OPTIMAL ACTIVE VIBRATION SUPPRESSION OF SMART COMPOSITE WIND TURBINE BLADES

BY

SHERIF IBRAHIM ABD EL-MAKSOUD MOHAMED

A Thesis Presented to the

DEANSHIP OF GRADUATE STUDIES

KING FAHD UNIVERSITY OF PETROLEUM & MINERALS

DHAHRAN, SAUDI ARABIA

In Partial Fulfillment of the
Requirements for the Degree of

MASTER OF SCIENCE

In

AEROSPACE ENGINEERING
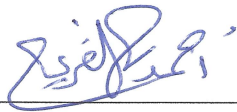
DHU AL-QA'DAH 1435

SEPTEMBER 2014

KING FAHD UNIVERSITY OF PETROLEUM and MINERALS

DHAHRAN- 31261, SAUDI ARABIA

DEANSHIP OF GRADUATE STUDIES

This thesis, written by **Sherif Ibrahim Abd El-Maksoud Mohamed** under the direction

his thesis advisor and approved by his thesis committee, has been presented and accepted

by the Dean of Graduate Studies, in partial fulfillment of the requirements for the degree

of **MASTER OF SCIENCE IN AEROSPACE ENGINEERING.**

Dr. Wael G. Abdelrahman
(Advisor)

Dr. Ahmed Z. Al-Garni
Department Chairman
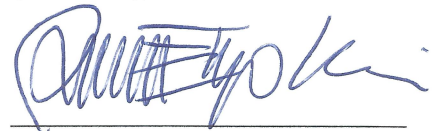
Dr. Ahmed Z. Al-Garni
(Co-Advisor)

Dr. Salam A. Zummo
Dean of Graduate Studies

Dr. Yehia A. Khulief
(Member)

16|10|14
Date

Dr. Mohammed A. Antar
(Member)

Dr. Prasetyo Edi
(Member)

To
my beloved parents, brother
and who has faith in me.

ACKNOWLEDGMENTS

IN THE NAME OF ALLAH, THE MOST BENEFICIENT, THE MOST MERCIFUL

Proclaim! In the name of thy Lord and Cherisher, Who created man, out a (mere) clot of congealed blood. Proclaim! And thy Lord is Most Bountiful, He who taught (the use of) the pen, taught man that which he knew not. Nay, but man doth transgress all bounds, in that he looketh upon himself as self-sufficient. Verily, to thy Lord is the return (of all). **(**Surah 96: Al 'Alaq, 1-8**)**

All praises belong to Allah (SWT), the Cherisher and Sustainer of the worlds, none is worthy of worship but Him. I am sincerely thankful to Him for His kindest blessings on me and all the members of my family. He was with me in the most difficult of times and always. Peace and blessings of Allah be upon our dearest prophet, Muhammad, his family and his companions.

I am grateful to King Fahd University of Petroleum and Minerals, for providing an adequate environment for research and education.

I want to express my appreciation to my advisor Dr. Wael G. Abdelrahman, for his help, guidance and efforts in this work.

My sincere and heart-felt thanks to Prof. Ahmed. Z. Al-Garni, my Co-Advisor and Chairman of Aerospace Engineering Department, due to his valuable suggestions, encouragement and support.

Special and sincere thanks also go to my thesis committee members, Prof. Yehia A. Khulief, Prof. Mohammed A. Antar and Dr. Edi Prasetyo for their cooperation and valuable advice.

I would also like to thank all AE faculty members (staff and students). Their advice and knowledge led me to finish this work in a very professional manner. I would also like to acknowledge my fellow research assistants, courses mates, colleagues and friends for their help, motivation and encouragement.

Last but not the least, I humbly offer my sincere thanks to my parents and brother for their incessant inspiration, blessings and prayers. They stood by me in my most difficult of times, and no words of appreciation can fully express my gratitude towards them. I always pray to Allah (SWT) to make them fine and to give us all Hidayah and Pardon our sins and grant us Paradise. Ameen

TABLE OF CONTENTS

LIST OF TABLES

LIST OF FIGURES

LIST OF ABBREVIATIONS

HAWT   Horizontal Axis Wind Turbine

VAWT   Vertical Axis Wind Turbine

PD   Proportional-Derivative controller

LQR   Linear Quadratic Regulator

PZT   Lead Zirconate Titanate

GR/E   Graphite/Epoxy

FEM   Finite Element Method

PVDF   Polyvinylidene Fluoride

FRP   Fiber Reinforced Polymer

GA   Genetic Algorithm

THESIS ABSTRACT (ENGLISH)

Full Name   : Sherif Ibrahim Abd El-Maksoud Mohamed

Thesis Title   : Optimal Active Vibration Suppression of Smart Composite Wind Turbine Blades

Major Field   : Aerospace Engineering

Date of Degree : September 2014

The purpose of this study is to apply active vibration control technique numerically for suppressing the vibrational level of a horizontal axis wind turbine blade. Two systems are studied to apply active vibration control on the wind turbine blade model, the first is a uniform cantilever beam and the other system is a non-uniform (tapered) cantilever beam. A single piezoelectric actuator and sensor are bonded on the upper and lower surface of the systems, respectively. The vibration analysis and dynamic characteristics of smart systems are obtained using approximate analytical methods. The entire structure is modeled in the state space form using the state space method, generalized coordinates and piezoelectric theory. Two types of controllers are designed to study the performance of the piezoelectric active controller. The first is a Proportional-Derivative (PD) controller and the other type is a Linear Quadratic Regulator (LQR). The Linear Quadratic Regulator (LQR) demonstrates better results for vibration suppression. The MATLAB code Simulink is used to simulate the different cases.

THESIS ABSTRACT (ARABIC)

إن الهدف من هذه الدراسة هو تطبيق أسلوب التحكم النشط للإهتزازات عدديا من أجل خفض مستوى الإهتزاز لريش التوربينات الهوائية ذات المحور الأفقي والتحكم بها. ومن أجل تطبيق أسلوب التحكم النشط للإهتزازات على نموذج لريشة توربينة هوائية، تم دراسة نظامين، الأول هو شعاع منتظم، والثاني هو شعاع غير منتظم (مدبب). وقد تم إستخدام مشغل واحد كهربي إجهادي وجهاز إستشعار واحد كهربي إجهادي على السطح العلوي والسفلي للأنظمة، على التوالي. ويعتبر تحليل الاهتزاز والخصائص الديناميكية للأنظمة الذكية ذات أولوية وقد تم الحصول عليها من خلال إستخدام أساليب التحليل التقريبية. وقد تم صياغة التمثيل المصفوفي للمعادلات التفاضلية من خلال إستخدام صيغة التمثيل المصفوفي، الإحداثيات المعممة ونظرية كهربائية الإجهاد. وقد تم تصميم نوعين من وحدات التحكم لتحديد مقدار القوة المتطلبة التي يحتاجها المشغل لتأثير على الأنظمة الذكية. الأول هو وحدة التحكم النسبي المشتقة (PD) والثاني هو المنظم التربيعي الخطي (LQR). وأظهرت النتائج أن المنظم التربيعي الخطي (LQR) يبين نتائج أفضل لقمع الإهتزازات. وقد تم إستخدام برنامج الماتلاب والسيميولينك لمحاكاة الحالات المختلفة.

CHAPTER 1

INTRODUCTION

Wind energy is considered one of the most important, sustainable, competitive, reliable and economical source of energy from other renewable energies globally because no fossil fuel is used, more efficient, less space than power station and it provides reliable supply of electrical energy. According to the U.S. Department of energy, wind energy is considered the fastest source among other sources for generating electricity. In Saudi Arabia, this source is yet to be fully utilized. It can reduce, to some extent, the dependence on fossil fuel, particularly in remote location with abundant wind. The generated electricity will reduce the 20 % of KSA oil production being used to generate electricity and distill water. Wind turbines are the devices that generate wind energy and electricity. Wind turbine blades are the main components of the wind turbines that differentiate vibrations among other components. When excessive vibrations occur to wind turbine blades, these vibrations cause catastrophic effects such as fatigue, structure problems, decrease in control accuracy, great damage in the mechanical and electrical components and efficiency reduction.

Lightweight and thin-walled structures are considered the most commonly used in various fields, especially in aerospace, mechanical and electrical fields. In aerospace, they are used in various industries such as designing spacecrafts, wings, bodies and tails

of the aircraft and in wind turbine blades [1]. However, these types of structures are prone to excessive vibrations. Vibrations are considered a type of motion, which coexist with movement of the systems. When vibrations exceed the limit, they cause catastrophic effects on the mechanical and electrical components. They reduce the system efficiency, control accuracy and cause resonance effects.

Many researches, experimentally and numerically, were conducted for vibration reduction. One of these methods is active vibration control, which attracts many researchers because of the rapid growth of electronic technologies.

Active vibration control method mainly consists of a sensor to capture the dynamic behavior of the structure, a processor to make some manipulation in the signals that come from the sensor, an actuator that applies force on the structure, and a source of energy or a controller to actuate the actuators. This is called a "smart structure". Therefore, a smart structure is a conventional structure that has been combined with sensing and actuating mechanisms [2]. Recently, piezoelectric sensors and actuators (patches) are used extensively due to their fast response, flexibility, light weight and small size, low cost, lower power consumption, high actuating force, high operating bandwidth, ease in manufacturing and convenience to embed into structures.

The purpose of this study is reducing the vibration response of a horizontal axis wind turbine blade by using active vibration control method numerically.

This research is organized as follows: First of all, Introduction about wind turbines, smart materials, vibration control, and the objective are presented in chapter one. Then, in chapter two, the previous studies about active vibration control, tasks and methodology

are discussed. Mathematical modeling of smart structures and numerical results are presented in chapter three. In chapter four, PD and LQR controller design are discussed. Results and discussion of the models and controllers effects are presented in chapter five. Finally, in chapter six, this research is closed with a conclusions section which includes some concluding remarks.

1.1   Wind Turbines

Wind turbines are the devices that are used to capture the kinetic energy contained in the wind or in the air and convert it to electrical power or wind energy. So, how do wind turbines generate electrical energy? Simply, the wind turns the rotor blades, which spin a rotor shaft, which connects to a generator which generates electricity. There are three locations for wind turbines installation, offshore, plains and hills. The power generation improves even more with increasing wind turbines sizes.

1.1.1   Types of Wind Turbines

There are two general types of wind turbines, Horizontal and Vertical Axis Wind Turbines:

- **Vertical Axis Wind Turbine**

It is a category of wind turbines where the main rotor shaft is located vertically and the other main parts are placed at the bottom of the wind turbine, as shown in Figure 1-1.

- **Horizontal Axis Wind Turbine**

It is a category of wind turbines where the main rotor shaft is located horizontally and the other main parts such as the electrical generator are placed at the top of the wind turbine,

as shown in Figure 1-2. Table 1-1 shows a comparison between Vertical and Horizontal

Axis Wind Turbines.

Figure 1-1: Vertical Axis Wind Turbine [3]

Figure 1-2: Horizontal Axis Wind Turbine [4]

Table 1-1: Comparison between Vertical and Horizontal Axis Wind Turbines

	Vertical Axis Wind Turbines	Horizontal Axis Wind Turbines
Advantages	1- Easier to maintain 2- Produce more power than HAWT 3- Enormously quieter than HAWT 4- Withstand extreme weather 5- Need less service	1- High System stability 2- Self starting 3- Higher efficiency and cheaper 4- Less damage 5- More efficient
Disadvantages	1- Structurally less stable 2- Very low starting torque 3- Sensitive to off-design conditions 4- Complicated in structure	1- Fatigue and structure problems 2- Vibration problems 3- Difficulties in maintenance 4- Difficulties in installation

1.1.2 Components of Wind Turbines

The major components of a wind turbine are foundation, tower, nacelle and rotor blades. Foundation is used for the stability of the wind turbine. The height of the tower is an essential component, the power energy increases with tower height. Blades rotate when the wind is blown over them, causing the rotor shaft to spin. Nacelle consists of a generator that generates electrical energy and a gear box that connects the low speed shaft to the high speed shaft and increases the rotation to around 1500 rpm, as shown in Figure 1-3. Horizontal Axis Wind Turbine (HAWT) is focused due to the vibration and structure problems in its blades. In Figure 1-4, the various parts of Horizontal Axis Wind Turbine are shown.
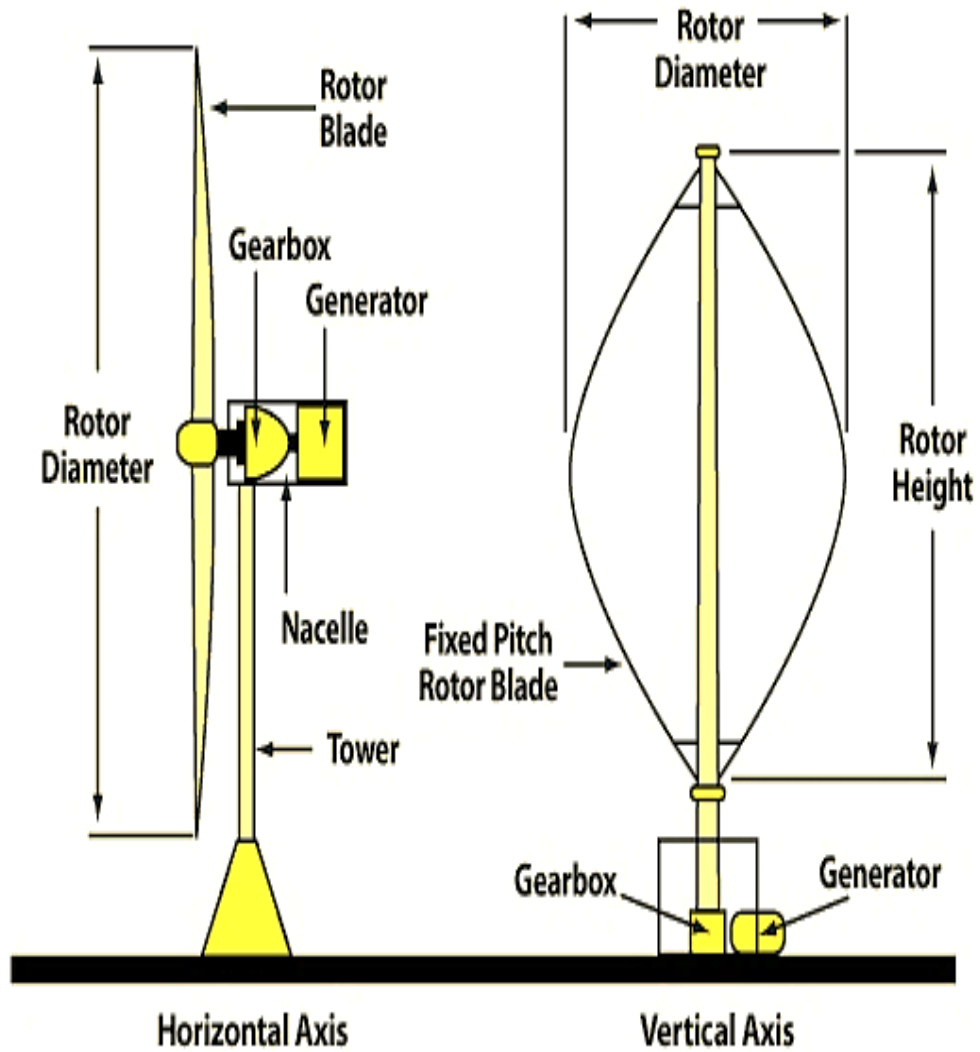
Figure 1-3: Components of Vertical and Horizontal Axis Wind Turbine [5]
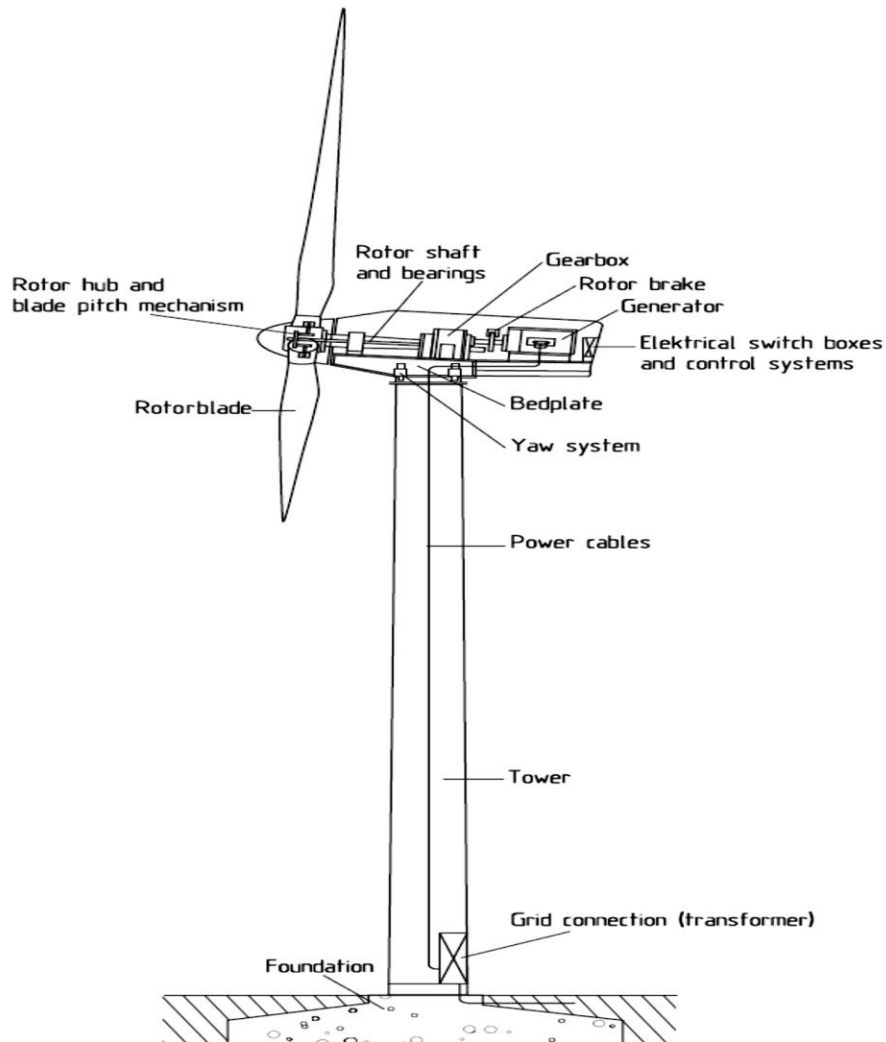
Figure 1-4: Components of Horizontal Axis Wind Turbine [4]

1.2   Smart Materials

Smart materials are designed materials that have one or more properties which interact with a conventional system and exhibit adaptive characteristics. There are several types of smart materials such as piezoelectric materials, Shape - memory alloys, thermoelectric materials, photomechanical materials, etc. A Smart structure is a combination between the structure and a set of actuators and sensors coupled by a controller, as shown in Figure 1-5. Frequently, piezoelectric actuators and sensors are used because they are

7

small in size, light weight, large bandwidth, flexibility, easy integration with various structures, and easy to design and manufacture, as shown in Figure 1-6.

High degree of integration
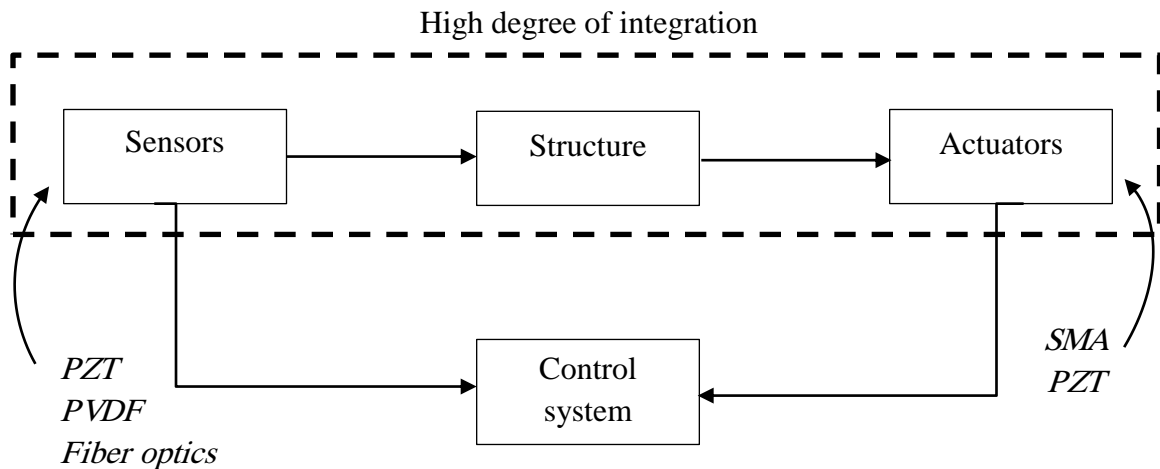
Figure 1-5: A structure equipped with three versions of suspension system: (a) passive; (b) active; (c) semi-active [6]
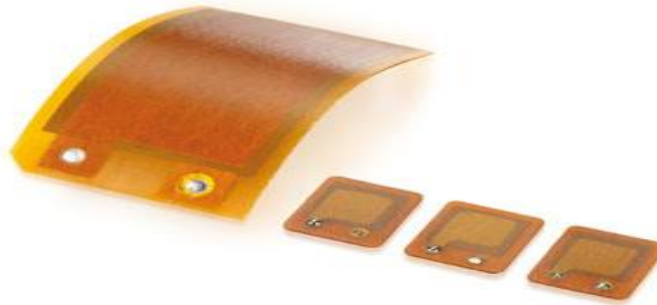
Figure 1-6: Piezoelectric patches [7]

Piezoelectric materials can be fabricated in form of patches and can be easily bonded on or imbedded into conventional structures. Piezoelectric patches are ferromagnetic materials that have the ability to expand or contract when subjected to electric or

magnetic field. Piezoelectricity means "electricity by pressure". The process of generating an electric field due to loads or stresses called "direct piezoelectric effect" whereas the process of imposing voltage under similar circumstance that cause deformation in the materials or strains is called "reverse piezoelectric effect", as shown in Figure 1-7.
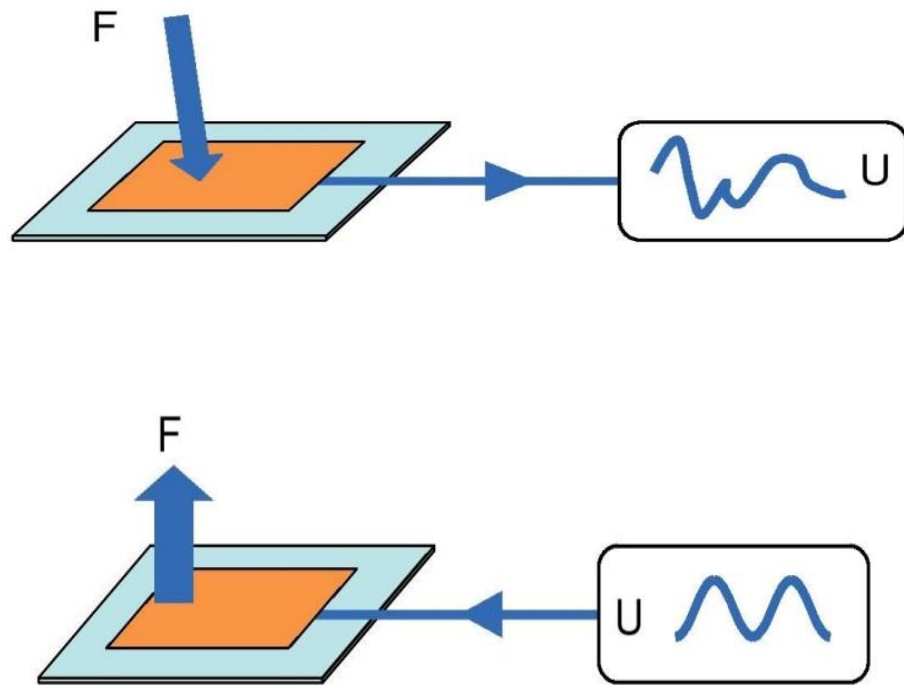
Figure 1-7: Direct and reverse piezoelectric effect [7]

1.2.1 Working Principle

Piezoelectric patches can be considered as capacitors. When voltage is imposed, an electric field parallel to the polarization is generated due to the voltage difference between the electrodes. This field causes a transverse contraction of the ceramic normal to the electric field direction [8], as shown in Figure 1-8.

9

$$M_p = - e_{31}Vb\, z_m$$
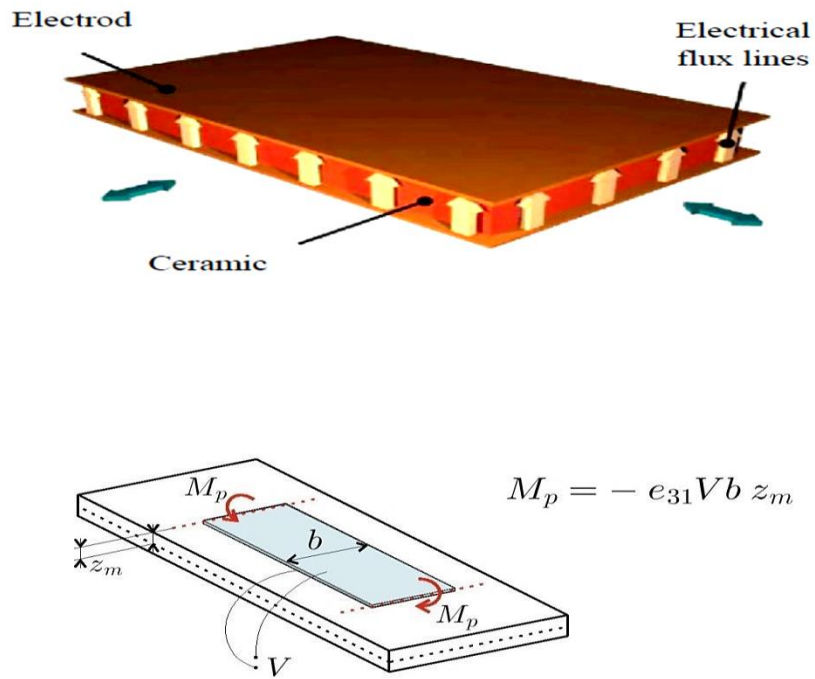
Figure 1-8: Transverse piezoelectric effect [7], [9]

Piezoelectric patches are consisted of a thin piezoceramic film which is covered with electrically conducting materials to provide the electrical contact. Mechanical preload and electrical insulation cover this piezoceramic film to apply it on curved surfaces, as shown in Figure 1-9.
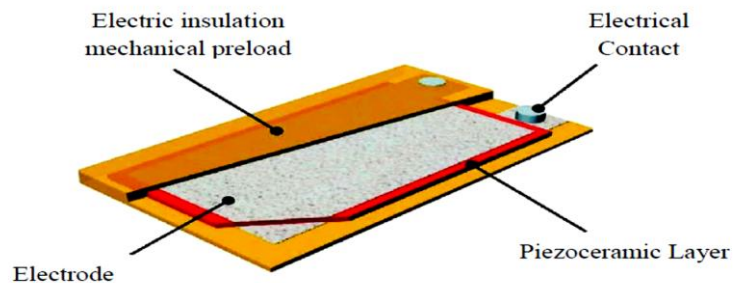
Figure 1-9: Component of piezoelectric patches [7]

1.3 Vibration Control

Vibration suppression of structures is considered a significant application in various engineering fields. Vibrations have catastrophic influences, when they exceed the limit, on device performance, effectiveness, operation accuracy and efficiency. According to that, controlling the vibrational level is considered a very important issue. The control system is considered challenging because one must achieve the desired motion while ensuring that the system is still or becomes stable. Different control techniques have been conducted such as optimal control, neural network, genetic algorithm, adaptive nonlinear boundary control, etc. [6], [9].

1.3.1 Classification of Vibration Control

The vibration control is divided into three categories, Active, passive and semi-active, as shown in Figure 1-10. The classification depends on the amount of external power source required [6], [9], as shown in Table 1-2.
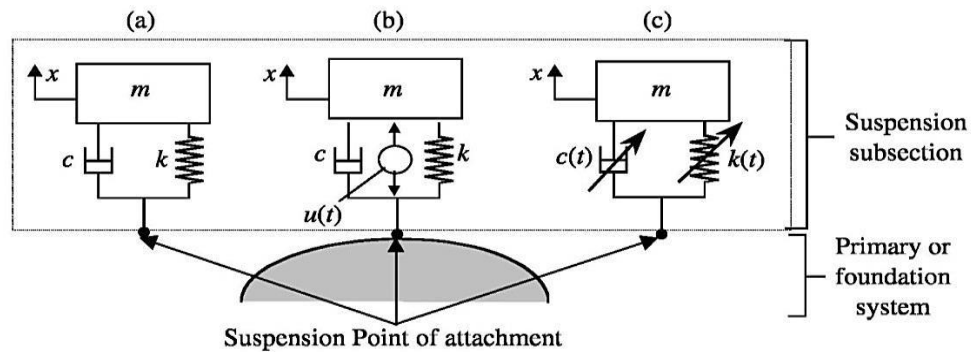
Figure 1-10: A structure equipped with three types of suspension systems: (a) passive; (b) active and (c) Semi-Active configurations [6], [9]

Table 1-2: Types of Vibration Control

Active	Passive	Semi-Active
• Needs a large external power source to work and control actuators that apply forces to the smart structures [10].	• Designed in a suitable way without the need of any external power source to work. It is constructed of the physical component.	• It is a combination of active and passive control system that needs less external power source to achieve the desired characteristic.
• Used to add and dissipate energy in the structures and very Effective for vibration suppression of the system.	• Effective for stability of the system and uses resistive or reactive devices to absorb vibrational energy.	• Used to control the real time or damping and making the system stable. Low energy requirement and cost.
• Control-induced instability and the need of large control effort are considered very significant problems	• Not effective in suppressing the vibrational level and has some limitations in structural applications.	• It can't add or remove energy to the structure.
(e.g., Actuators)	(e.g., Mechanical spring)	(e.g., Variable rate damper)

In passive vibration control, it is not possible to regulate the control forces that are generated in real time. Moreover, no external power sources exist and not effective in reducing the vibration response. Therefore, active vibration control technique is designed for vibration suppression and for adding and dissipating energy.

1.4   Active Vibration Control

Due to the shortcomings of passive vibration control, the active vibration control method has attracted large amount of investing actions in various fields. An active vibration control method is used to reduce the vibrational level by using external power source to operate its function. A schematic diagram of an active vibration control is shown in Figure 1-11. It consists of

1) A plant (vibrating system) whose vibration needs to be controlled and reduced.

2) Sensors used to monitor and measure the response of the system in term of displacement, velocity or acceleration.

3) Actuators that receive a control signal from the controller and apply a force to the system.

4) A microprocessor-based system that consists of:

- Analog-Digital converter (ADC) that is used to convert the analog signal measured by the sensors to digital form that is compatible with the computer that generates the control signal.

- Digital-Analog converter (DAC) that converts the digital signal to analog form that is compatible with the actuator.

- The controller (control algorithm) that is programmed in the computer and is used to determine how much force the actuators need to apply.

- An amplifier that is used to amplify the analog signal to appropriate level for the actuator

- A filter that is used to remove noise and disturbances.

- An external power source.

The sensors measure the response of the system and provide feedback to the controller. The controller makes a comparison between the desired response and the sensed response, and uses the error to generate the appropriate control signal (control law). Actuators drive the control signal and apply a force to the system whose vibration needs to be reduced may be an integral part of the plant or may be an external part bonded on the plant (e.g., a piezoelectric patches or electromagnetic actuator).
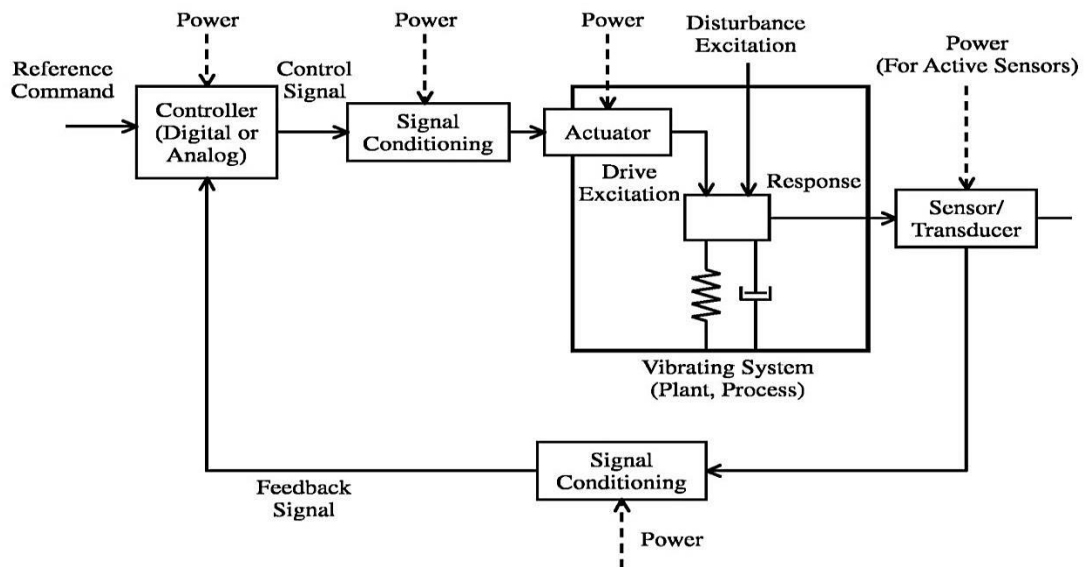
Figure 1-11: A system for active vibration control [6]

1.4.1 Control Techniques

Controller strategy is considered one of the major elements for active vibration control method. The control logic compares the sensed response with the desired response to generate the error and to determine the proper control signal. This system is known as a feedback control system, as shown in Figure 1-12. A feedback control system provides a

mechanism for tailoring system behavior to an appropriate manner. Many control law (the relation that generates the control signal from the sensed response) have been developed for technical and practical applications in various fields. In order to design a feedback control system appropriately, the performance must be defined in term of system specifications. Standard performance measures are usually defined in term of step response. The general objectives are the speed of the response, the rate of damping, stability and accuracy. There are two major control techniques for vibration control, classical approach and Modern control. One of the well-known classical approaches is proportional-integral-derivative (PID) controller whereas optimal control represents modern control. In this study, LQR optimal control and PD controller are designed and a comparison between them is done.
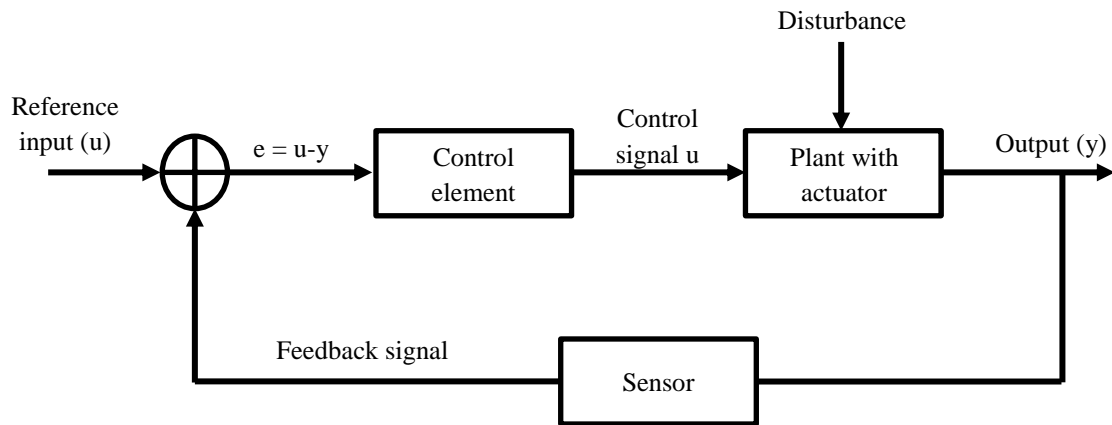
Figure 1-12: Feedback control system

1.5   Objective of this study

Due to the energy crisis, power consumption and environmental problems, renewable energy; e.g. wind power generation, is considered a very significant requirement globally. Blades are considered the main components in wind turbines that differentiate wind and vibrations from other components. With increasing size of wind turbine blades for more power generation, blades are prone to excessive vibrations. When vibrations exceed the limit, they cause catastrophic effects on mechanical and electrical components. They reduce the system efficiency, control accuracy and cause resonance effects. So the need to control and reduce vibrational level to avoid these problems is considered crucial to the system's performance and safety.

The aim of this study is to apply active vibration control technique for suppressing the vibration response of a horizontal axis wind turbine blade. To apply active vibration control technique on wind turbine blade, several tasks are carried out. These include modelling of the smart system, response description and controllers design.

CHAPTER 2

LITERATURE REVIEW

A wind turbine blade model can be idealized as a tapered cantilever beam because the length of the span is very large relative to the chord and thickness, and the wind turbine blade model can be considered as a one dimensional beam. To study a tapered cantilever beam, a uniform cantilever beam is studied as a type of validation. To study the physical systems such as plates, bars and beams, the equations that describe these systems are usually in the form of partial differential equations, which the exact solution of these systems is considered very difficult to solve or the boundary conditions are very complex. Ganesan and Engels [11], studied the dynamics of the Timoshenko beam based on the general assumed modes method with interface restrained assumed modes and static constraint modes. Han et al. [12], investigated the transverse vibration analysis of a uniform beam using four theories: Euler-Bernoulli, Rayleigh, shear and Timoshenko beam, as shown in Table 2-1.

Table 2-1: Four beam theories [12]

Beam models	Bending moment	Lateral displacement	Shear deformation	Rotary inertia
Euler-Bernoulli	✔	✔	✖	✖
Rayleigh	✔	✔	✖	✔
Shear	✔	✔	✔	✖
Timoshenko	✔	✔	✔	✔

In 1992, Bazoune and khulief [13], developed a finite beam element for vibration characteristics of a rotating (tapered) Timoshenko beam. The effect of shear deformation, setting angle and rotary inertia are included into the finite element model. The results showed high accuracy when compared with other numerical results. Khulief [14–16], developed a finite element approach for vibration reduction in rotating elastic beams and in elastic structural systems using active vibration control method. Wereley et al. [17], studied numerically and experimentally the vibration characteristics of a uniform cantilever beam to obtain the mode shapes and the natural frequencies. Four methods were used; exact solution, lumped parameter method, assumed modes method and finite element method. The results showed agreeable accuracy when compared with the measured results. Achawakorn and jearsiripongkul [18], determined the vibration characteristics and natural frequencies for uniform and non-uniform (tapered) beams using approximate analytical methods. The results showed agreeable accuracy when compared with the analytical solution. Zhen et al. [19], developed the finite model method for analyzing the free vibration of horizontal axis wind turbine blades. Flap-wise, edge-wise, and torsional natural frequencies of a variable length blade have been determined. The results revealed that the approach used in this study is very efficient.

With recent developments in sensor/actuator technologies, extensive studies were conducted for vibration reduction using smart materials such as piezoelectric patches. Many studies have concentrated on modeling of piezoelectric materials or intelligent materials for structure modeling. Crawley and Luis [20], showed the development of piezoelectric actuators and sensors as parts of smart structures analytically and experimentally. The results revealed that the effectiveness of piezoelectric actuators does

not only depend on the dimensions of the structures but on their capability on transmitting strain to the structures. Song et al. [21], studied numerically and experimentally active vibration control of an E-glass/epoxy laminated composite cantilever beam using piezoelectric sensors and actuators. Finite element method is used to obtain the natural frequencies and mode shapes of a smart beam. Positive position feedback (PPF) and strain rate feedback (SRF) were used to reduce the vibrational level of the plant. The results showed that the vibrational level of the smart system are reduced using the proposed controller. Kapuria and Yasin [22], studied active vibration control of hybrid composite and fiber metal laminate (FML) plates incorporated with monolithic piezoelectric fiber reinforced composite (PFRC) actuators and sensors using layer-wise plate theory, optimal control and velocity feedback for reducing the vibration of the smart systems. Staino et al. [23], studied active vibration control of a wind turbine blade for controlling the edge-wise vibrations using piezoelectric actuators and sensors. The mathematical model of the wind turbine blade with the piezoelectric layers has been derived using Euler-Lagrangian approach to describe the dynamics of the edge-wise vibrations. A Linear Quadratic Regulator (LQR) has been designed to control the actuation force and is compared with Direct Velocity Feedback (DVF) to study their effectiveness. The results revealed that the desired performance can be achieved using the proposed controller.

Controller design is considered one of the major elements for active vibration control method. The major benefit of active vibration control is reducing the vibrational level of smart structures. The effectiveness of this action is based on the types of the controller algorithms and their designs. Earlier, Han et al. [24], studied experimentally and

numerically active vibration control of smart composite cantilever beam and plates. The classical laminated beam theory and Ritz method were used to obtain the natural frequencies and the mode shapes of the composite cantilever beam with piezoelectric patches. A Linear Quadratic Gaussian (LQG) and classical control methods are implemented to reduce the vibration rates of smart structures. The results revealed that LQG method is very efficient for vibration suppression and robustness to noise compared with the classical control methods. Manjunath and Bandyopadhyay [25–28], studied the design of a Fast Output Sampling (FOS) based discrete sliding mode control and a Periodic Output feedback (POF) control to suppress the vibrational level of a smart flexible cantilever beam. One of the results revealed that when the location of the piezoelectric sensor is moved from the structure support end to the free end, the sensor output decreased due to the heavy distribution of the bending moment near the fixed end whereas when the location of the piezoelectric actuator is moved from the structure support end to the free end, a large amount of control effort is required. Also, the proposed controllers ensure system stability, better performance and easy implementation in real time. Song and Gu [29], investigated experimentally active vibration control of an Aluminum cantilever beam using sliding mode controller. Piezoceramic sensor and actuators are bonded to the structure to control and monitor the vibration response. The advantages of sliding mode based controller are easier in implementation, insensitivity to the unmodeled dynamics and strong robustness to model parameters. Proportional-Derivative (PD) controller and lead compensation were designed for making comparison with the proposed controller. The results showed that sliding mode controller suppressed the vibration rates of smart system quickly and more effectively. Zhang et al. [30–31],

20

studied active vibration control of flexible structures with bonded piezoelectric sensors and actuators for vibration reduction using Linear Quadratic regulator (LQR), Linear Quadratic Gauss (LQG) and robust H_∞ control. The results revealed that H_∞ control has strong robustness to model parameters, high performance and can suppress the vibrational level better than LQG. Rahman and Alam [32], investigated experimentally active vibration suppression of a smart cantilever beam integrated with piezoelectric sensors and actuators using proportional integral derivative (PID) controller. The results showed that the proposed control method is very efficient and effective. Jarzyna et al. [33], Studied the design of LQR controller and PD controller for vibration suppression of a composite cantilever beam using piezoelectric Macro Fiber Composite actuator. The results revealed that LQR controller demonstrated better results than PD controller. The PD controller was very sensitive to the variations of parameters which lead to an increase in oscillations. Roy and Chakraborty [34], designed a Linear quadratic regulator (LQR) with the help of genetic algorithm (GA) for vibration suppression of a smart fiber reinforced polymer (FRP) composite shell structures integrated with piezoelectric actuators and sensors. The results revealed that the proposed LQR controller could control the dynamic oscillation and the static displacement which was not possible with conventional LQR controller. Recently, neural network is considered very important technique for modeling, analyzing and predicting the output results [35–37]. Kumar and Chhabra [38], designed a Linear Quadratic Regulator (LQR) with the help of neural network controller for vibration reduction of a cantilever plate incorporated with piezoelectric patches. Zoric et al. [2], presented the optimized fuzzy logic controller (FLC) with on-line tuning of scaling factors for active vibration control of a cantilever

composite beams. Particle Swarm Optimization (PSO) is used to optimize the membership functions of the proposed FLC. The results are compared with (LQR) optimal control and optimized fuzzy logic controller (FLC) with constant scaling factors. The results showed that the Particle swarm optimization (PSO)-optimized self-tuning fuzzy logic controller (FLC) is much more effective and efficient in vibration suppression from others.

The sizes and locations of piezoelectric sensors and actuators are considered very significant parameters for control effectiveness and for the performance of smart systems. Bruant et al. [39], studied the optimal placement and orientation of piezoelectric sensors and actuators for active vibration control of a simply supported plate using genetic algorithm. The results revealed that the GA is very efficient for optimization in the more complex structures. Zoric et al [1], presented the optimal control, size and location of the piezoelectric patches bonded on a composite cantilever beam for active vibration suppression. In this study, the fuzzy optimization strategy based on the Particle Swarm Optimization (PSO) algorithm is used. The optimization criteria are based on eigenvalues of the controllability Grammian matrix. The results showed that The PSO algorithm ensures fast convergence, easy in implementation and handling, and computational effectiveness. Furthermore, this technique leads to maximize the closed loop modal damping ratios, minimize the maximum applied control voltages and can be implemented for more complex structures. Schulz et al. [40], analyzed the optimization of piezoelectric patches allocation in cantilever composite structures for vibration reduction using a Linear quadratic regulator (LQR) and Genetic Algorithm (GA) as optimization tool.

Active vibration control can be used to suppress the vibrational level of wind turbine blades due to the external forces and strong winds. Qiao et al. [41], presented a finite element model of smart wind turbine blade for vibration suppression control.

2.1 Tasks and Methodology

Based on literature review and to accomplish this study, the following tasks are studied:

a. Obtain the vibration characteristics and the dynamic behavior of a uniform beam, a non-uniform (tapered) beam and a wind turbine blade.

b. Study and validate the simulation model with known data in literature.

c. The entire structures are modeled in state space form using state space method, modal coordinates and piezoelectric theory.

d. Design the proposed controller and study the controller effectiveness and performance.

e. Study the effect of the different parameters and variables.

f. Validate using available experimental, numerical or published data.

g. Make recommendations for future study.

h. Report/publish important finding of this study.

The above tasks are arranged in the following order to accomplish this study. In order to suppress the vibration response of the wind turbine blade model, an active vibration control method is applied on two systems, the first is a uniform cantilever beam and the second is a non-uniform (tapered) cantilever beam. Ritz method and assumed modes method are used to obtain the dynamic characteristics of smart systems. The equations of

motion of the smart structures are converted to state space form using state space method, modal coordinates and piezoelectric theory. Two types of controllers are designed to study the performance of the piezoelectric active controller. The first is a Proportional-Derivative (PD) controller and the other type is a Linear Quadratic Regulator (LQR). The criteria that are used for designing the controllers are minimizing the settling time and the control input not exceed ± 90 V because the maximum voltage that could be applied to the piezoelectric actuator is ± 90 V. The MATLAB code Simulink is used to simulate the different cases. Validation of results is conducted with known data in the literature. The methodology of active vibration control of the smart structures is shown in Figure 2-1.
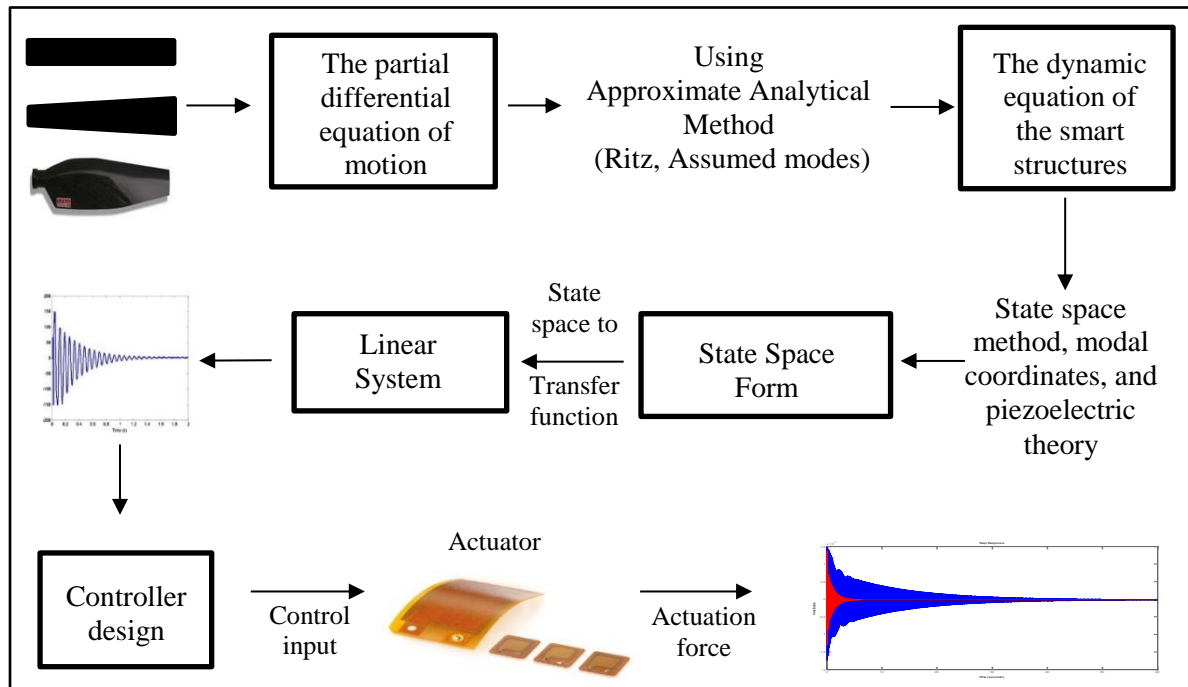
Figure 2-1: Active vibration control of smart structures

CHAPTER 3

MATHEMATICAL MODEL

The exact solution of various continuous systems is considered very complex and difficult due to the non-uniform mass and stiffness distributions or due to the boundary conditions are very complicated. In these cases, approximate analytical methods may be used for obtaining the natural frequencies, mode shapes and dynamic characteristics of the system. The partial differential equation is reduced to ordinary differential equation using approximate analytical methods. To obtain the dynamic characteristics of wind turbine blade model, two systems are studied, the first is a uniform cantilever beam and the other system is a non-uniform (tapered) cantilever beam. Wind turbine blade can be idealized as a tapered cantilever beam.

3.1 Rayleigh-Ritz Method

The partial differential equation of motion for an Euler-Bernoulli beam where the transverse deflection $w(x, t)$ and for free vibration can be expressed as:

$$\rho A(x)\frac{\partial^2 \omega(x,t)}{\partial t^2} + \frac{\partial^2}{\partial x^2}\left[EI(x)\frac{\partial^2 \omega(x,t)}{\partial x^2}\right] = 0 \qquad (3.1)$$

Where E is Young's modulus, $A(x)$ is the cross section area of the beam, $I(x)$ is the moment of inertia of the beam, ρ is the density and for the free vibration, $f(x,t) = 0$.

The Rayleigh-Ritz Method based on the fact that Rayleigh's quotient is larger than or equal to the first eigenvalue, $\lambda_i = \omega_i^2$:

$$R(X(x)) \geq \lambda_1 \tag{3.2}$$

In the Rayleigh-Ritz method, the transverse displacement of the continuous system, $w(x)$, is approximated using a series of trial functions (admissible functions) that satisfy the geometric boundary conditions of the system:

$$w(x) = \sum_{i=1}^{n} c_i \, \emptyset_i \tag{3.3}$$

Where $c_1, c_2, \ldots, c_n$ are called Ritz coefficients, and $\emptyset_1(x), \emptyset_2(x), \ldots, \emptyset_n(x)$ are called trial functions.

Rayleigh's quotient becomes a function of Ritz coefficients $c_1, c_2, \ldots, c_n$.

$$R = R(c_1, c_2, \ldots, c_n) \tag{3.4}$$

The Ritz coefficients $c_1, c_2, \ldots, c_n$ are selected to minimize Rayleigh's quotient using the necessary conditions:

$$\frac{\partial R}{\partial c_i} = 0, \qquad i = 1,2,\ldots,n \tag{3.5}$$

Rayleigh's quotient is indicated as

$$R = \omega^2 = \frac{\pi_{max}}{T_{max}^*} \tag{3.6}$$

26

Where π_{max} and T^*_{max} denote the maximum strain energy and reference maximum kinetic energy of the continuous system, respectively. The reference maximum kinetic energy (T^*_{max}) is related to the maximum kinetic energy (T_{max}) as,

$$T_{max} = \omega^2 T^*_{max} \tag{3.7}$$

The maximum strain energy and the reference kinetic energy can be expressed as

$$\pi = N = \frac{1}{2} \sum_{i=1}^{n} \sum_{j=1}^{n} K_{ij} c_i c_j \tag{3.8}$$

$$T = D = \frac{1}{2} \sum_{i=1}^{n} \sum_{j=1}^{n} m_{ij} c_i c_j \tag{3.9}$$

Where $[k] = [k_{ij}]$ is the stiffness matrix, $[m] = [m_{ij}]$ is the mass matrix,

$$\vec{c} = \begin{Bmatrix} c_1 \\ c_2 \\ . \\ . \\ c_n \end{Bmatrix} \tag{3.10}$$

In the case of transverse vibration of a uniform and a non-uniform beam, k_{ij} and m_{ij} are given by

$$k_{ij} = \int_0^l EI(x) \frac{d\emptyset_i}{dx} \frac{d\emptyset_j}{dx} dx \tag{3.11}$$

$$m_{ij} = \int_0^l \rho A(x) \emptyset_i \emptyset_j dx \tag{3.12}$$

So, the Rayleigh's quotient is expressed as

$$R(c_1, c_2, \dots \dots, c_n) = \frac{N(c_1, c_2, \dots \dots, c_n)}{D(c_1, c_2, \dots \dots, c_n)} \tag{3.13}$$

The condition for the minimum of Rayleigh's quotient is

$$\frac{\partial R}{\partial c_i} = \frac{D(\partial N/\partial c_i) - N(\partial D/\partial c_i)}{D^2} = 0, \qquad i = 1,2,\dots,n$$

$$\frac{1}{D}\left(\frac{\partial N}{\partial c_i} - \frac{N}{D}\frac{\partial D}{\partial c_i}\right) = \frac{1}{D}\left(\frac{\partial N}{\partial c_i} - \frac{N}{D}\frac{\partial D}{\partial c_i}\right) = 0, \quad i = 1,2,\dots.,n \qquad (3.14)$$

For each natural frequency ω_i, the corresponding vector of Ritz coefficients $\vec{c}^{(i)}$ can be evaluated by solving the linear simultaneous homogeneous equations:

$$\left[[K] - \lambda_i^{(n)}[m]\right]\vec{c}^{(i)} = \vec{0} \qquad (3.15)$$

Equation (3.15) denotes an algebraic eigenvalue problem of order n.

In Matrix form as

$$\begin{bmatrix} K_{11} - \lambda_i^{(n)}m_{11} & K_{12} - \lambda_i^{(n)}m_{12} & \dots & K_{1n} - \lambda_i^{(n)}m_{1n} \\ K_{21} - \lambda_i^{(n)}m_{21} & K_{22} - \lambda_i^{(n)}m_{22} & \dots & K_{2n} - \lambda_i^{(n)}m_{1n} \\ \cdot & \cdot & & \cdot \\ \cdot & \cdot & & \cdot \\ K_{n1} - \lambda_i^{(n)}m_{n1} & K_{n2} - \lambda_i^{(n)}m_{n2} & \dots & K_{nn} - \lambda_i^{(n)}m_{nn} \end{bmatrix} \begin{Bmatrix} c_1^{(i)} \\ c_2^{(i)} \\ \cdot \\ \cdot \\ \cdot \\ c_n^{(i)} \end{Bmatrix} = \begin{Bmatrix} 0 \\ 0 \\ \cdot \\ \cdot \\ 0 \end{Bmatrix}$$

$$i = 1,2,..,n \qquad (3.16)$$

3.2 Assumed Modes Method

It is related to the Rayleigh-Ritz method but the major difference between the two techniques is that the Rayleigh-Ritz method used for solving the eigenvalue problems, whereas the assumed modes method is used to solve the forced vibration problems.

The displacement solution $w(x,t)$ is assumed to be

$$w(x,t) = \sum_{i=1}^{n} \emptyset_i(x)\, \eta_i(t) \tag{3.17}$$

Where $\emptyset_i(x)$ are known trial functions (admissible functions) that can be a set of assumed mode shapes, polynomials, or even eigenfunctions and depend on the boundary condition of the system, $\eta_i(t)$ called generalized coordinates. For forced vibration problem, the expression of strain energy (π), kinetic energy (T), and virtual work of non-conservative force, δW, are expressed in terms of assumed modes solution.

$$\pi(t) = \frac{1}{2}\sum_{i=1}^{n}\sum_{j=1}^{n} K_{ij}\eta_i(t)\eta_j(t) \tag{3.18}$$

$$T(t) = \frac{1}{2}\sum_{i=1}^{n}\sum_{j=1}^{n} m_{ij}\dot{\eta}_i(t)\dot{\eta}_j(t) \tag{3.19}$$

$$\delta W = \sum_{i=1}^{n} Q_{i_{nc}}(t)\, \delta\eta_i(t) \tag{3.20}$$

Where

$$Q_{i_{nc}}(t) = \int_0^l f(x,t)\emptyset_i(x)dx \qquad i = 1,2,\dots n \qquad (3.21)$$

The Lagrange equation can be expressed as

$$\frac{d}{dt}\left(\frac{\partial T}{\partial \dot{\eta}_i}\right) - \frac{\partial T}{\partial \eta_i} + \frac{\partial \pi}{\partial \eta_i} = Q_{i_{nc}}(t) \qquad (3.22)$$

Substituting Eqs. (3.18), (3.19) and (3.21) into Eq. (3.22), the equation of motion of the system can be derived as

$$[m]\ddot{\eta}(t) + [k]\eta(t) = Q_{i_{nc}}(t) \qquad (3.23)$$

3.3   Piezoelectric Strain Rate Sensors and Actuators

The linear piezoelectric coupling between the electric field and the elastic field or between the mechanical and electrical characteristics as follows:

$$D_i = d\,\sigma + e^T E_f \qquad (3.24)$$

$$\varepsilon = S^E\,\sigma + dE_f \qquad (3.25)$$

Where σ and ε represent the stress and strain, respectively, E_f and D_i represent the electric field and dielectric displacement, respectively. d, S^E and e^T represent piezoelectric strain / charge coefficient, elastic compliance of the medium and electric permittivity of the medium, respectively. A cantilever beam with bonded piezoelectric actuator and sensor is shown in Figure 3-1.
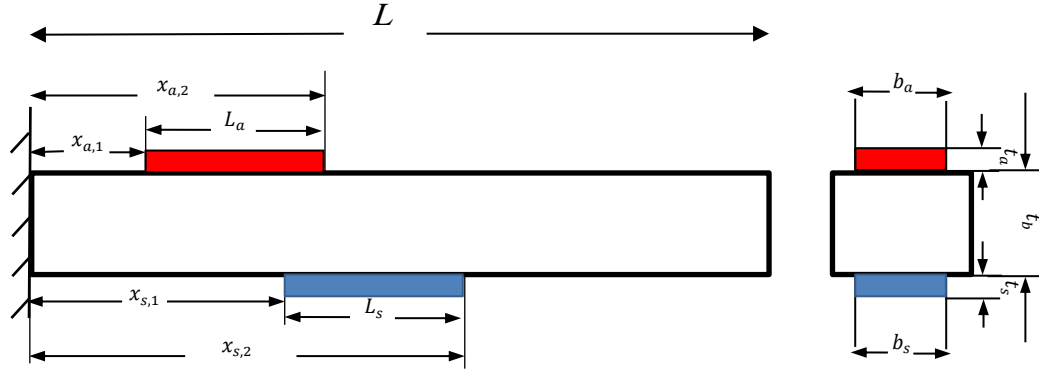
Figure 3-1: Cantilever beam with bonded piezoelectric actuator and sensor [42]

3.3.1 Sensor Equation

It is the process of generating an electric field due to loads or stresses on the structures or calculating the output charge produced by the strain in the structure, which called 'Direct piezoelectric effect'. The total charge of the piezoelectric sensor $Q(t)$ is the summation of the electric charge distribution over the entire length.

The electric charge distribution $q(x,t)$ is expressed as

$$q(x,t) = \left(\frac{K_{31}^2}{g_{31}}\right)\varepsilon_c(x,t) \tag{3.26}$$

Where K_{31} is the coupling coefficient, g_{31} is the piezoelectric voltage coefficient and $\varepsilon_c(x,t)$ is the strain in the sensor patches.

The total charge accumulated on the piezoelectric patches (sensor) can be expressed as

$$Q(t) = -b_s \int_{x_1}^{x_2} q(x,t)dx = -b_s \left(t_P + \frac{t_b}{2}\right)\left(\frac{K_{31}^2}{g_{31}}\right)\frac{\partial^2 w(x,t)}{\partial x^2} \qquad (3.27)$$

Where b_s, t_P, t_b, $w(x,t)$ represent the width of the piezoelectric sensor, the thickness (height) of the piezoelectric sensor, the thickness of the beam and the transverse displacement, respectively. x_1 and x_2 represent the location the piezoelectric sensor on the structures.

The sensor equation can be expressed as

$$V^s(t) = P^T \dot{q} = y(t) \qquad (3.28)$$

Where P^T represents a constant vector which is based on the sensor type and its location on the structure. $V^s(t)$ and $y(t)$ represent the sensor voltage and the output of the system, respectively.

3.3.2 Actuator equation

It is the process of imposing voltage on the actuator layer which leads to deformation in the structure or strains, which called 'reverse piezoelectric effect'. The strain developed by the applied electric field E_f on the actuator is expressed as

$$\varepsilon_A = d_{31}E_f = d_{31}\frac{V^a(t)}{t_a} \qquad (3.29)$$

Where d_{31}, t_a and $V^a(t)$ represent piezoelectric strain constant, actuator thickness (height) and input voltage to the actuator, respectively.

When the input voltage to the actuator is applied in the thickness direction, the stress developed is

$$\sigma_A = E_P d_{31} \frac{V^a(t)}{t_a}$$

(3.30)

Where E_P represents the piezoelectric Young's modulus

The moment M_A which is acting on the beam due to the stress is obtained by

$$M_A = E_P d_{31} z V^a(t)$$

(3.31)

Finally, the control force applied by the actuator can be expressed as

$$f_{ctrl} = h V^a(t) = h K_{ctrl} V^s(t)$$

(3.32)

Where K_{ctrl} and h represent the controller gain and a constant vector depends on the actuator type and its location on the structure, respectively.

3.4   Dynamic Equation of Smart Structure

The equation of motion of smart structure is

$$M\ddot{q}(t) + Kq(t) = f_{ext} + f_{ctrl}$$

(3.33)

Where M, K, f_{ext}, f_{ctrl} are the global mass matrix, the global stiffness matrix, the external force applied to the beam, the controlling force from the actuator, respectively.

By utilizing modal coordinates, the following modal transformation is introduced

$$q = T\eta$$

(3.34)

Where T is the modal transformation matrix.

33

By applying the modal transformation and multiplying by T^T on both sides and simplifying, we get

$$M^* \ddot{q}(t) + K^* q(t) = f^*_{ext} + f^*_{ctrl} \tag{3.35}$$

Where M^*, K^*, f^*_{ext}, f^*_{ctrl} are the modal form of the mass matrix, the modal form of the stiffness matrix, the generalized external force applied to the beam, the generalized controlling force from the actuator, respectively.

$$M^* = T^T M T \tag{3.36}$$

$$K^* = T^T K T \tag{3.37}$$

$$f^*_{ext} = T^T f_{ext} \tag{3.38}$$

$$f_{ctrl}^* = T^T f_{ctrl} \tag{3.39}$$

The modal form of the damping matrix is

$$C^* = \alpha M^* + \beta K^* \tag{3.40}$$

Where C^* is the proportional damping matrix (Rayleigh damping). α and β are the frictional damping constant and the structural damping constants.

The dynamic equation of the smart structure can be given as

$$M^* \ddot{\eta}(t) + C^* \dot{\eta}(t) + K^* \eta(t) = f^*_{ext} + f^*_{ctrl} \tag{3.41}$$

$$f^*_{ext} = T^T f r(t) \tag{3.42}$$

$$f^*_{ctrl} = T^T f_{ctrl} = T^T h V^a(t) = T^T h u^a(t) \tag{3.43}$$

Where $r(t)$, $u^a(t)$, f and h represent the external force input (impulse disturbance), the control input voltage to the actuator from the controller, external force coefficient vector and a constant vector depends on the actuator type and its location on the structure, respectively.

3.5   State Space Model

The governing equation in Eq. (3.41) is written in the state space form as

$$\eta = x \tag{3.44}$$

$$\dot{X} = Ax(t) + Bu(t) + E\,r(t) \tag{3.45}$$

$$
\begin{bmatrix} \dot{x}_1 \\ \dot{x}_1 \\ \cdot \\ \cdot \\ \cdot \\ \dot{x}_n \end{bmatrix}
= \begin{bmatrix} 0 & I \\ -M^{*-1}K^* & -M^{*-1}C^* \end{bmatrix}_{n\times n}
\begin{bmatrix} x_1 \\ x_1 \\ \cdot \\ \cdot \\ \cdot \\ x_n \end{bmatrix}
+ \begin{bmatrix} 0 \\ [M^{*-1}T^T h] \end{bmatrix}
\begin{Bmatrix} u_1(t) \\ u_2(t) \\ \cdot \\ \cdot \\ u_n(t) \end{Bmatrix}
$$

$$
+ \begin{bmatrix} 0 \\ [M^{*-1}T^T f] \end{bmatrix}
\begin{Bmatrix} r_1(t) \\ r(t) \\ \cdot \\ \cdot \\ r_n(t) \end{Bmatrix} \tag{3.46}
$$

$$y(t) = C\,x(t) + Du(t) \tag{3.47}$$

$$D = null\ Matrix$$

$$y(t) = [0\ 0\ \ P^T T] \begin{bmatrix} x_1 \\ x_1 \\ . \\ . \\ . \\ x_n \end{bmatrix} + D \begin{Bmatrix} u_1(t) \\ u_2(t) \\ . \\ . \\ u_n(t) \end{Bmatrix} \tag{3.48}$$

Where the size of h and P^T depend on the number of element.

$$h = E_P d_{31} b\bar{z}\,[-1\ \ 1\ \ ...\,] \tag{3.49}$$

$$P^T = G_c e_{31} bz\,[-1\ \ 1\ \ ...\,] \tag{3.50}$$

Where

$$z = \left(t_P + \frac{t_b}{2}\right)$$

$$\bar{z} = \left(\frac{t_b + t_P}{2}\right)$$

$A, B, C, D, x(t), u(t), y(t), r(t)$ represent the system (plant) matrix (n x n), the control or input matrix (n x p), the output matrix (q x n), the transmission matrix (q x p), the state vector, the control input, the system output and the external force input (impulse disturbance), respectively. $\bar{z}$ is the distance between the natural axis of the beam and the piezoelectric patches, G_c is device gain, and e_{31} is the piezoelectric stress / charge constant.

3.6   Validation

To obtain the vibration analysis and the dynamic properties of a wind turbine blade

model, two systems are studied; the first is a uniform cantilever beam and the other

system is a non-uniform (tapered) cantilever beam. The wind turbine blade model can be

considered as a tapered cantilever beam. A single piezoelectric actuator and sensor

bonded on the upper and lower surface, respectively. It is assumed that the piezoelectric

patches span the entire width of the structures. The mass and stiffness of the piezoelectric

patches are being neglected. In modeling of the smart structures, the mass and stiffness of

the adhesive used to bond the actuator / sensor pair to the master structure are being

neglected. The cable capacitance between the piezoelectric patches and the signal-

conditioning device is considered negligible and the temperature effects are neglected.

The Rayleigh-Ritz Method is used to obtain the natural frequencies (eigenvalues) and

mode shapes (eigenvectors) for the free vibration problems. The numerical results of the

simulation models are validated with known data in the literature, as follows:

- **Uniform Beam**

The first case in this study is a uniform cantilever beam. The length, width and thickness

of the uniform beam are 61.2775 cm, 2.54 cm, and 1.0583 mm, respectively, as shown in

Figure 3-2. The material properties that are used in the analysis are Al-alloy 6061 properties. Al-alloy 6061 has Young's Modulus (E) of 69 GPa and density (ρ) of 2705 kg/m^3. The damping constants (α and β) are 0.001 and 0.001, respectively. The dimensions and properties of the piezoelectric sensor / actuator used are given in Table 3-1. The natural frequencies of the uniform beam are given in Table 3-2.

Figure 3-2: Schematic of a uniform cantilever Beam

Table 3-1: Properties of piezoelectric sensor/actuator of uniform beam

Properties	Units	Sensor	Actuator
L (length)	cm	11.3	11.3
W (width)	cm	2.54	2.54
t (thickness)	mm	0.8	0.8
d_{31}(piezo strain constant)	m/V	-125×10^{-12}	-125×10^{-12}
g_{31}(voltage constant)	mV/N	-1.16×10^{-2}	-1.16×10^{-2}
K_{31}(coupling coefficient)	--------	0.35	0.35
e_{31}(piezo stress/charge constant)	C/m^2	-10.62	-10.62
E (Young's modulus)	GPa	63	63
ρ (density)	Kg/m^3	7600	7600

Table 3-2: Measured and predicted modal frequencies of a uniform cantilever beam neglecting effects of stiffness and mass of the piezoelectric patches

Mode	$\omega_n(Hz)$ Measured experimentally [17]	$\omega_n(Hz)$ Finite element analysis [17]	$\omega_n(Hz)$ Ritz [*Present work*]	% Difference
1	2.22	2.3	2.299	-3.55
2	13.64	14.42	14.410	-5.64
3	36.46	40.40	41.358	-13.43

- **Non-Uniform Beam**

The second case is a non-uniform (tapered) beam, as shown in Figure 3-3. The material properties that are used in the analysis are Al-alloy 6061 properties. Al-alloy 6061 has Young's Modulus (E) of 69 GPa and density (ρ) of 2705 kg/m^3. The damping constants (α and β) are 0.001 and 0.0001, respectively. The length and thickness of the non-uniform beam are 20 cm and 2 mm, respectively. The width of the non-uniform beam is increasing along the length and is equal to $b(x) = 0.02e^{4x}$. The dimensions and properties of the piezoelectric sensor / actuator used are given in Table 3-3. The natural frequencies of non-uniform beam are given in Table 3-4.
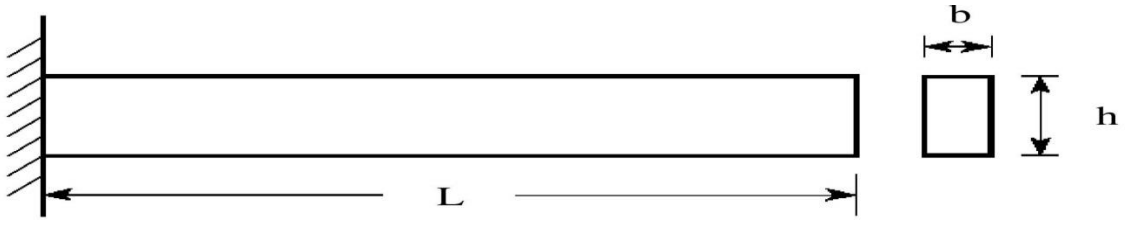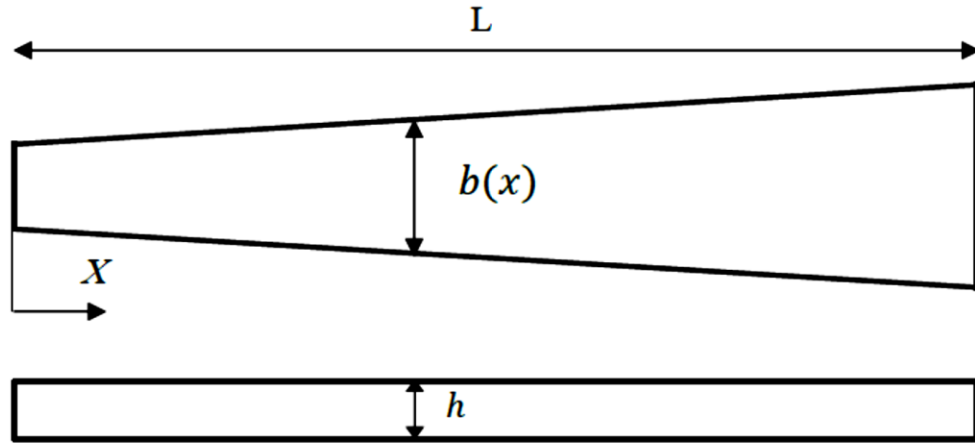
Figure 3-3: Top and side views of non-uniform (tapered) beam

Table 3-3: Properties of piezoelectric sensor/actuator of tapered beam

Properties	Units	Sensor	Actuator
L (length)	cm	5	5
W (width)	cm	2.54	2.54
t (thickness)	mm	0.8	0.8
d_{31} (piezo strain constant)	m/V	-125×10^{-12}	-125×10^{-12}
g_{31} (voltage constant)	mV/N	-1.16×10^{-2}	-1.16×10^{-2}
K_{31} (coupling coefficient)	--------	0.35	0.35
e_{31} (piezo stress/charge constant)	C/m^2	-10.62	-10.62
E (Young's modulus)	GPa	63	63
ρ (density)	Kg/m^3	7600	7600

Table 3-4: Measured and predicted modal frequencies of a non-uniform beam neglecting effects of stiffness and mass of the piezoelectric patches

Mode	$\omega_n(Hz)$ Analytical solution [18]	$\omega_n(Hz)$ Finite element method [18]	$\omega_n(Hz)$ Ritz [*Present Work*]	% Diff
1	31.42	32.11	31.744	-1.031
2	234.28	239.37	236.991	-1.157
3	695.44	706.42	712.202	-2.41

▪ **Wind Turbine Blade Model**

Wind turbine blade model can be idealized as a tapered cantilever beam. There are many types of airfoils but a few types that have been used in wind turbine blades such as NACA 0012, NACA 4415 and NACA 63(2)-215 [43]. The NACA 0012 is a 12 % thick symmetric airfoil, as shown in Figure 3-4 and Figure 3-5. The material properties that are used in the analysis are Al-alloy 6061 properties.
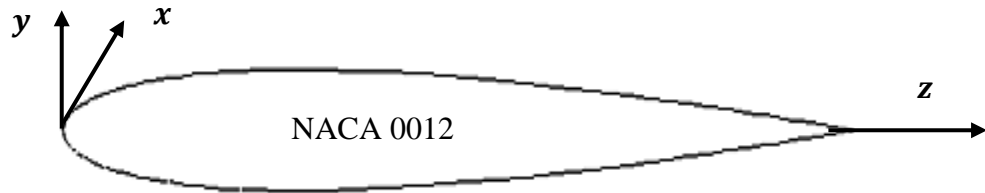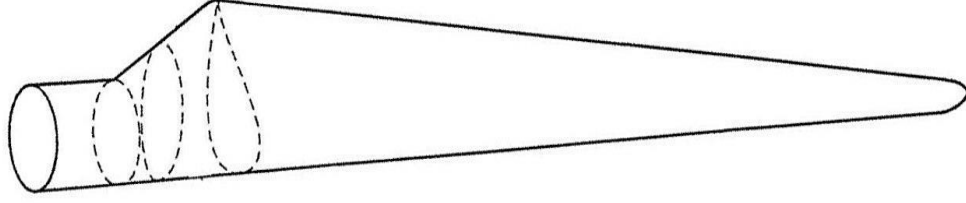

Figure 3-4: NACA 0012 airfoil

Figure 3-5: Wind Turbine Blade

In order to determine the area and the moment of inertia properties, the thickness distribution is required. Therefore, the Thickness distribution for a symmetrical 4-digit NACA airfoil [44]

$$y_t = \frac{Tc}{0.2}\left[a_1\sqrt{\frac{z}{c}} + a_2\frac{z}{c} + a_3\left(\frac{z}{c}\right)^2 + a_4\left(\frac{z}{c}\right)^3 + a_5\left(\frac{z}{c}\right)^4\right] \tag{3.51}$$

Where

$a_1 = 0.2969,\ a_2 = -0.126,\ a_3 = -0.3516,\ a_4 = 0.2843,\ a_5 = -0.1015$

Integrate equation (3.51) with respect to dz to calculate the area under the curve. Then double that to get the total cross sectional area.

The moment of inertia of the wind turbine blade is expressed as:

$$I = \int y_t{}^2 dA = \int_0^c \int_0^y y_t{}^2\, dy dz \tag{3.52}$$

Characteristic of wind turbine blade model and properties of piezoelectric sensor / actuator used are given in Table 3-5 and Table 3-6, respectively. The natural frequencies of wind turbine blade model for NACA 0012 are given in Table 3-7.

Table 3-5: Properties of wind turbine blade model

L (Length)$= 2\ m$	$\alpha = 0.001$ $\beta = 0.0001$
C_t(Tip chord)$= 0.1\ m$	C_r (Root chord)$= 0.25\ m$
ρ (Density) $= 2705\ kg/m^3$	E (Young's modulus) $= 69\ GPa$
T(Thickness to chord ratio) $= t/c = 0.12$ (for NACA 0012)	
$Chord\ = -0.075x + 0.25$	

Table 3-6: Properties of piezoelectric sensor/actuator of wind turbine blade model

Properties	Units	Sensor	Actuator
L (length)	cm	11.3	11.3
W (width)	cm	10.7	10.7
t (thickness)	mm	0.5	0.5
d_{31}(piezo strain constant)	m/V	-125×10^{-12}	-125×10^{-12}
g_{31}(voltage constant)	mV/N	-1.16×10^{-2}	-1.16×10^{-2}
K_{31}(coupling coefficient)	--------	0.35	0.35
e_{31}(piezo stress/charge constant)	C/m^2	-10.62	-10.62
E (Young's modulus)	GPa	63	63
ρ (density)	Kg/m^3	7600	7600

Table 3-7: Natural frequencies of a wind turbine blade model neglecting effects of stiffness and mass of the piezoelectric patches for NACA 0012

Mode	1	2	3
Natural Frequencies (Hz)	7.242	27.591	66.592

CHAPTER 4

CONTROLLER DESIGN

In this chapter, two controllers are discussed to study the performance of the piezoelectric active controller. The first is a Proportional-Derivative (PD) controller. The other controller is a Linear Quadratic Regulator (LQR) optimal control. The MATLAB code Simulink is used to implement the two types and study their effectiveness for vibration suppression.

4.1 Proportional-Integral-Derivative (PID) controller

Proportional-Integral-Derivative (PID) controller is considered the most common control algorithm in many applications due to its simplicity. In engineering applications, the controller appears in different cases: as stand-alone controller, as part of hierarchical, distributed control systems, or into embedded part [45].

The ideal form of PID controller is

$$u(t) = k_p e(t) + k_i \int_0^t e(\tau)d\tau + k_d \frac{de}{dt} \tag{4.1}$$

Where u represents the control input, e is the control error ($e = r - y$) where r and y represent the control reference and the output of the system, respectively, as shown in Figure 4-1.

k_p, k_i and k_d represent the proportional gain that is proportional to the error signal, the integral gain that is proportional to the total error (the integral of the error) and the derivative gain which provides corrections before the error becomes large (the derivative of the error), respectively. The advantages and disadvantages of PID gains are shown in Table. 4-1.

The proportional term acts on the present value of the error, the integral term is considered an average of the past errors and the derivative term represents a prediction of the future errors, as shown in Figure 4-2. The time response of the dynamic system is showed in Figure 4-3.
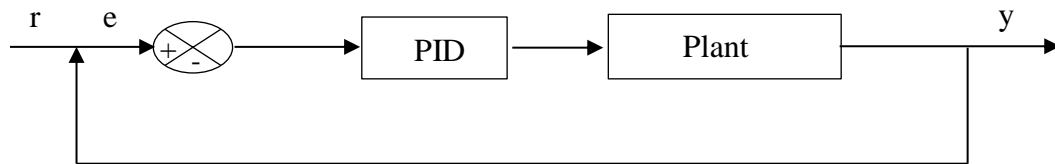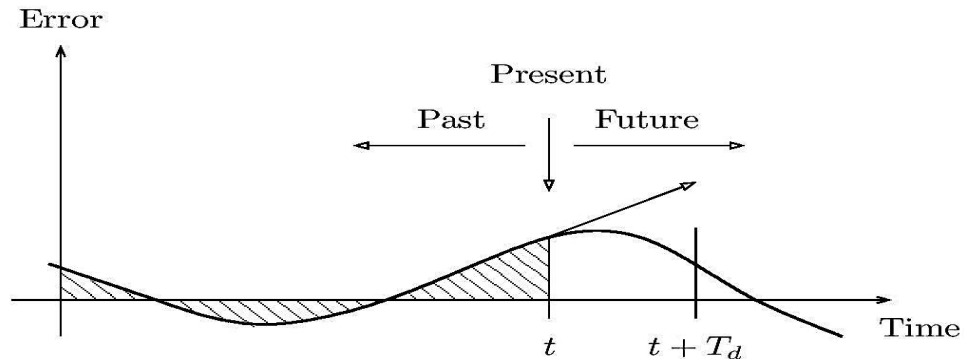

Figure 4-1: System with PID controller

Figure 4-2: A PID controller takes control action based on past, present and prediction of future control errors [45]

Table 4-1: The advantages and disadvantages of PID gains

| k_p	k_i	k_d
• Minimizes fluctuations. • Very simple. • Decreases the error with increasing the gain	• Proportional to both the magnitude and duration of the error (accumulated error)	• Provides large corrections before the error increases and becomes large
• Has steady-state errors • With increasing the gain, the oscillations increase.	• Integral windup • Makes the system less stable	• Noise problems
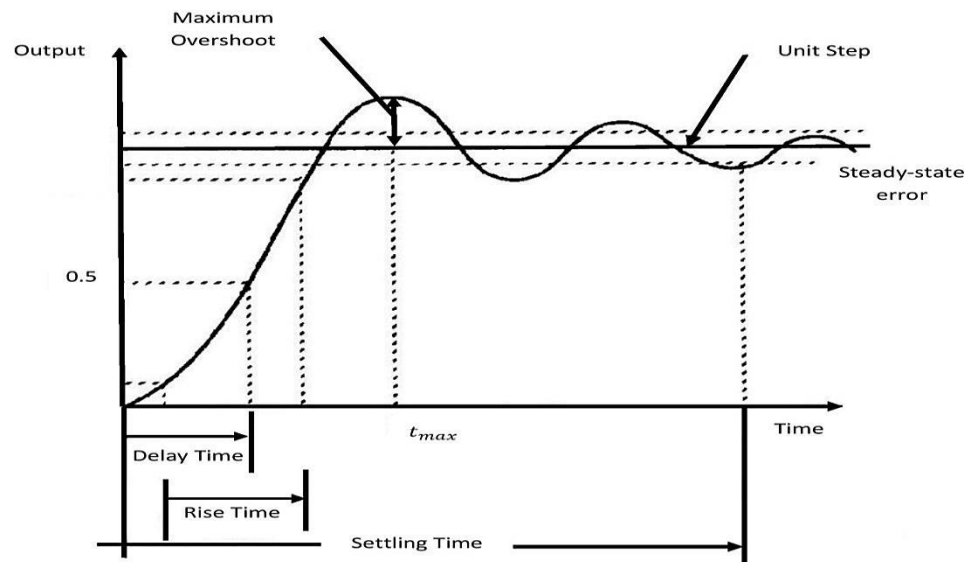
Figure 4-3: Time response of a system

Each of these gains – proportional, integral and derivative – has its advantages and disadvantages. So by combining all three gains into a single PID controller, the model of PID controller is expressed as

$$C(s) = k_p + \frac{k_i}{s} + k_d s \qquad (4.2)$$

This model is linear, however, there are some nonlinear effects that must be considered due to some limitations in the actuators, which called 'actuators saturation'. Due to the integral term, saturation increases to an effect called 'integral windup'. Integral windup is defined as the situation when the feedback controller exceeds the maximum actuator limits and becomes not able to respond to the changes in the control error. When this phenomenon occurs, the system runs with an open loop instead of feedback closed loop. To avoid this problem in this study, a Proportional-Derivative (PD) controller is used. The model of PD controller is expressed by

$$C(s) = k_p + k_d s \qquad (4.3)$$

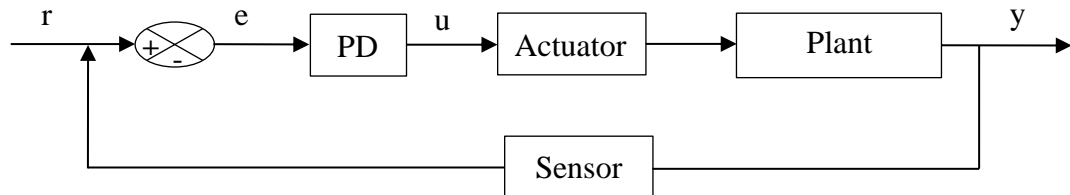The block diagram of system with PD controller is illustrated in Figure 4-4.

Figure 4-4: System with PD controller

4.2   Linear Quadratic Regulator (LQR)

In this section, the closed loop optimal control of a linear model is discussed. Let us consider a linear vibration system that is represented by a state space model:

$$\dot{x} = Ax(t) + Bu(t) + Er(t) \qquad (4.4)$$

By designing observer, all the states **x** are observed, and all the mode shapes are controllable. Then, the linear state control law becomes:

$$u(t) = -Gx(t)$$

Where G is the feedback gain to minimize the objective function (quadratic function) and $u(t)$ represents the control input.

The general form of a Linear Quadratic Regulator (LQR) index performance is:

$$J = \frac{1}{2} \int_{0}^{\infty} (x^T(t)Qx(t) + u^T(t)Ru(t))dt \qquad (4.5)$$

Where Q and R are weighted matrices.

Q is the $m \times m$ dimensional symmetric non-negative matrix, which is the weighting matrix of state variables x in the objective function J. For a more rapid vibration reduction and rapid response, a larger value of Q can be chosen.

R is the $n \times n$ dimensional symmetric positive matrix, which is the weighting matrix of input variables u in the objective function J. For a smaller energy consumption, a larger value of R can be selected.

According to LQR, the optimal controller gain that minimizes the objective function (performance index function) is expressed as:

$$G = R^{-1}B^T P \qquad (4.6)$$

Where P is the symmetric positive solution of algebra Riccati equation described by the following equations:

$$PA + A^T P + Q - PBR^{-1}B^T P = 0 \qquad (4.7)$$

Obviously, feedback gain G affects the pole placement and the time response performance index of the system. The optimal state feedback gain G depends mainly on the weighting matrices Q and R. There are many techniques for obtaining Q and R: neural network, genetic algorithm, evolutionary computation or may be by trial and error [24, 34, 38, 46 and 47].

Many researchers focus on Linear Quadratic Regulator (LQR) due to its infinitely amplitude margin and phase margin that is larger than sixty degree [46], ensures stable operation in a closed loop system, insensitive to small parameter changes [33] and its control efficiency. However, there are some limitations, as follows: the solution of Riccati equation, the need to measure all the state variables and the level of stability that is achieved cannot be directly determined [6]. The state feedback controller and the observer are illustrated in Figure 4-5.
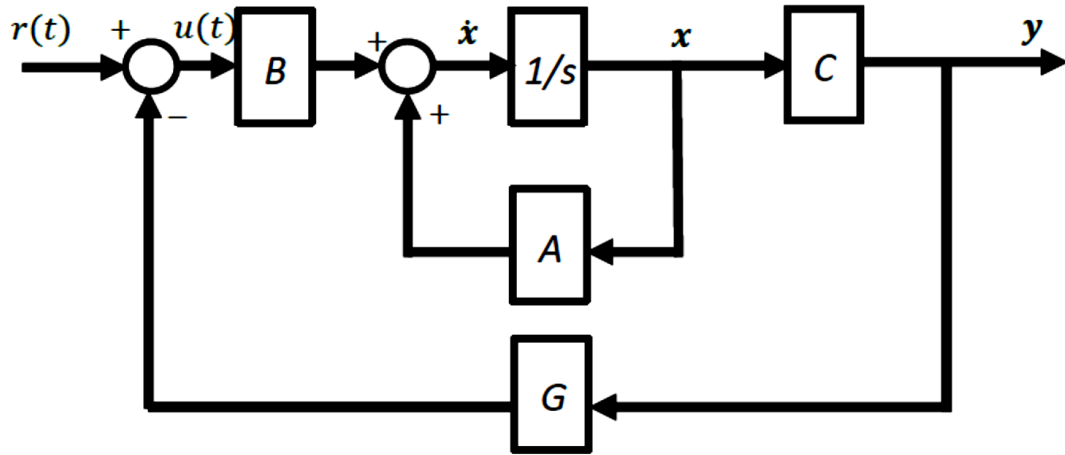
Figure 4-5: A system with LQR controller

4.2.1 Observability and Controllability

Controllability and observability of the state space dynamic system are studied to prove whether the system is controllable and observable. Controllability deals with whether the states of the dynamic model are influenced by the control input. A structure is controllable if the integrated actuators excite all the mode shapes of smart structures [1].

The state space dynamic system is illustrated by

$$\dot{x} = Ax + bu$$

$$y = cx + Dy$$

The controllability matrix U is expressed by

$$U = [B, AB, A^2B, \ldots, A^{n-1}B] \tag{4.8}$$

The system becomes controllable if the rank of the matrix U equals to the number of states or the order of the system.

Observability is concerned with whether the states of the system can be identified from the output of the system.

The observable matrix V is defined as

$$V = [C^T, A^T C^T, \ldots, (A^T)^{n-1} C^T] \tag{4.9}$$

The system becomes observable if the rank of the matrix V equals to the number of states or the order of the system.

4.2.2 State Observer

In the preceding section, Linear Quadratic Regulator (LQR) needs to estimate all the state variables for obtaining the control input u. In some systems, the state variables cannot be obtained directly due to the complexity of the systems or the high cost of the sensing devices or transducers, so a device must be designed to estimate the state variables, this device called state observer. The design of a state observer can be divided into two parts. The first is the original model where u and y represent the input and the output of the system, respectively, with the knowledge of A, B, C, and D. the other part is a duplicate of the original system as:

$$\dot{\bar{x}} = A\bar{x}(t) + Bu(t) \tag{4.10}$$

The output of the original part $y(t) = cx(t)$ is compared with the output of the duplicating part $\bar{y}(t) = c\bar{x}(t)$. The difference between the two outputs is passing through a constant gain vector l which is used to reduce the error and as a correction term, as shown in Figure 4-6.
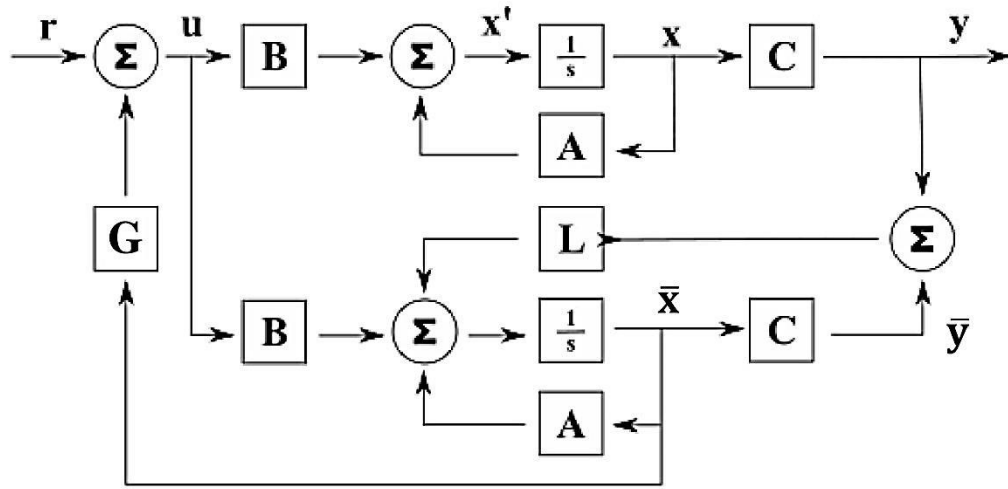

Figure 4-6: Closed loop state observer

The dynamic behavior of the observer can be expressed as:

$$\dot{\bar{x}}(t) = (A - LC)\bar{x} + Bu + ly \qquad (4.11)$$

Let us define the error between the actual and duplicated state.

$$e(t) = x(t) - \bar{x}(t) \qquad (4.12)$$

The equation that governs the estimation of the error can be expressed by

$$\dot{e}(t) = (A - LC)e(t) \qquad (4.13)$$

53

The eigenvalues of the observer have to be faster than the eigenvalues of the system being controlled which mean the eigenvalues of the estimator should be slightly more negative than the eigenvalues of the system [48–49].

CHAPTER 5

RESULTS AND DISCUSSION

The purpose of this study is reducing the vibrational level of a wind turbine blade model. Therefore, in order to study active vibration control of a clamped wind turbine blade model, two cases are discussed and tested: a uniform cantilever beam, a non-uniform (tapered) cantilever beam. These models do not consider the shear effects because shear deformation is insignificant in comparison with bending deformation. The effects of rotary inertia are neglected because with including the effects of rotary inertia, the dynamic stiffening of the structure increases which is undesirable. They have undesirable effects in case of unbalanced system. A single piezoelectric actuator and sensor are bonded on the upper and lower surface, respectively, as shown in Figure 5-1. It is assumed that the piezoelectric patches span the entire width of the systems. Rayleigh-Ritz method and assumed modes method are used to obtain the natural frequencies (eigenvalues), the mode shapes (eigenvectors) and the generalized force term. The damping matrix is assumed to be obtained by a linear combination of the stiffness and the mass matrices (Proportional damping). There are two inputs effect on the master structures; the first is the external force input f_{ext} (impulse disturbance), and the other input is the control input u to the actuator from the controller. The entire structures are modeled in the state space form by using the state space method, modal coordinates and piezoelectric theory. In this study, two types of controllers are designed to study the

performance of the piezoelectric active controller. The first is a Proportional-Derivative (PD) controller and the second is a Linear Quadratic Regulator (LQR). All cases are considered to have two degree of freedom (DOF) at each nodal point; modal displacement and modal velocity. The modal displacement is measured at a single point on the structure.
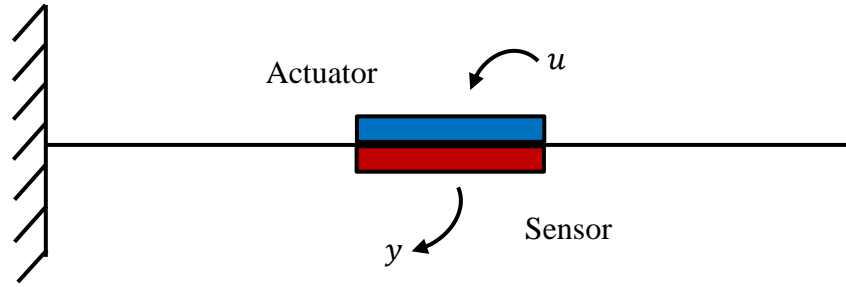

Figure 5-1: Smart system consisting of clamped structure, piezoelectric sensor and actuator

5.1   System Response

After the dynamic equation of smart structure is determined, the state space model is obtained by utilizing the state space form, modal coordinates and piezoelectric theory. The signal conditioning device gain G_c which is used to convert the current into the open circuit sensor voltage V^s is assumed to be 100. The root locus, bode plot, poles, step and impulse response of open loop smart system are illustrated for each case, as follows:

- **Uniform Beam**

The poles (eigenvalues) of smart uniform beam are:

$\lambda_{1,2} = -10.229 \mp 142.6621i$ and $\lambda_{3,4} = -0.1058 \mp 14.5163i$

The system is stable because all the poles are lying in the left half portion of the imaginary (complex plane) axis. Figure 5-2 to Figure 5-4, show the root locus, bode plot and sensor output (voltage) of step and impulse input for the open loop smart system, respectively. In case of step input, the peak amplitude is 0.000028 V and the settling time is 33.3 sec whereas for impulse input, the peak amplitude is 0.000671 V and the settling time is 23.7 sec:
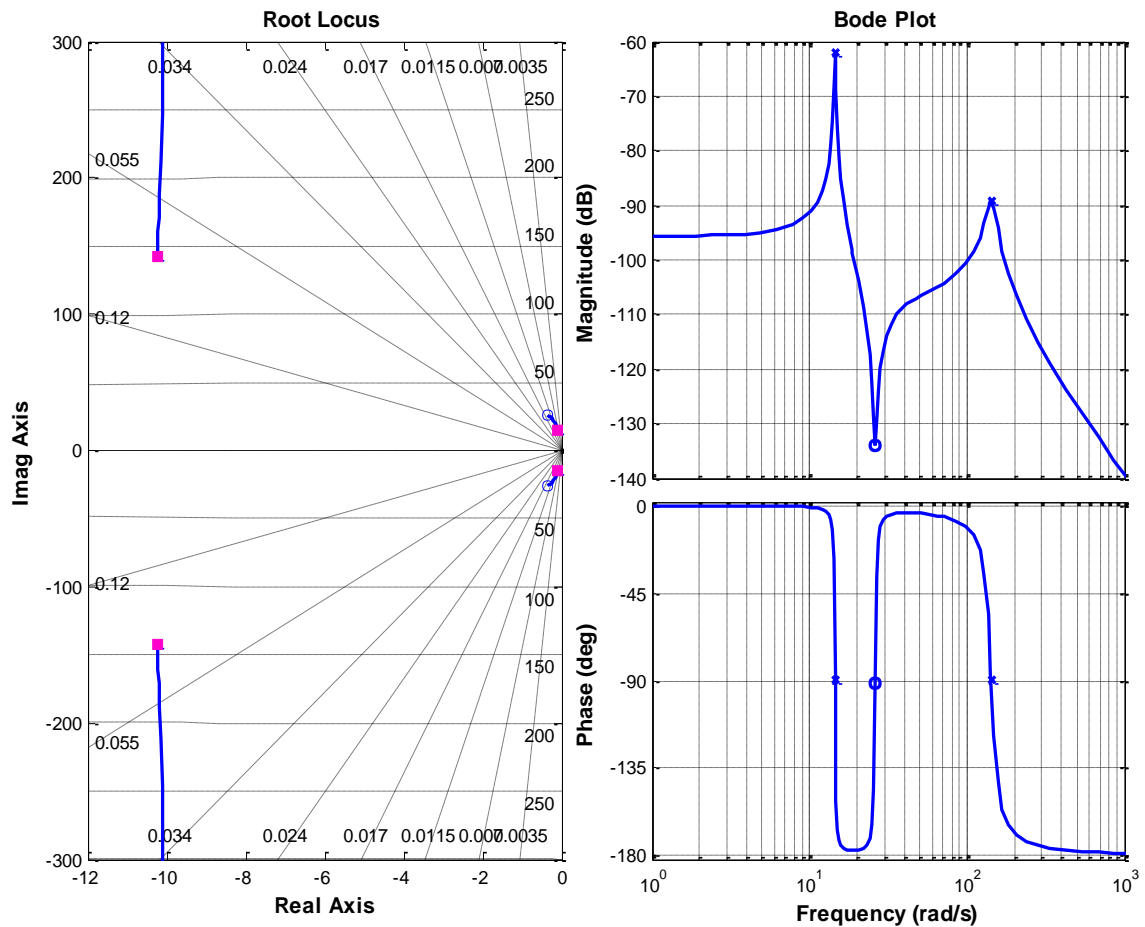

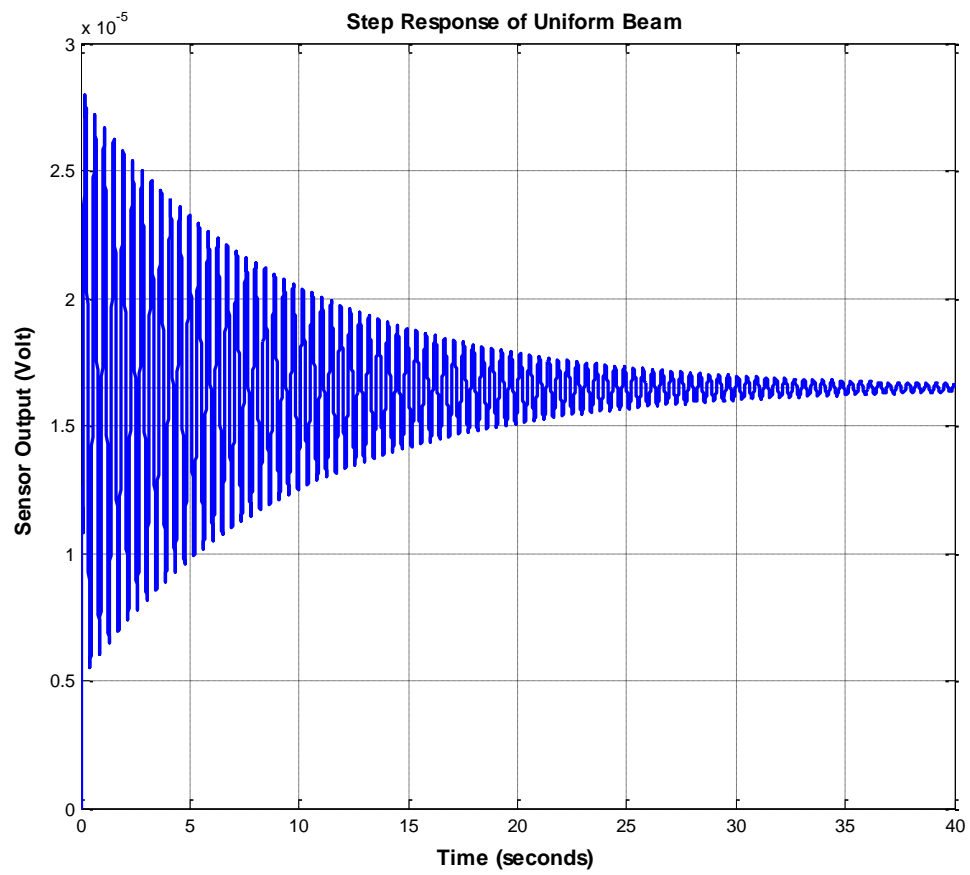**Figure 5-2: The root locus and bode plot of uniform beam**

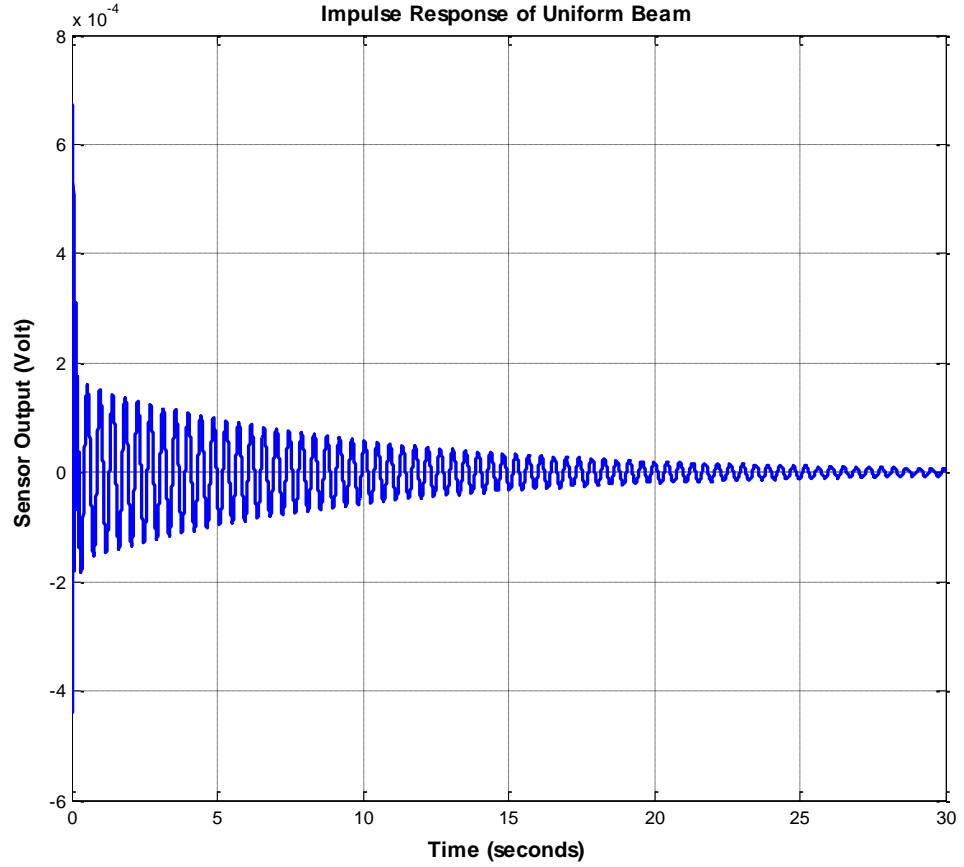**Figure 5-3: Step response of uniform beam**

Figure 5-4: Impulse response of uniform beam

▪ **Non-Uniform (Tapered) Beam**

The poles of smart non-uniform (tapered) beam are:

$\lambda_{1,2} = -348.9789 \mp 2618.7368i$ and $\lambda_{3,4} = -2.0718 \mp 203.5258i$

The system is stable because all the poles are lying in the left half portion of the imaginary axis. Figure 5-5 to Figure 5-7, show the root locus, bode plot and sensor output of step and impulse input for the open loop system, respectively. In case of step input, the

peak amplitude is 0.302×10^{-6} V and the settling time is 1.76 sec whereas for impulse input, the peak amplitude is 0.084×10^{-3} V and settling time is 1.34 sec.
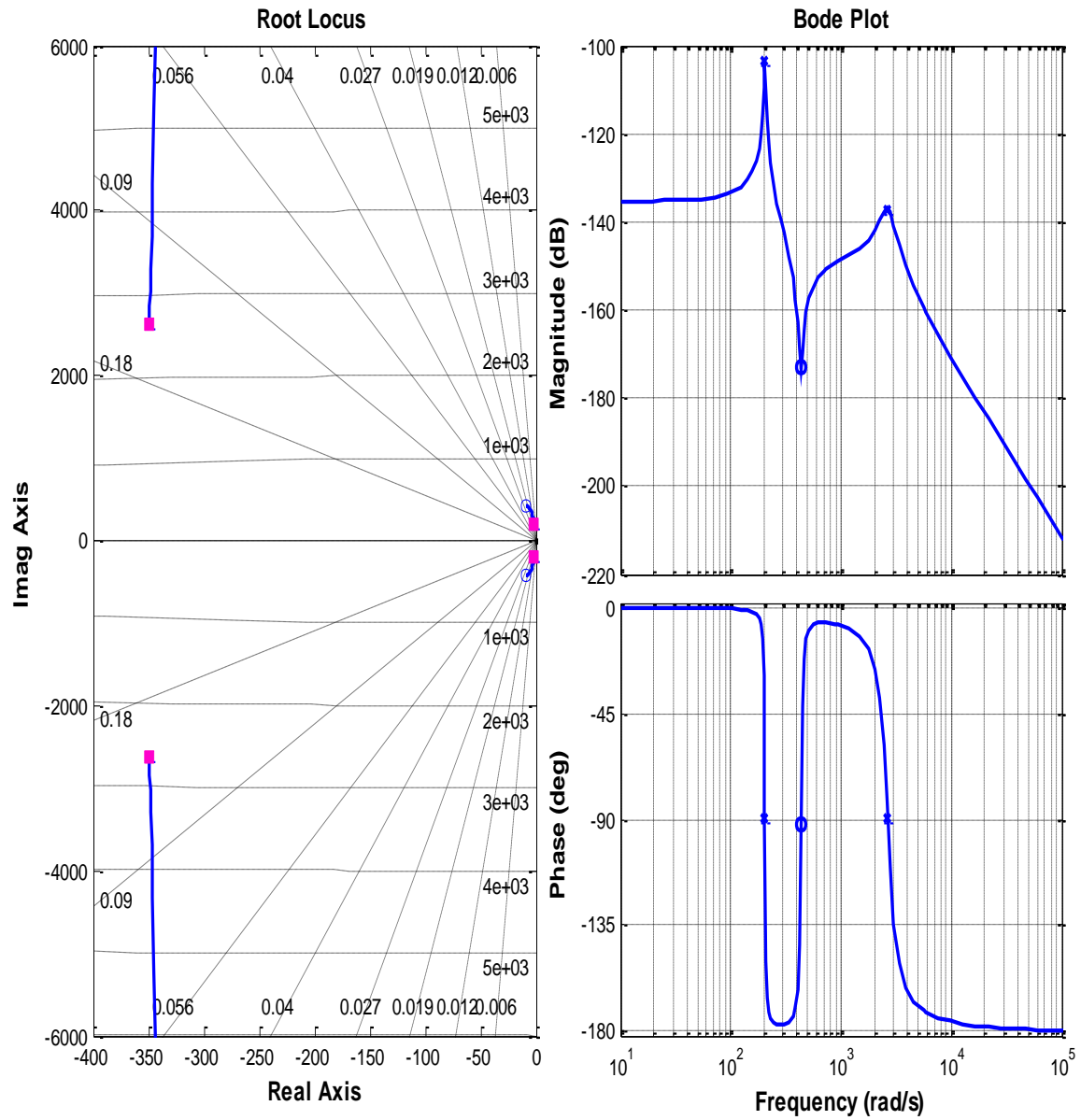

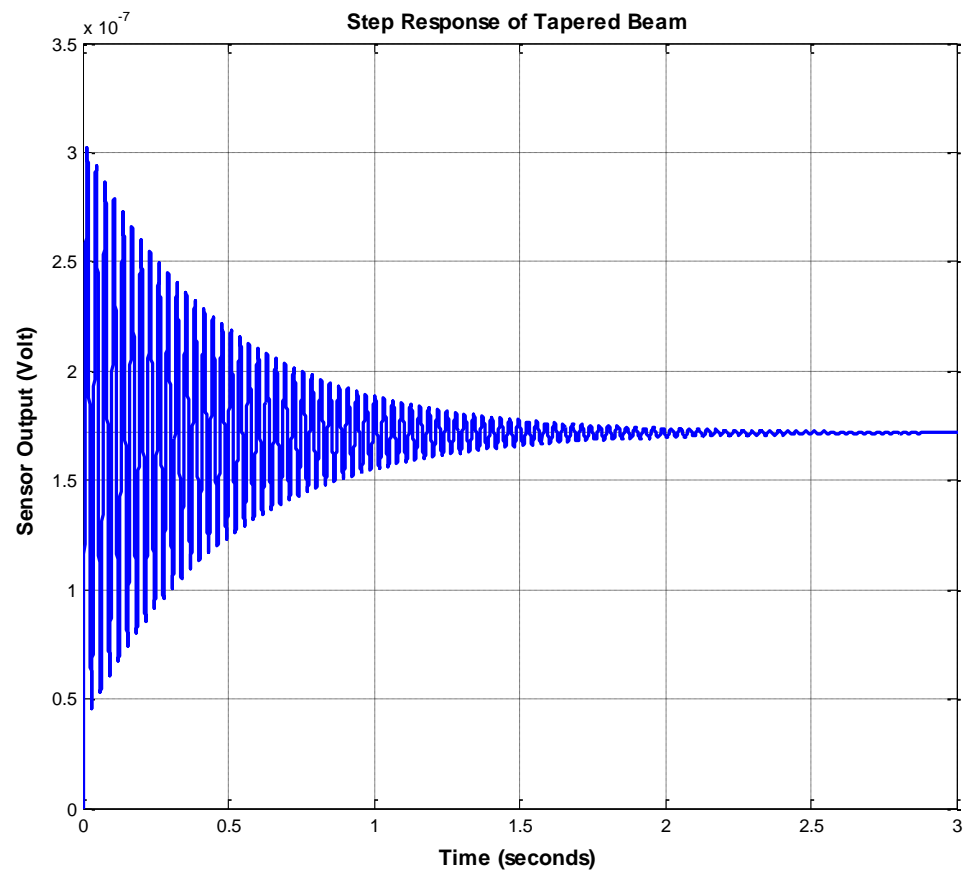**Figure 5-5: The root locus and bode plot of non-uniform beam**

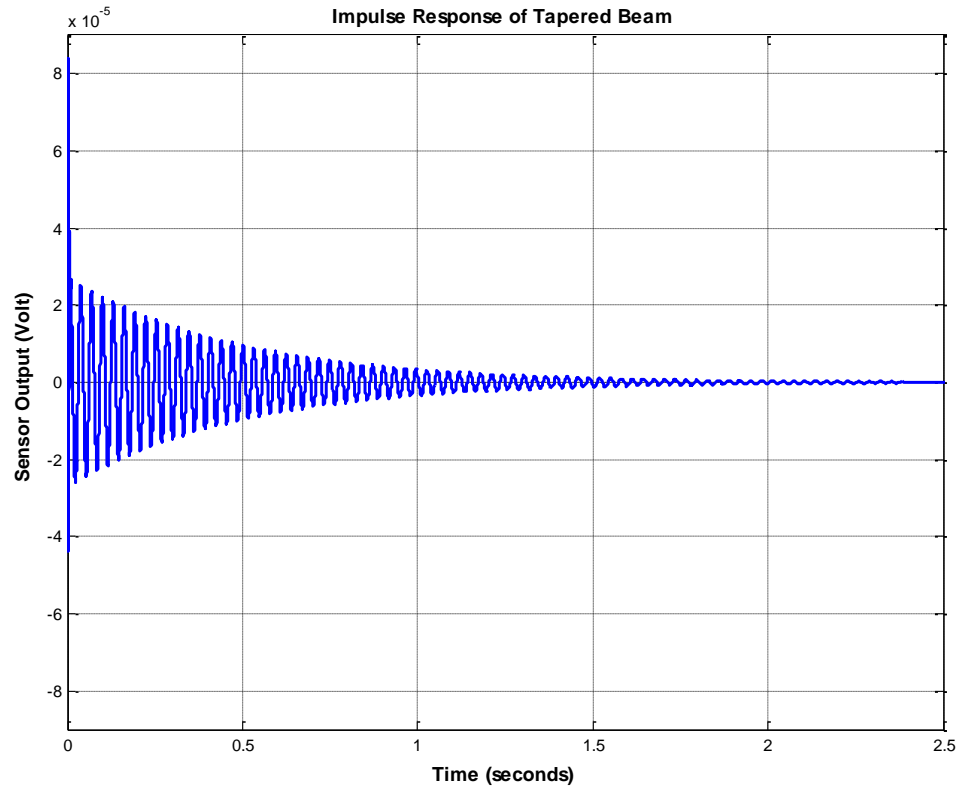**Figure 5-6: Step response of non-uniform beam**

Figure 5-7: Impulse response of non-uniform beam

- **Wind Turbine Blade**

For wind turbine blade model, The poles of smart wind turbine blade model (NACA 0012) are:

$\lambda_{1,2} = -1.7266 \mp 185.7965i$ and $\lambda_{3,4} = -0.1062 \mp 45.985i$

The system is stable because all the poles are lying in the left half portion of the imaginary (S-plane) axis. Figure 5-8 to Figure 5-10, show the root locus, bode plot and sensor output of step and impulse input for the open loop system, respectively. For case

of step input, the peak amplitude is 5.22×10^{-5} V and the settling time is 17.6 sec but

for impulse input, the peak amplitude is 0.00451 V and settling time is 5.71 sec.
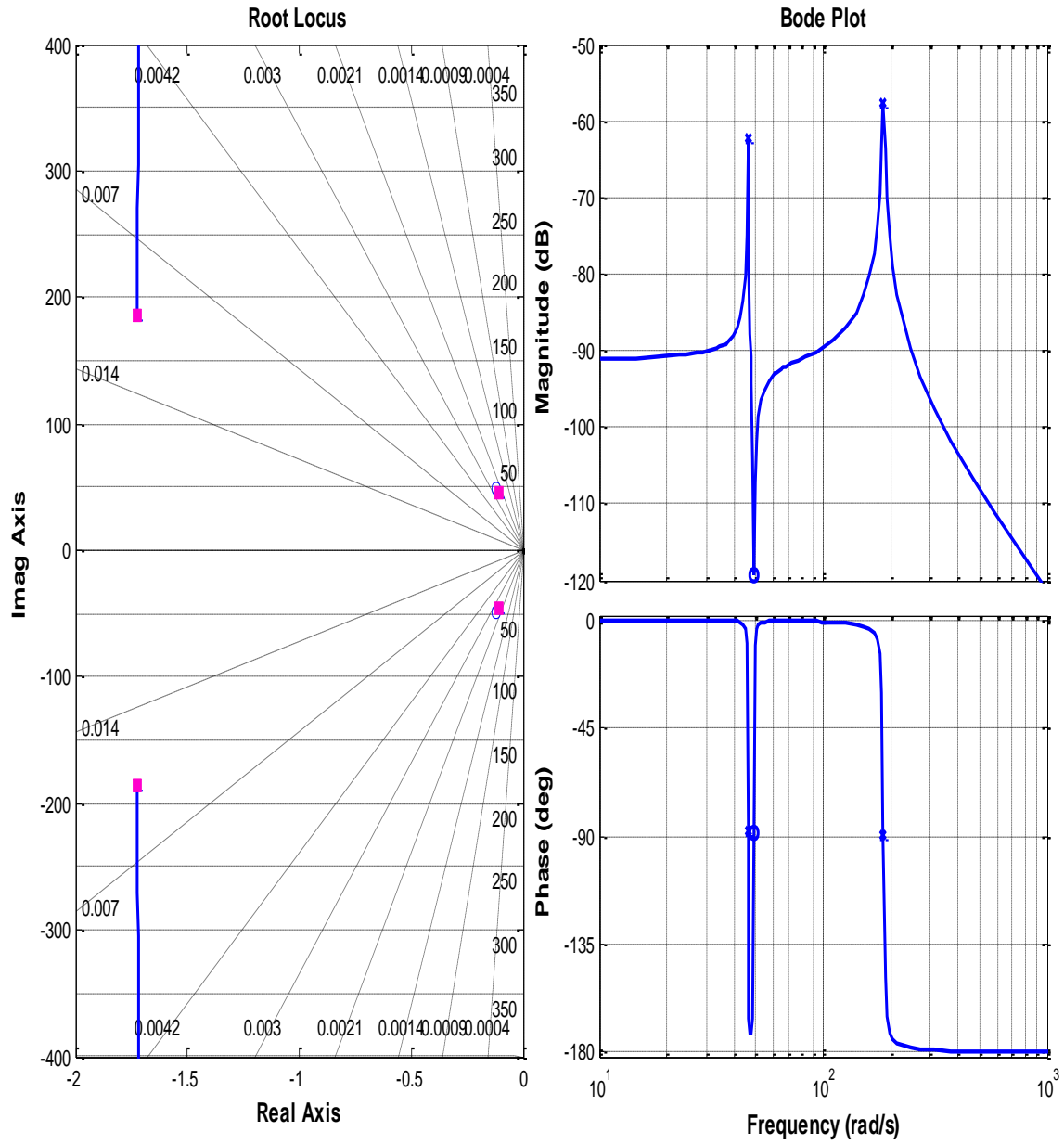

Figure 5-8: The root locus and bode plot of wind turbine blade model
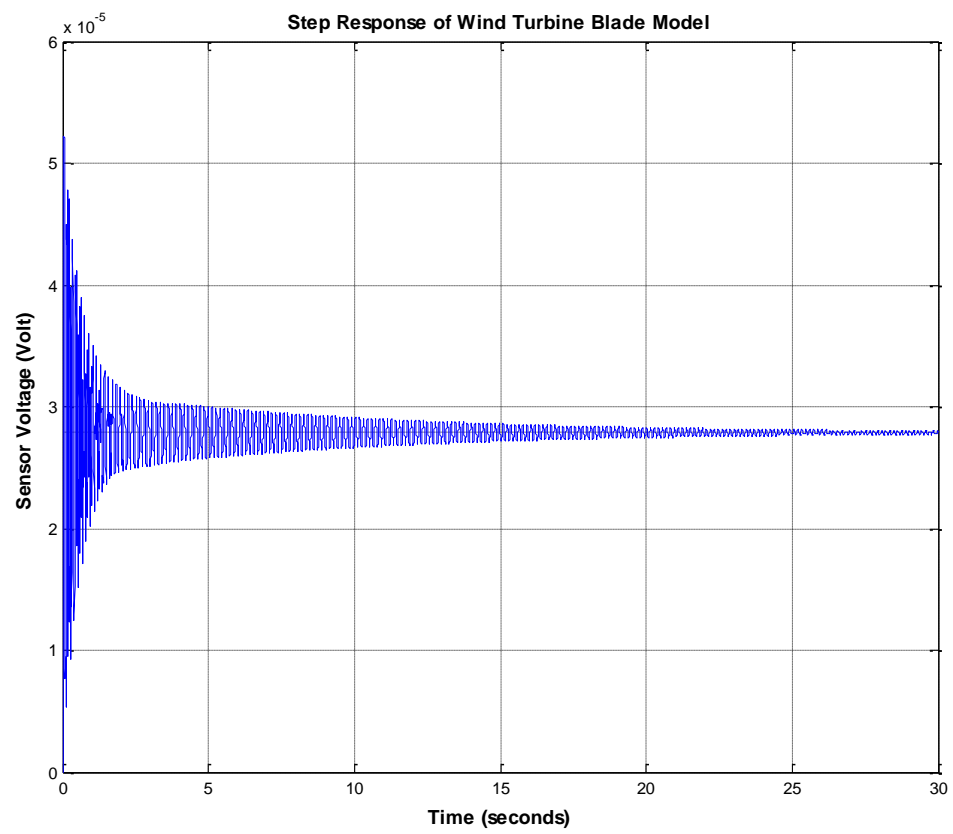
Figure 5-9: Step response of wind turbine blade model
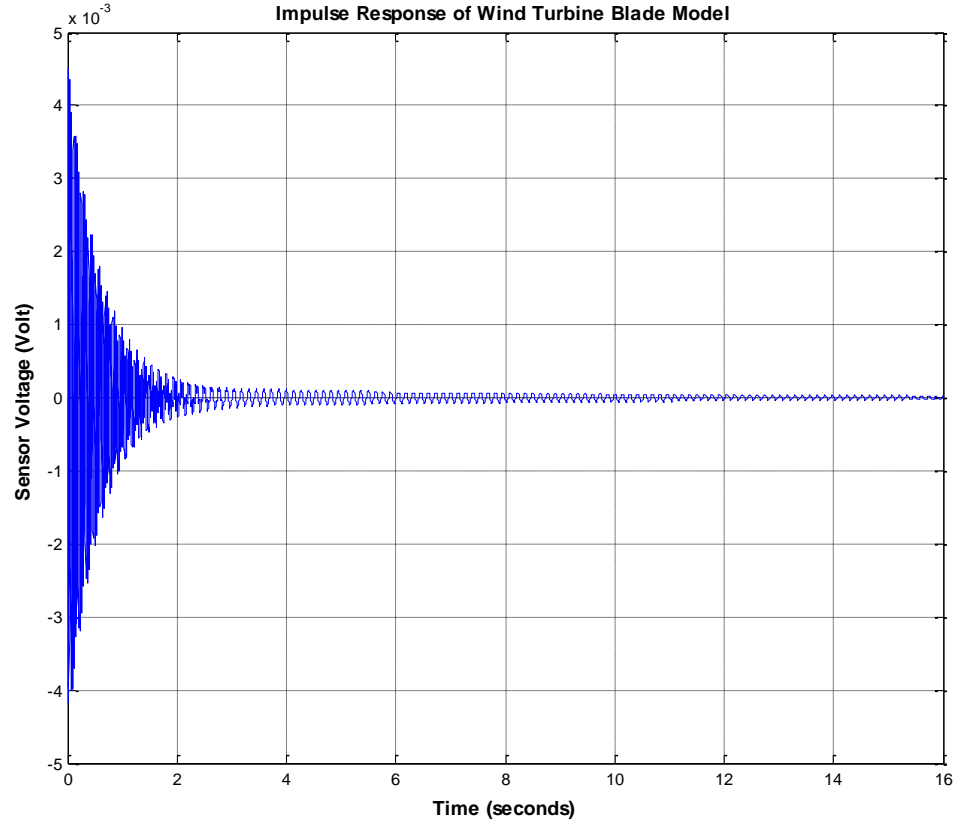
Figure 5-10: Impulse response of wind turbine blade model

5.2   Vibration Suppression using PD and LQR

An external aerodynamic force is applied to the smart structures. The shape of the distributed load is assumed to be cosine distribution. The external force (impulse disturbance $r(t)$) is 10 N for duration of 40 ms for all cases. The distributed load is expressed as $[cos(\pi x/2L)]$ for all cases. The MATLAB code Simulink is used to simulate the smart systems and their responses without and with controller, as shown in Figure 5-11:

Figure 5-11: Simulink block diagram of closed loop system with external force

Where the system (plant) block is shown in Figure 5-12:
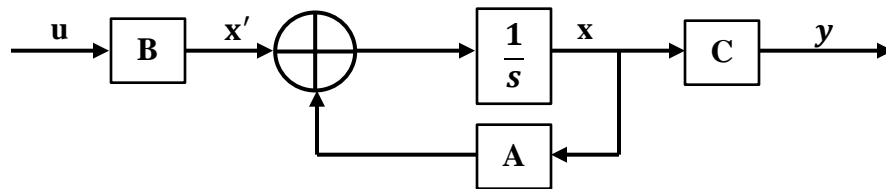
Figure 5-12: Simulink block diagram of open loop system

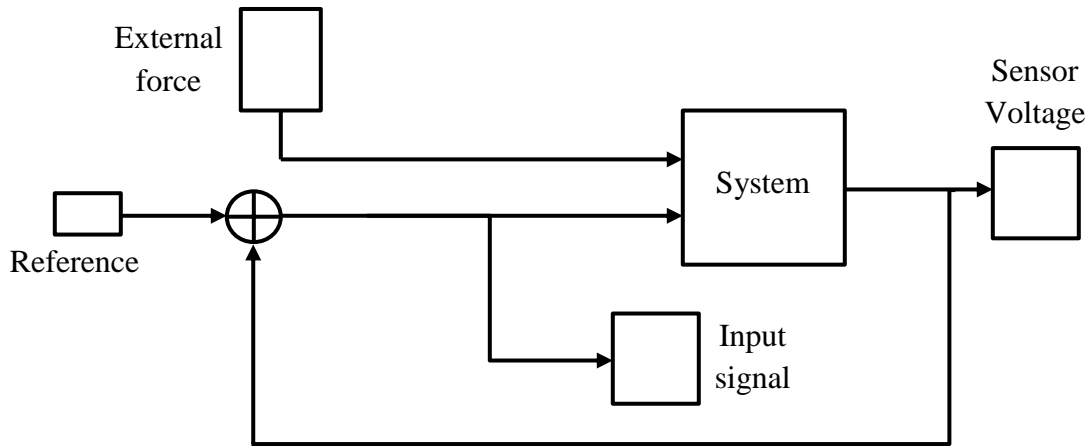A Proportional-Derivative (PD) controller is added to the smart systems to reduce the vibrational level, as shown in Figure 5-13. The optimal values of proportional and derivative gains (K_P and K_d) are obtained by trial and error technique. The criteria that are used to obtain the proportional and derivative gains are minimizing the settling time, the control input does not exceed ± 90 V because the maximum voltage that could be applied to the piezoelectric actuator is ± 90 V and the overshoot percentage does not exceed 71%. A filter (N) is added when PD controller is used. The benefits of the filter are reducing the noise and higher frequency modal vibration. If the noise and the higher

frequency modal vibration are amplified due to the derivative action, the system becomes unstable.
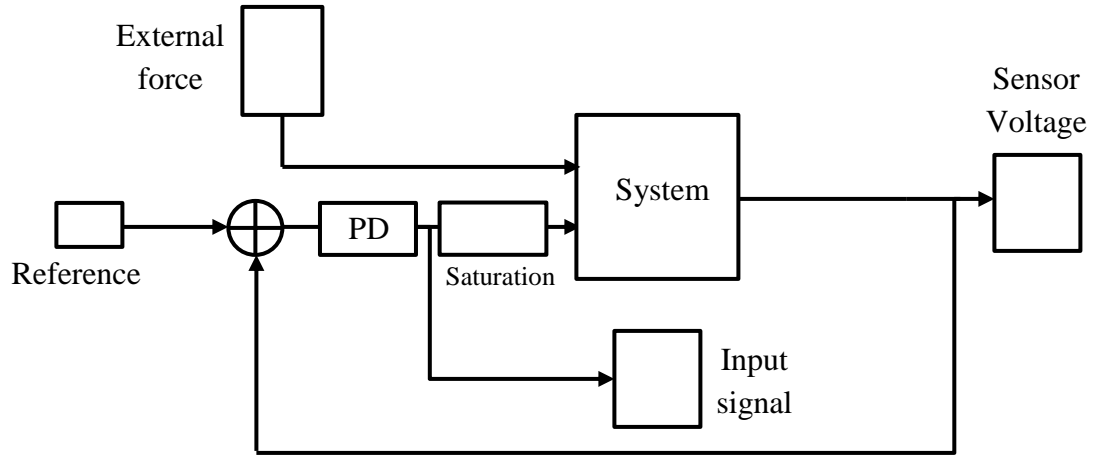
Figure 5-13: Simulink block diagram of closed loop system with PD controller

The other controller is A Linear Quadratic Regulator (LQR) which is added to the smart systems to suppress the vibrational level. The weighting matrices Q and R are considered very important parameters for designing optimal control. The optimal values of Q and R are obtained by trial and error technique. The criteria that are used for obtaining the weighting matrices are minimizing the settling time and the control input does not exceed ± 90 V because the maximum voltage that could be applied to the piezoelectric actuator is ± 90 V. The closed loop system with adding LQR controller is illustrated in Figure 5-14.
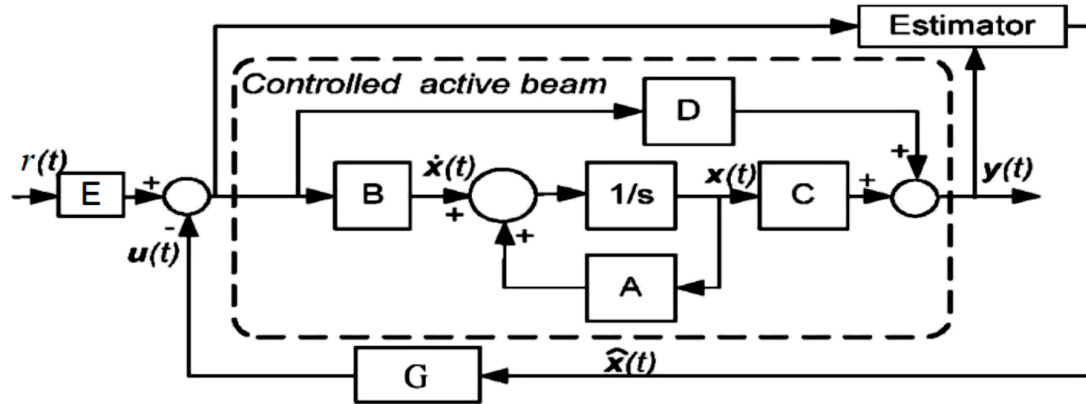
Figure 5-14: Simulink block diagram of closed loop system with adding LQR controller [33]

The following sections show the utilization of PD and LQR controller to suppress the vibration response of the first vibration mode of the uniform beam, the tapered beam, and the suggested wind turbine blade model, respectively, as follows:

5.2.1   Uniform Beam

The response of the closed loop smart uniform cantilever beam with adding the external force (disturbance) and without adding any type of controller is shown in Figure 5-15:
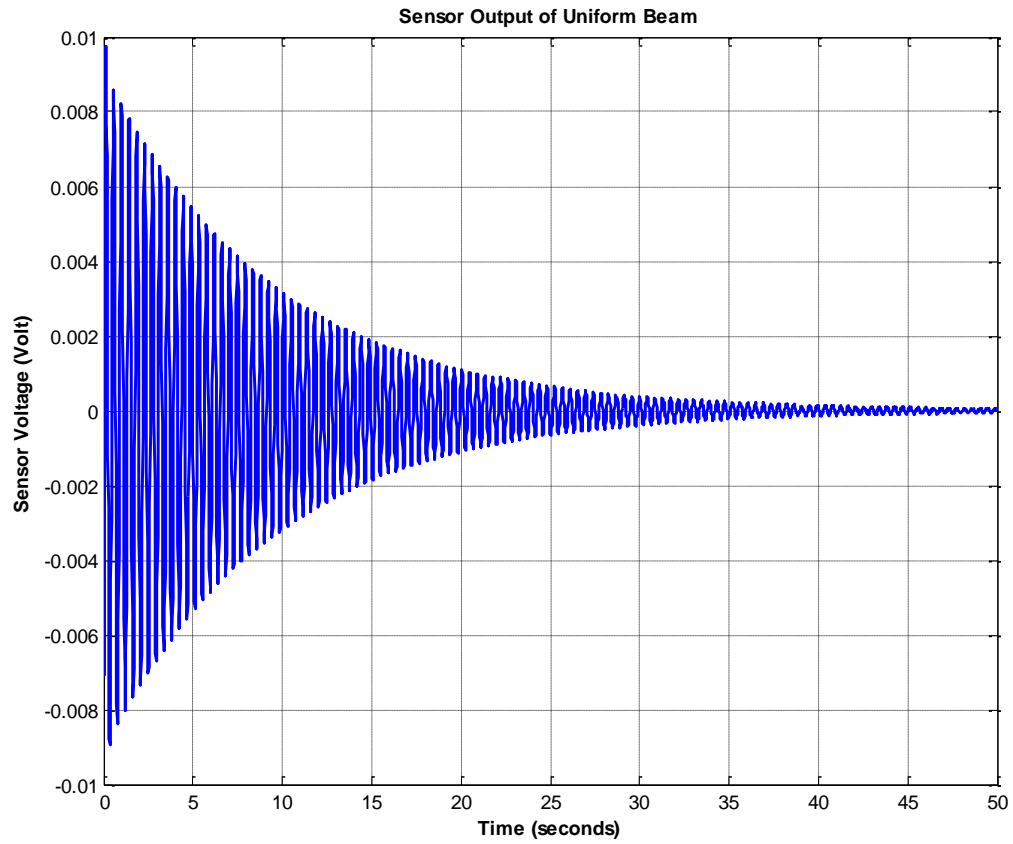
Figure 5-15: Closed loop sensor voltage of uniform beam without controller

▪ **PD controller results**

For the smart cantilever uniform beam, the proportional and derivative gains are taken as:

$(K_P = 8000, \ K_d = 119$ and N=2000). The response of the system with adding PD controller and the actuation force (input signal) are illustrated in Figure 5-16 and Figure 5-17:

69

Figure 5-16: Closed loop sensor voltage of uniform beam with PD controller

Figure 5-17: The actuation force of uniform beam with PD controller

▪ **LQR controller results**

The controllability and observability of the state space model are examined to prove whether the system is controllable and observable. The rank of the observability matrix and the controllability matrix are the same as the order of the system (equal 4), so the system is controllable and observable. The weighting matrices (Q and R) are taken as: ($Q = 2.1$, $R = 0.1$). The response of the system with adding LQR and the actuation force (input signal) are illustrated in Figure 5-18 to Figure 5-19:
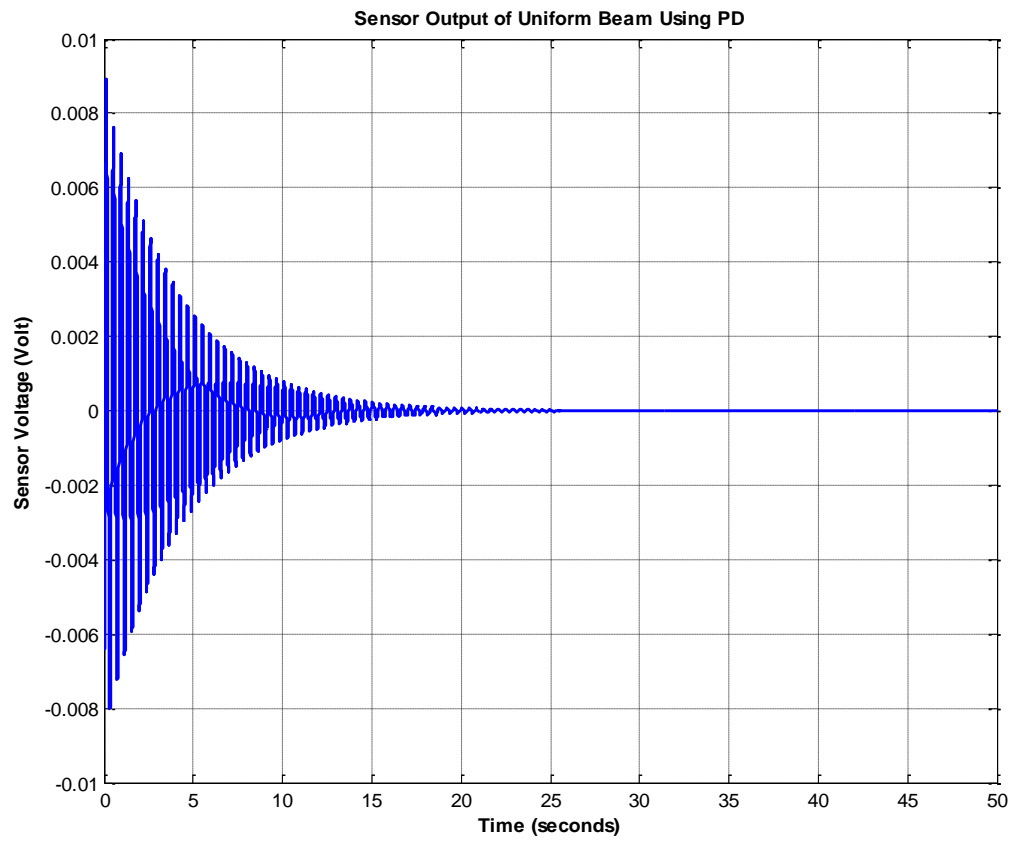
Figure 5-18: Closed loop sensor voltage of uniform beam with LQR controller
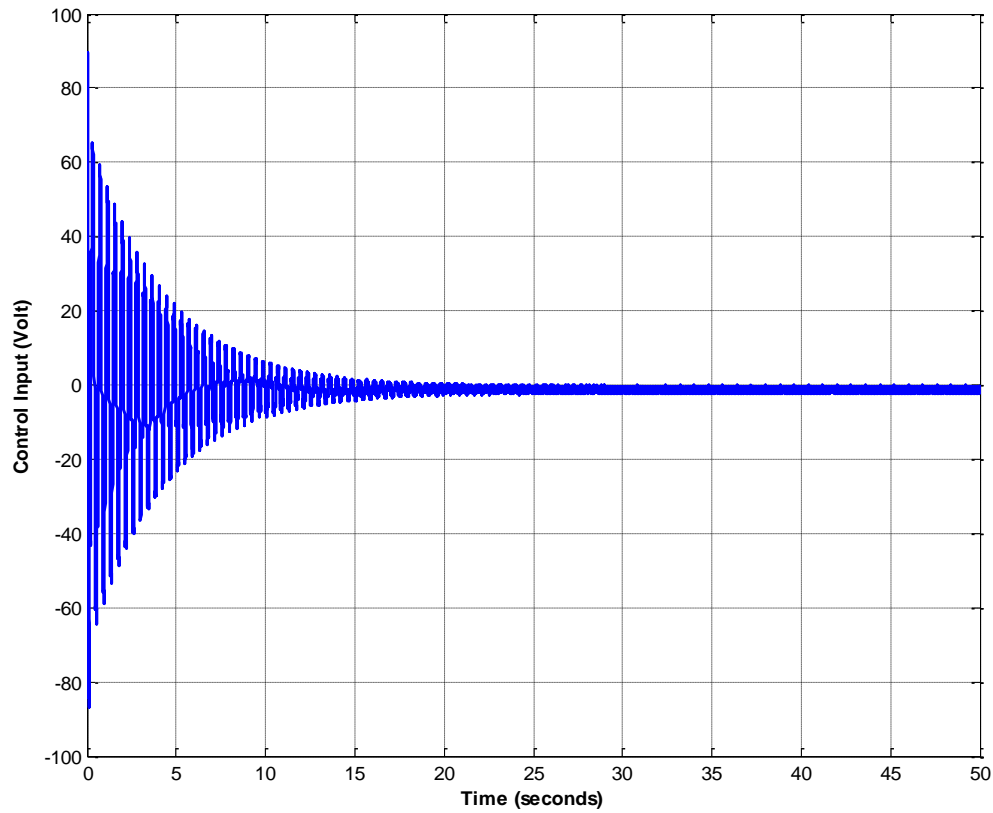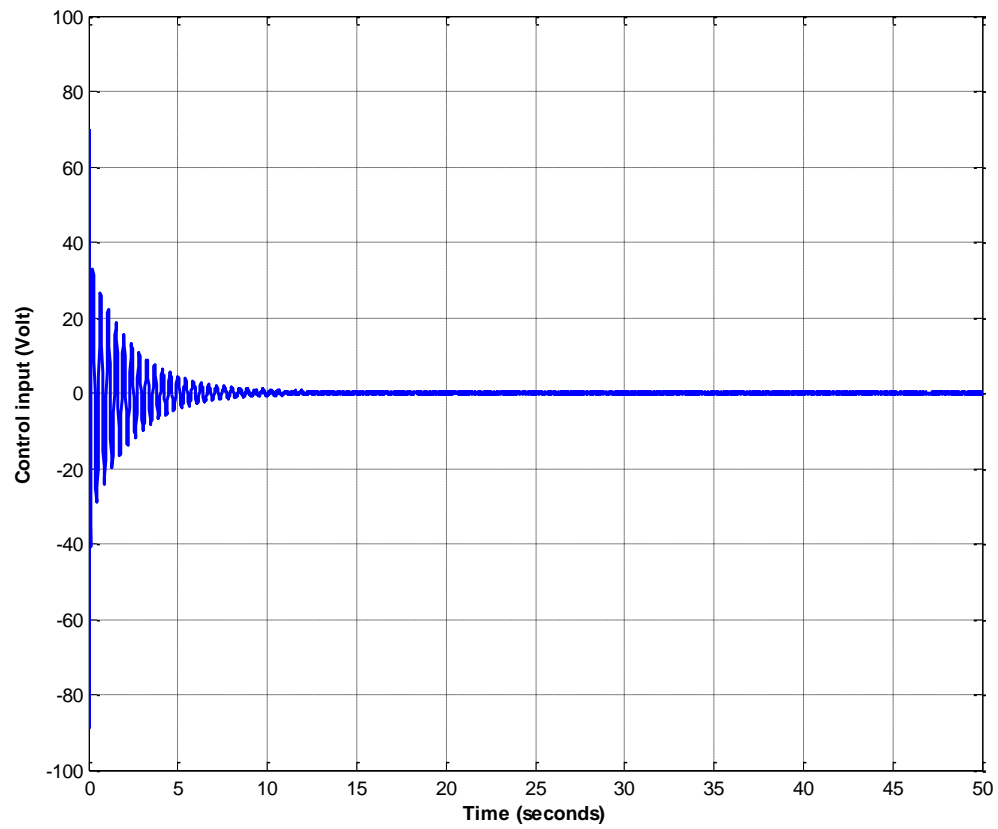
Figure 5-19: The actuation force of uniform beam with LQR controller

The sensor output of smart uniform cantilever beam without controller, with PD controller and with adding LQR controller is shown in Figure 5-20.

Figure 5-20: Comparison of sensor output of uniform cantilever beam without and with controller

The results revealed that the peak amplitude without adding controller is (-0.0089 V and +0.0097 V). The peak amplitude with adding PD is (-0.008 V and +0.0089 V) whereas the peak amplitude with adding LQR is (-0.008 V and +0.0091 V).

The maximum actuation force by adding PD controller is (-86.9 V and 89.7 V) whereas the maximum actuation force by adding LQR controller is (-88.82 V and 69.57 V).

At bandwidth 0.02%, the settling time without adding any type of controller is 36.927 sec whereas the settling time with adding PD and LQR controller are 15.698 and 9.007 sec, respectively.

5.2.2 Non-Uniform Beam

The response of the closed loop smart tapered cantilever beam with adding the external force (disturbance) and without adding any type of controller is shown in Figure 5-21:
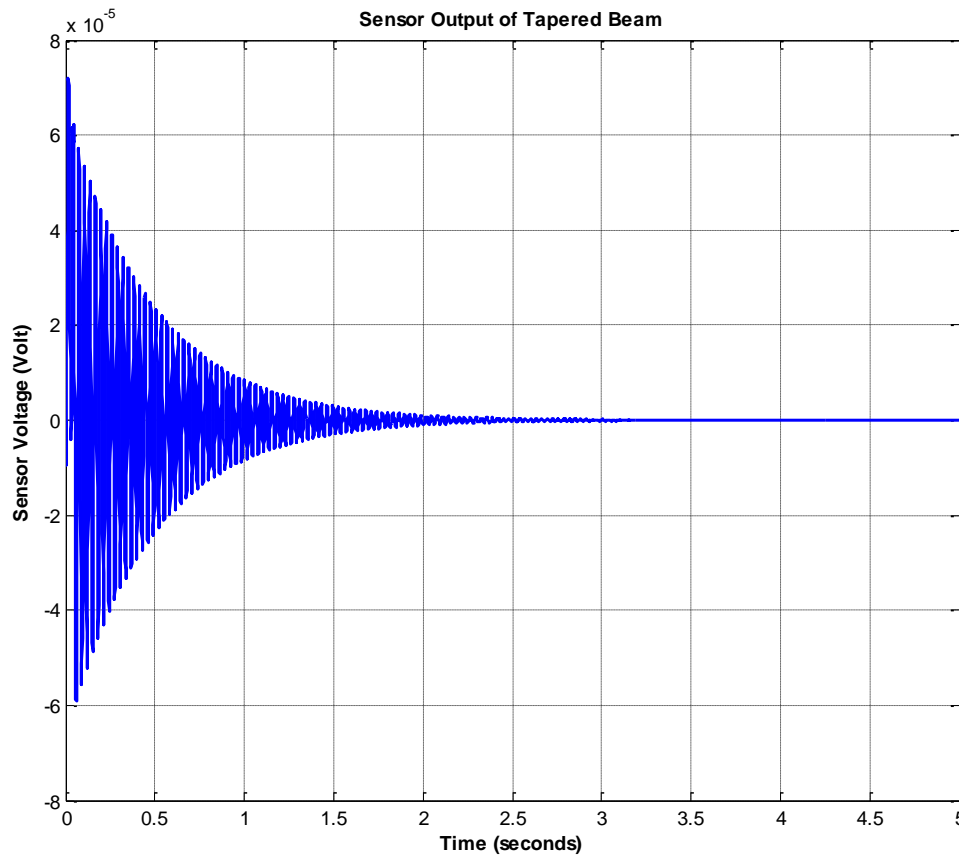
Figure 5-21: Closed loop sensor voltage of tapered beam without controller

- **PD controller results**

In case of the smart cantilever tapered beam, the proportional and derivative gains are taken as: ($K_P = 1300000$, $K_d = 900$ and $N = 20000$). The response of the system with adding PD controller and the actuation force (input signal) are illustrated in Figure 5-22 and Figure 5-23:
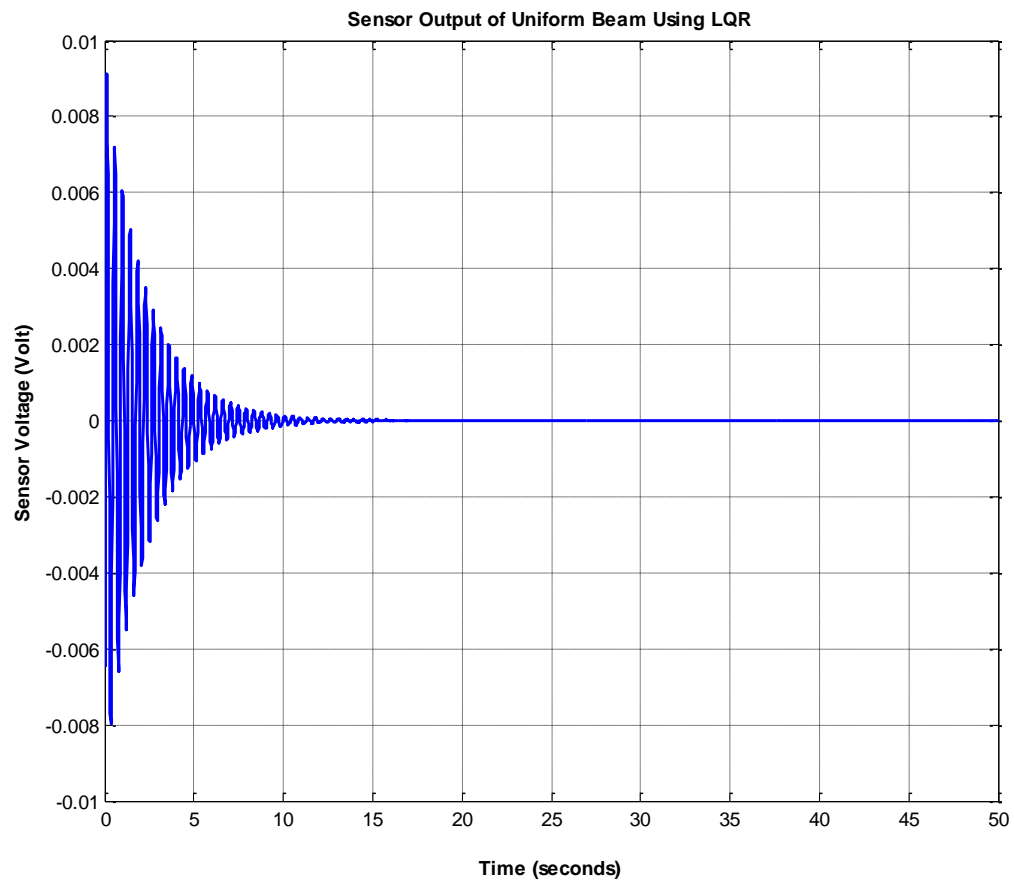

**Figure 5-22: Closed loop sensor voltage of tapered beam with PD controller**
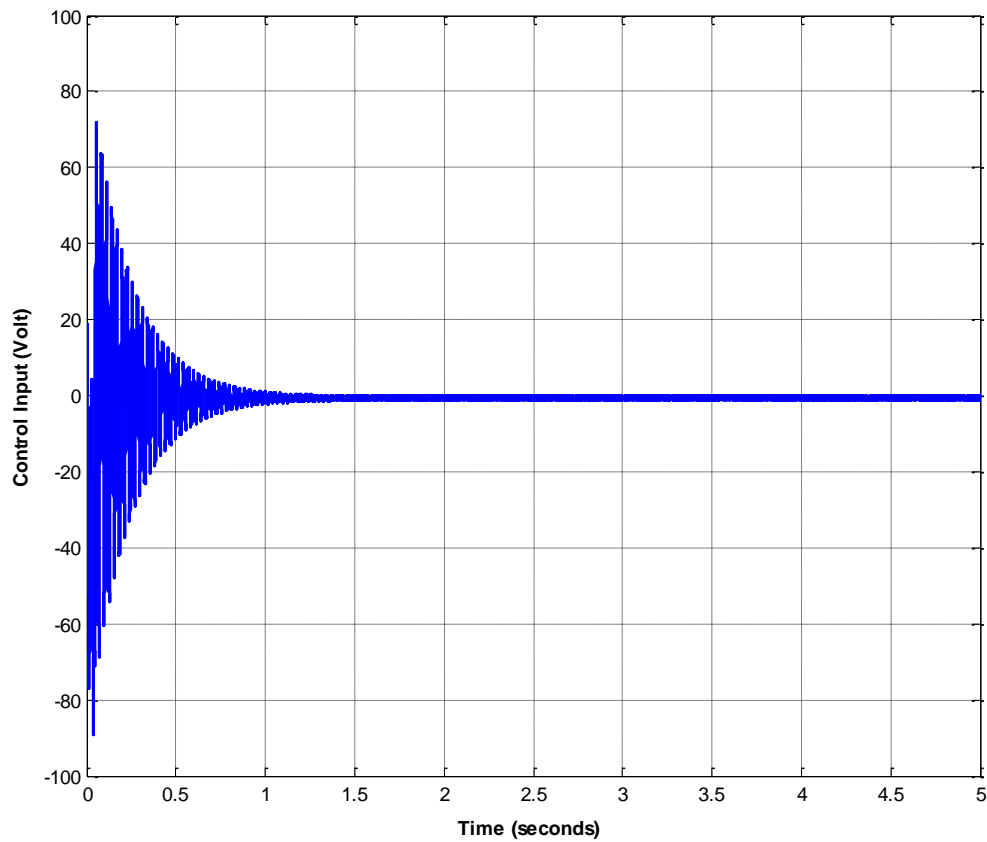
Figure 5-23: The actuation force of tapered beam with PD controller

- **LQR controller results**

The controllability and observability of the state space model are examined to prove whether the system is controllable and observable. The rank of the observability matrix and the controllability matrix are the same as the order of the system (equal 4), so the system is controllable and observable. The optimal values of Q and R are obtained by trial and error technique. The weighting matrices are taken as: $Q = 45$ and $R = 0.001$.

The response of the system with adding LQR controller and the actuation force (input signal) are illustrated in Figure 5-24 to Figure 5-25:

Figure 5-24: Closed loop sensor voltage of tapered beam with LQR controller
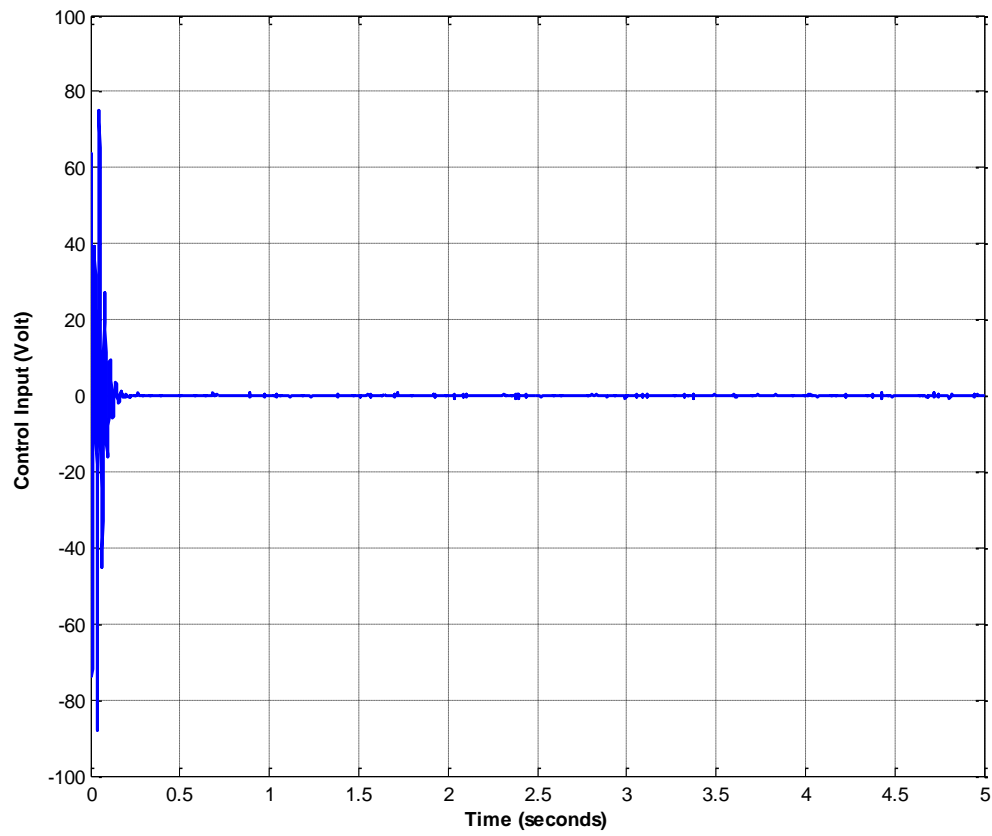
Figure 5-25: The actuation force of tapered beam with LQR controller

The sensor output of tapered cantilever beam without controller, with PD controller and with LQR optimal control is shown in Figure 5-26.
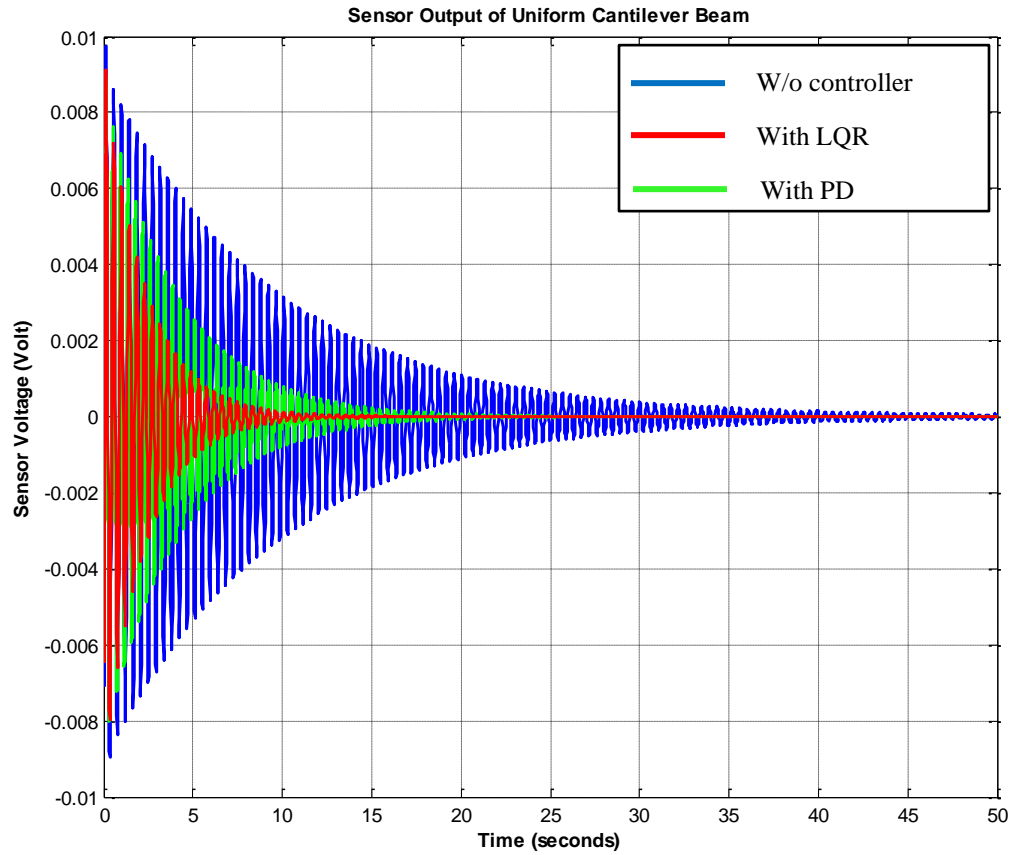
Figure 5-26: Comparison of sensor output of tapered cantilever beam without and with controller

The result revealed that the peak amplitude without adding any type of controllers is (-5.9 × 10^{-5} V and +7.21 × 10^{-5} V). The peak amplitude with adding PD is (-5.4857 × 10^{-5} V and +6.184 × 10^{-5} V) where the peak amplitude with adding LQR is (-2.5064 × 10^{-5} V and +5.6389 × 10^{-5} V).

The maximum actuation force by adding PD controller is (-89.25 V and 72.04 V) whereas the maximum actuation force by adding LQR controller is (-87.97 V and 75.18 V).

At bandwidth 0.0002%, the settling time without adding any type of controller is 1.687 sec whereas the settling time with adding PD and LQR controller are 0.8134 sec and 0.1231 sec, respectively.

5.2.3 Wind Turbine Blade

The response of the closed loop smart system with adding the external force (disturbance) and without using any type of controller is illustrated in Figure 5-27:
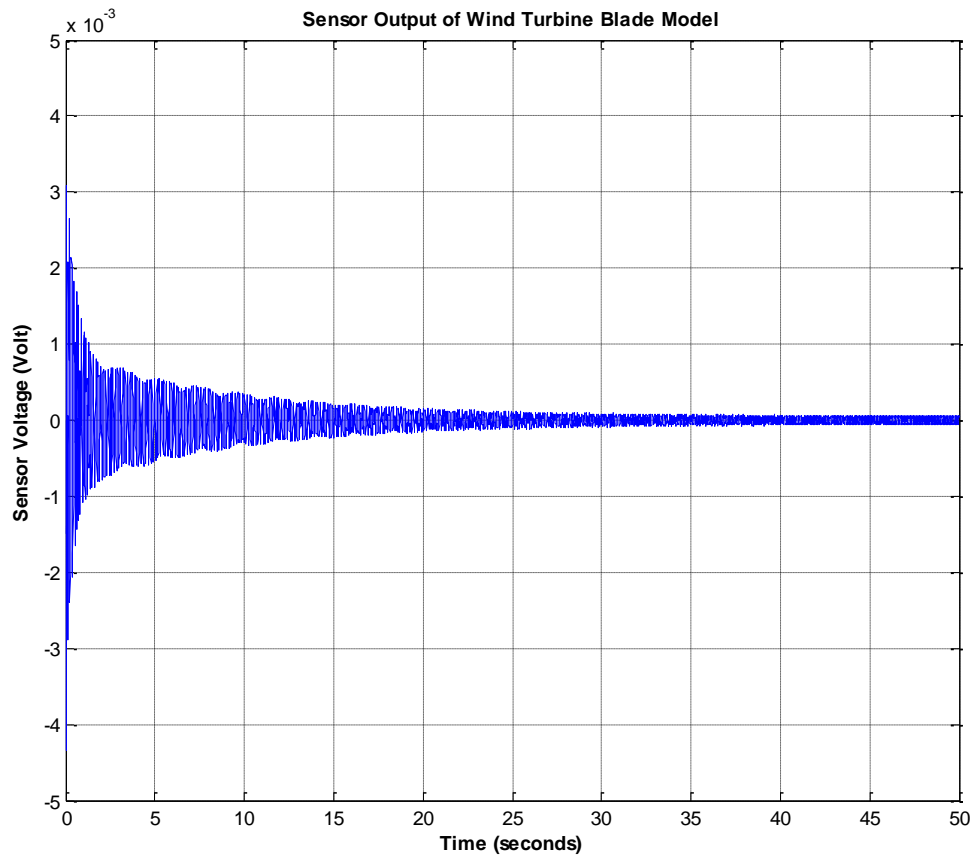
Figure 5-27: Closed loop sensor voltage of wind turbine blade without controller

- **PD controller results**

The proportional and derivative gains are taken as: ($K_P = 54252, K_d = 409$ and $N = 1648$). The response of the system with adding PD controller and the actuation force (input signal) are illustrated in Figure 5-28 and Figure 5-29:
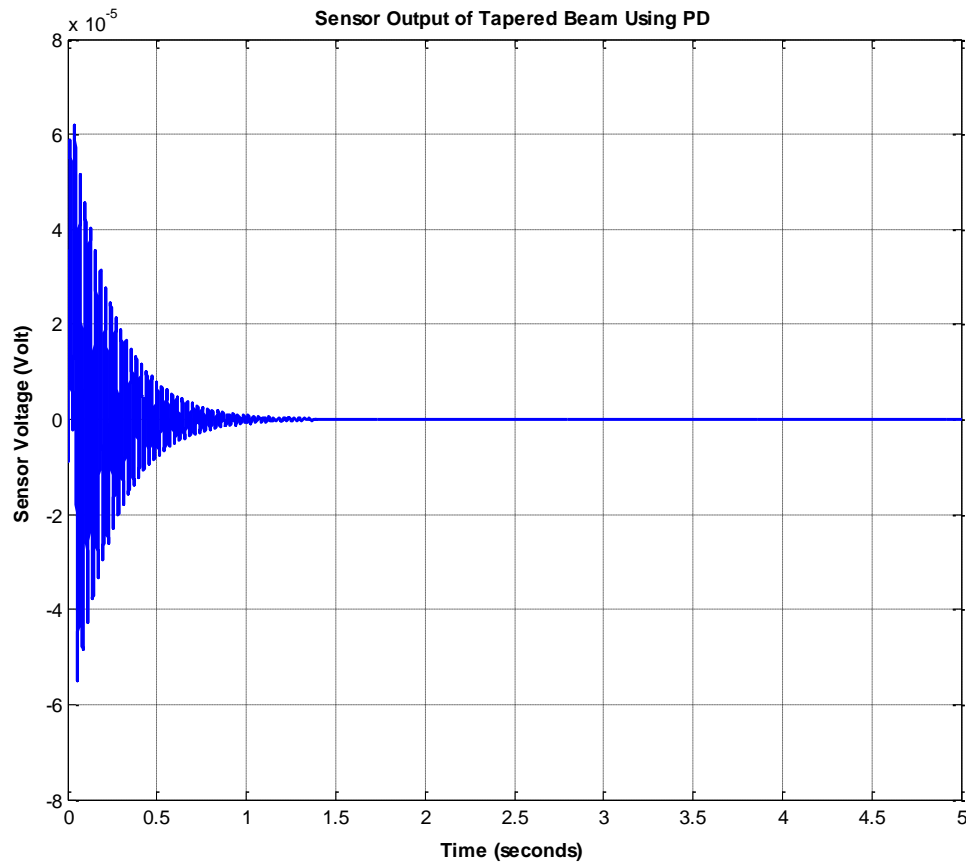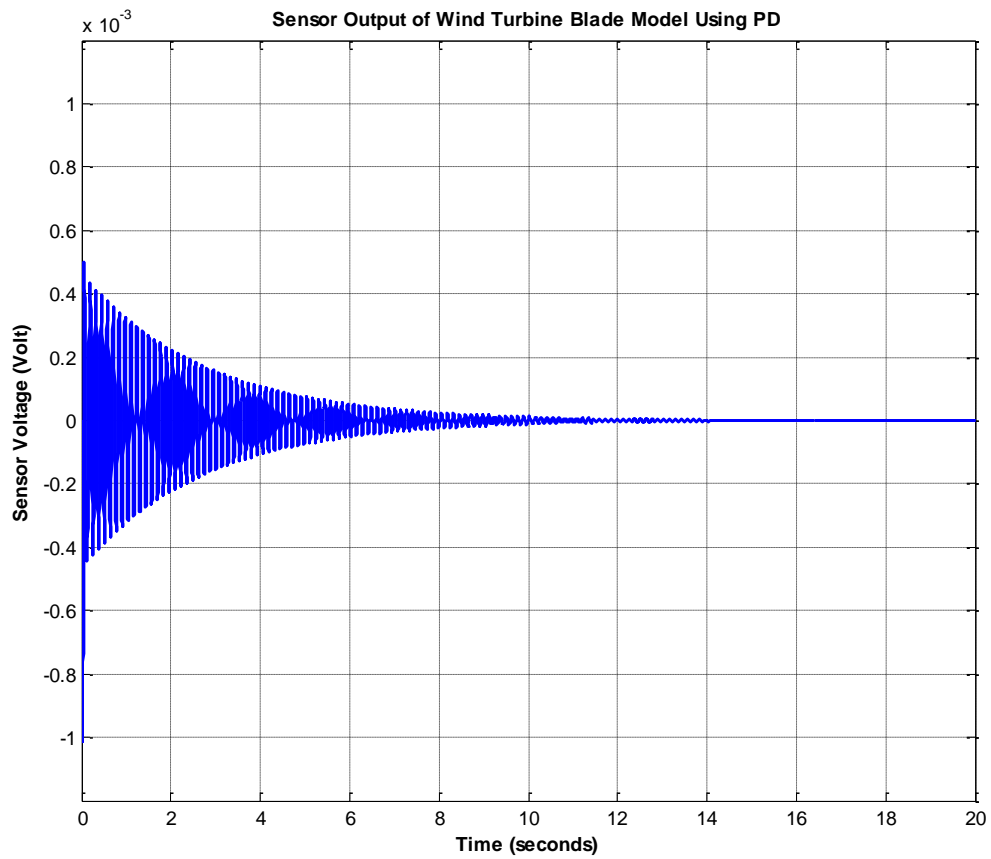

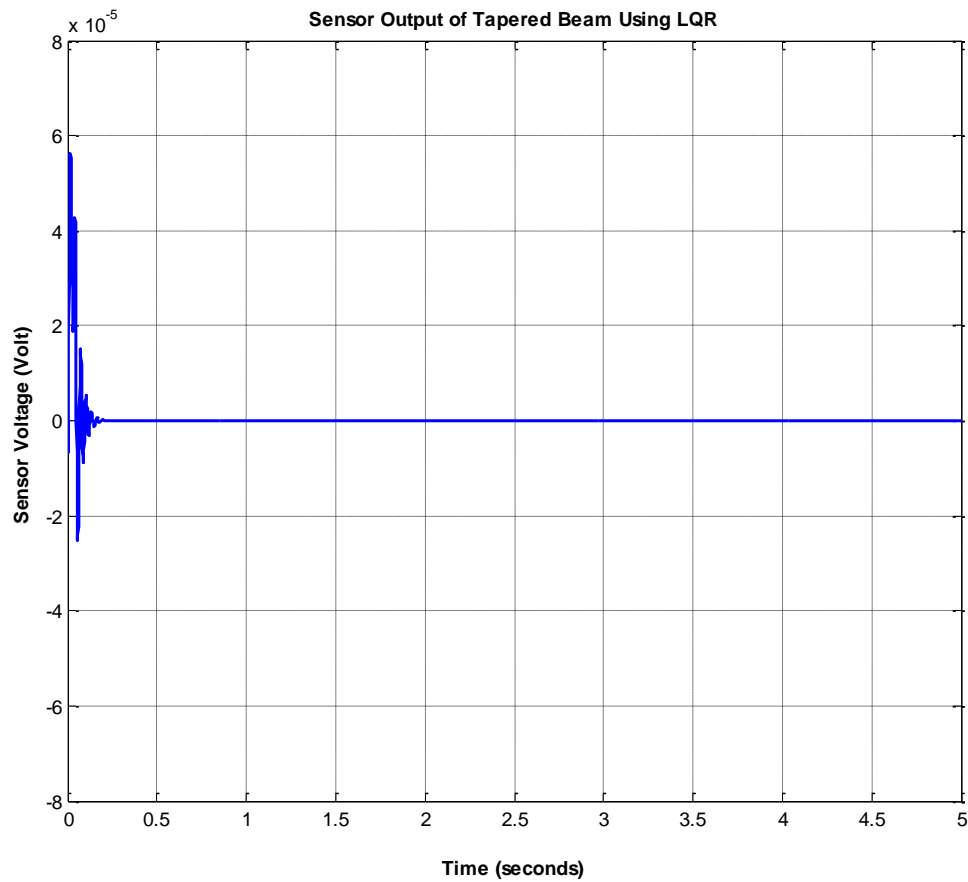**Figure 5-28: Closed loop sensor voltage of wind turbine blade with PD controller**
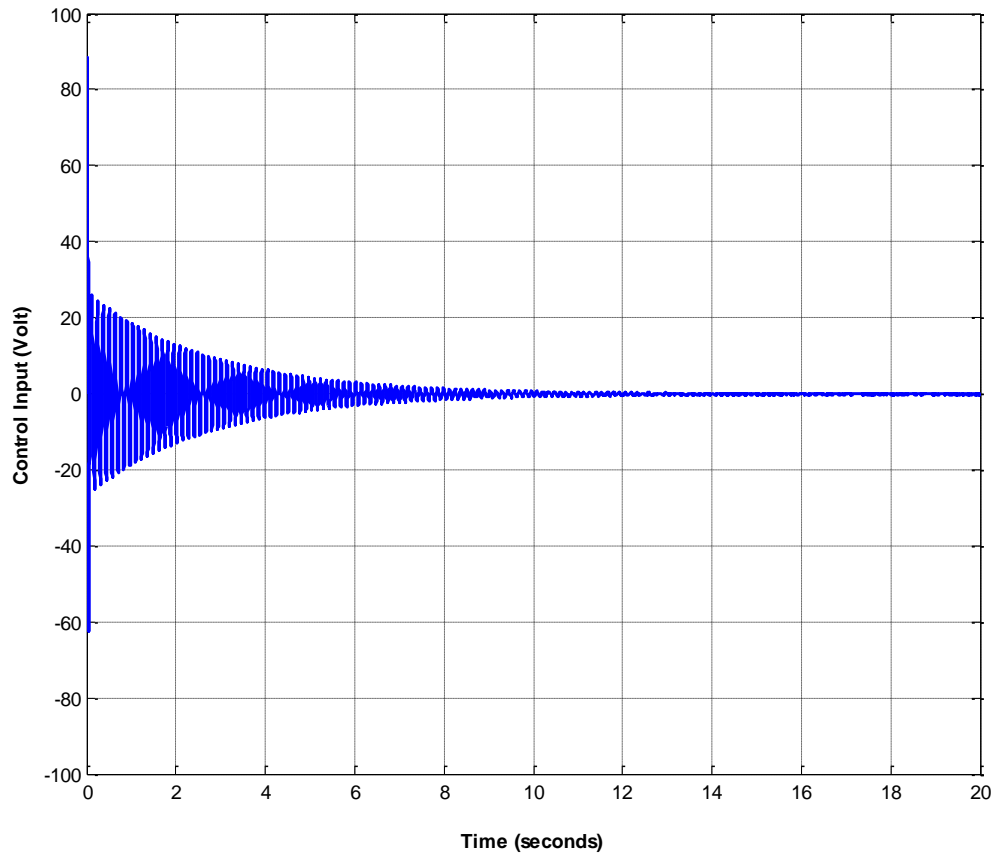
Figure 5-29: The actuation force of wind turbine blade with PD controller

▪ **LQR controller results**

In this case, a LQR optimal control is added to the system. The controllability and observability of the state space model are examined to prove whether the system is controllable and observable. The rank of the observability matrix and the controllability matrix are the same as the order of the system (equal 4), so the system is controllable and observable. The weighting matrices are obtained by trial and error technique. The weighting matrices are taken as: ($Q = 250$, $R = 0.001$). The response of the smart

system with adding LQR and the actuation force (input signal) are illustrated in Figure 5-30 to Figure 5-31:
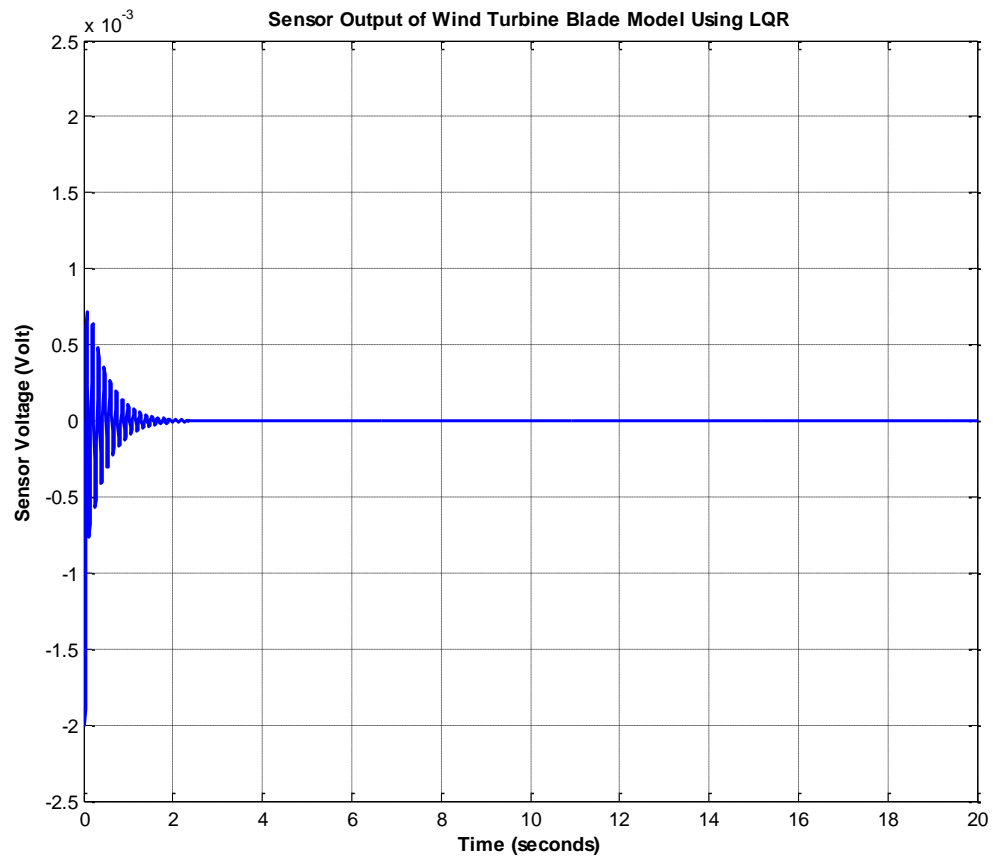
**Figure 5-30: Closed loop sensor voltage of wind turbine blade with LQR controller**
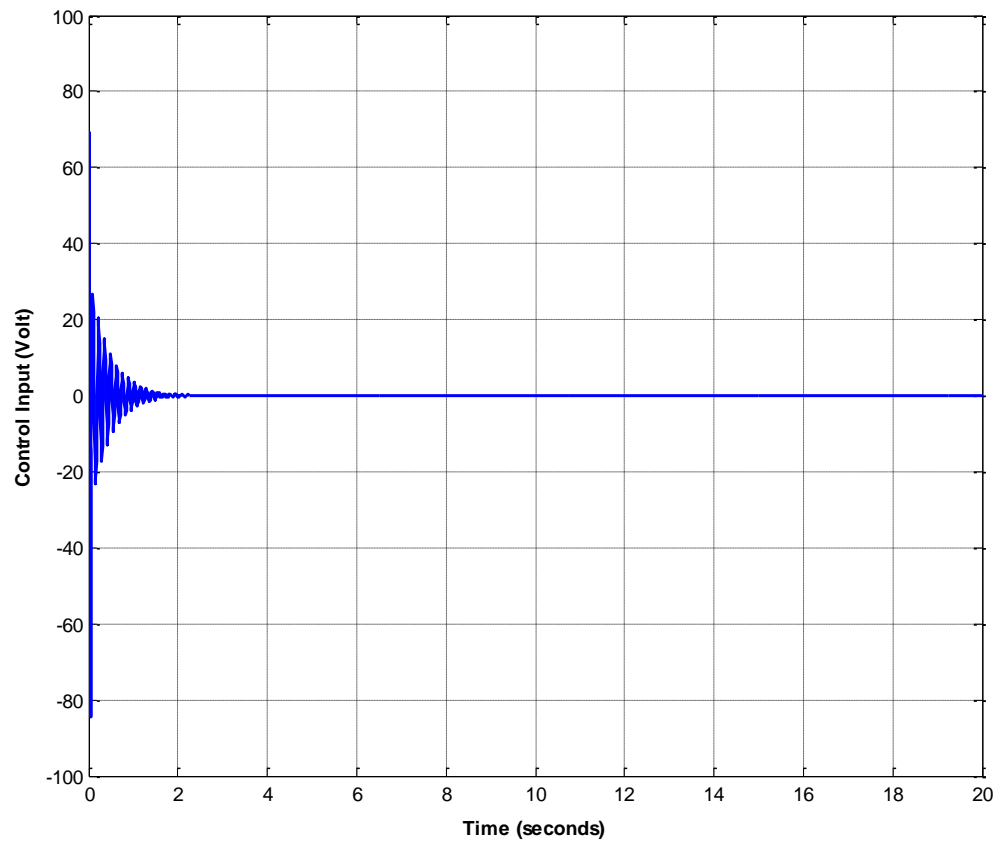
Figure 5-31: The actuation force of wind turbine blade with LQR controller

The sensor output of wind turbine blade model without controller, with PD controller and with LQR is shown in Figure 5-32.
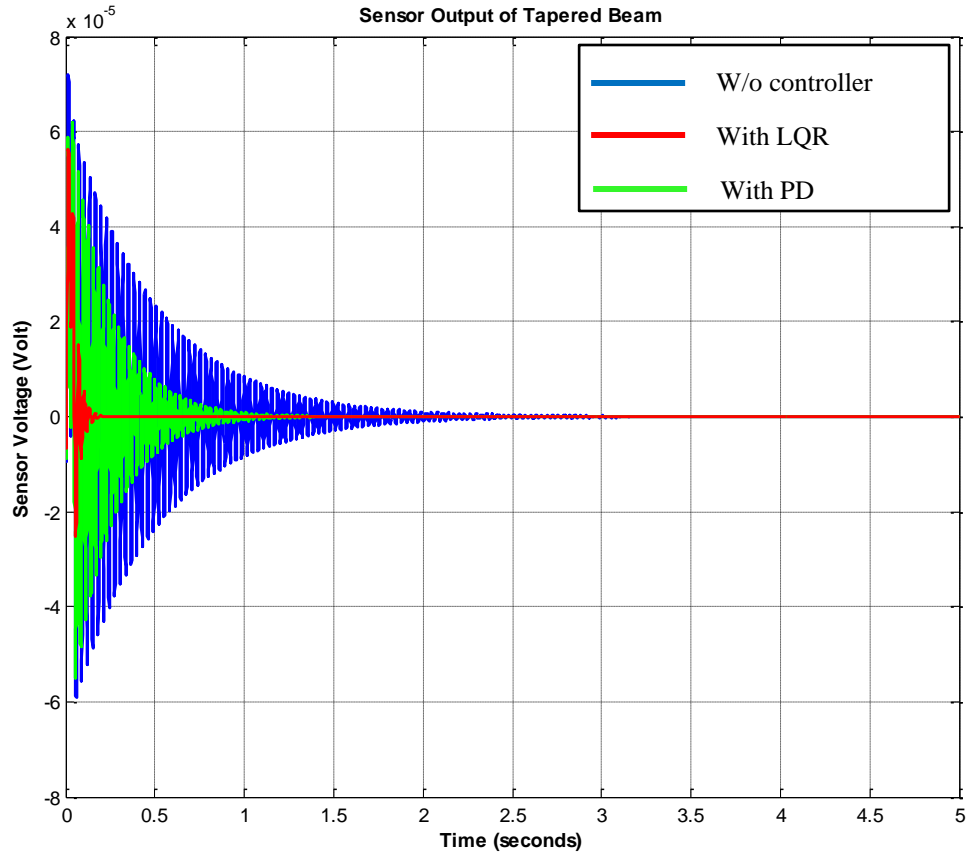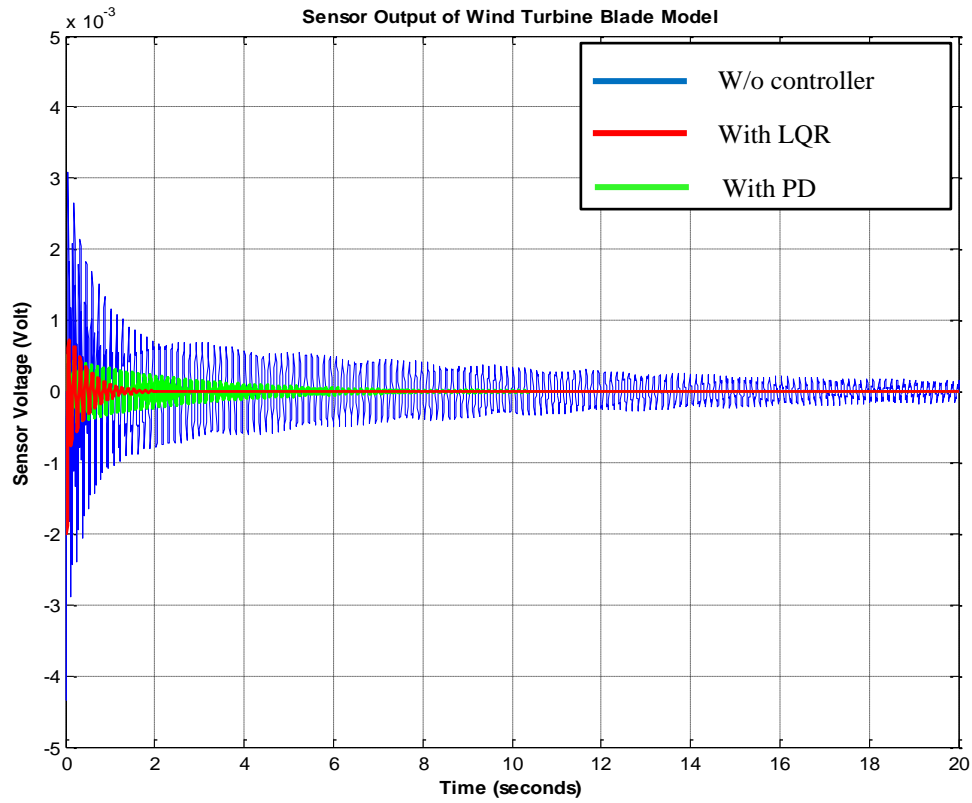
Figure 5-32: Comparison of sensor output of wind turbine blade model without and with controller

The result revealed that the peak amplitude without adding any type of controllers is (-0.0043 V and +0.0031 V). The peak amplitude with adding PD is (-0.001 V and +5.0121 $\times 10^{-4}$ V) whereas the peak amplitude with adding LQR is (-0.002 V and +7.1967 $\times 10^{-4}$ V).

The maximum actuation force with adding PD controller is (-62.557 V and 88.485 V) whereas the maximum actuation force with adding LQR controller is (-84.614 V and 69.008 V).

At bandwidth 0.02%, the settling time without adding any type of controller is 16.448 sec whereas the settling time with adding PD and LQR controller are 2.289 and 0.674 sec, respectively.

The following tables show summary of the three cases that are tested, the uniform cantilever beam idealization, the non-uniform cantilever beam idealization and the suggested wind turbine blade model, without and with using PD and LQR controller:

Table 5-1: Uniform beam results

	Without controller	PD controller	LQR controller
Settling Time (sec)	36.927	15.698	9.007
Peak Amplitude (V)	0.0097	0.0089	0.0091
Actuation Force (V)	………………	89.709	88.82
Max Disp (m)	0.472	0.432	0.442

Table 5-2: Non-uniform beam results

	Without controller	PD controller	LQR controller
Settling Time (sec)	1.687	0.813	0.123
Peak Amplitude (V)	7.211×10^{-5}	6.184×10^{-5}	5.638×10^{-5}
Actuation Force (V)	……………….	89.25	87.97
Max Disp (m)	0.0026	0.0023	0.0021

Table 5-3: Wind turbine blade results

	Without controller	PD controller	LQR controller
Settling Time (sec)	16.448	2.289	0.674
Peak Amplitude (V)	0.0043	0.001	0.002
Actuation Force (V)	…………….	88.485	84.614
Max Disp (m)	0.0037	8.623×10^{-4}	0.0017

5.3   Effect of Piezoelectric Size

The width and thickness of piezoelectric patches are considered very significant parameters in vibration suppression and the performance of smart structures. The effect of different values of thickness and width of piezoelectric patches are investigated with using LQR controller.

Several values of width and thickness of piezoelectric patches are checked. For constant thickness of 0.5 mm, the width values are 10, 15, 20, and 25 cm. And for constant width of 10.7 cm, the thickness values are 0.1, 1, 10, and 120 mm. The smart system that is used for this investigation is the wind turbine blade model. The other parameters such as the material properties are remain fixed. The material properties of the wind turbine blade that are used in this investigation are Al-alloy 6061 properties. The sensor output responses of smart wind turbine blade are illustrated in Figure 5-33 to Figure 5-40.

Summary of the eight cases of different values of width and thickness of piezoelectric patches is shown in Table 5-4 and Table 5-5.

Figure 5-33: Response of wind turbine blade (Width=0.1m and thickness=0.0005m)
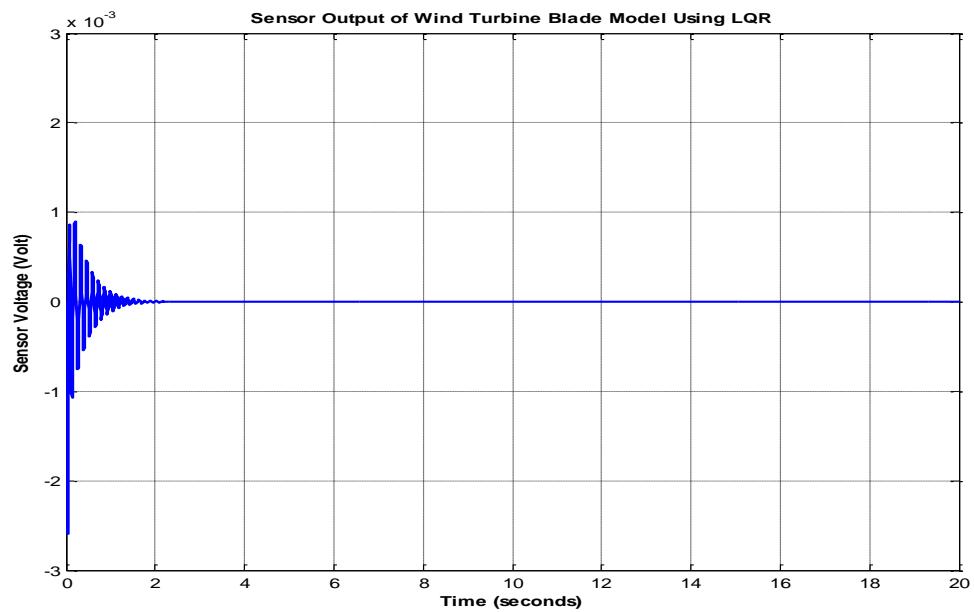
Figure 5-34: Response of wind turbine blade (Width=0.15m and thickness=0.0005m)
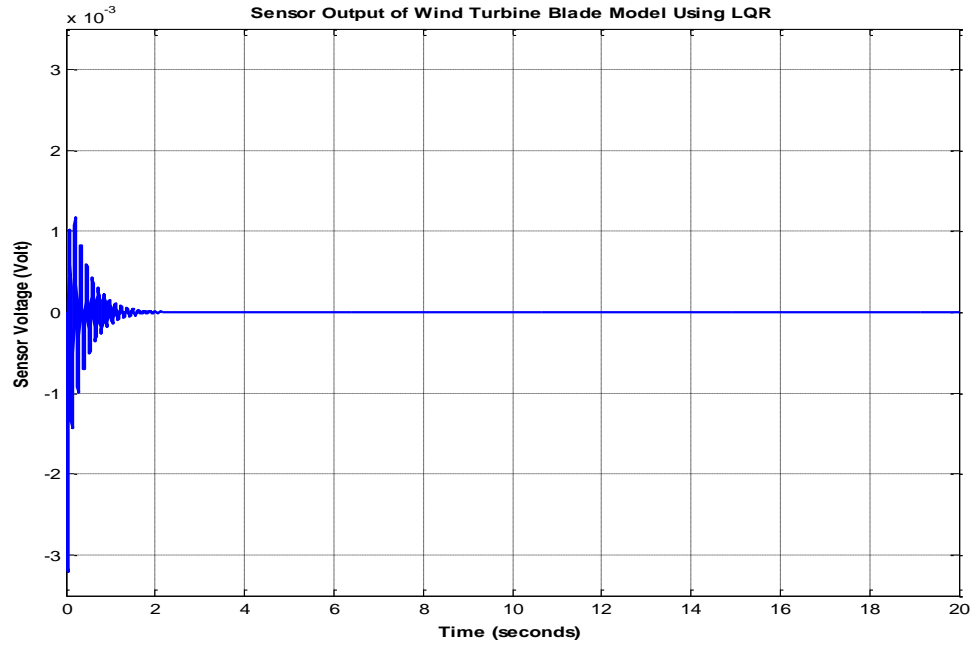
Figure 5-35: Response of wind turbine blade (Width=0.2m and thickness=0.0005m)
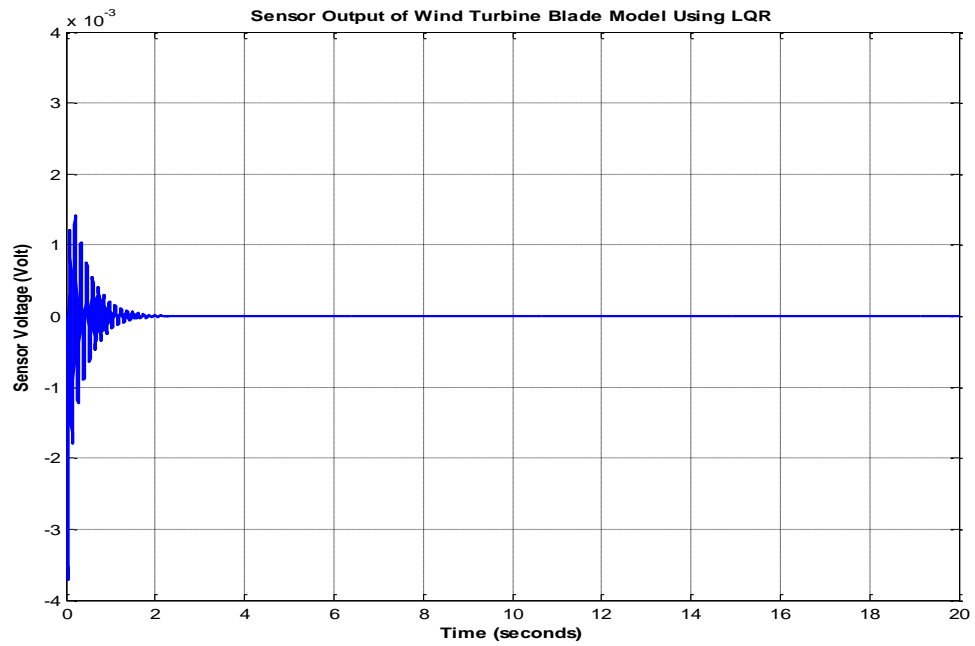
Figure 5-36: Response of wind turbine blade (Width=0.25m and thickness=0.0005m)
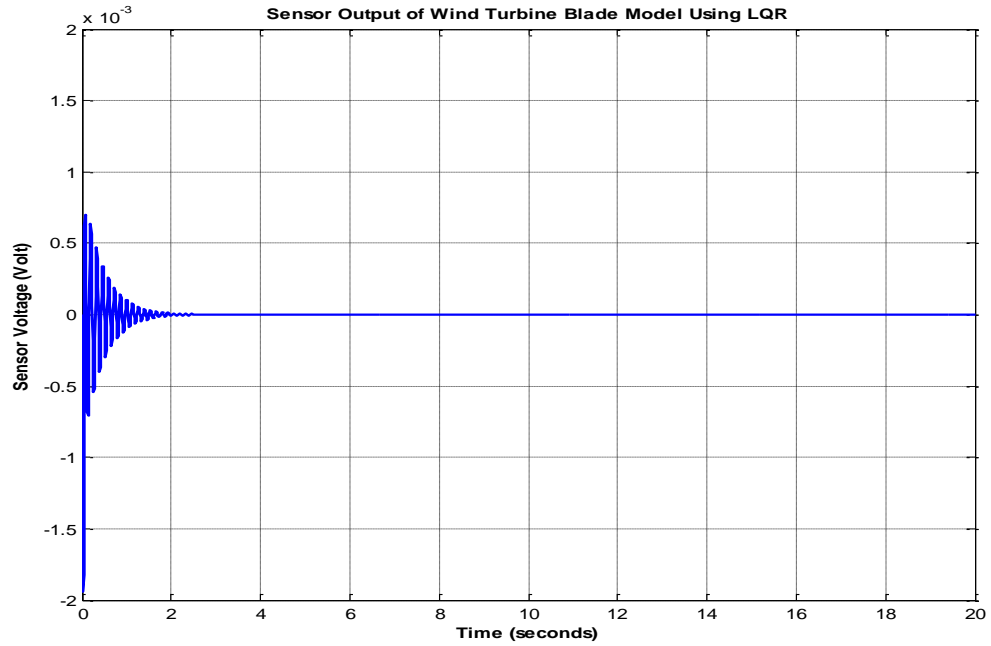
Figure 5-37: Response of wind turbine blade (Width=0.107m and thickness=0.0001m)
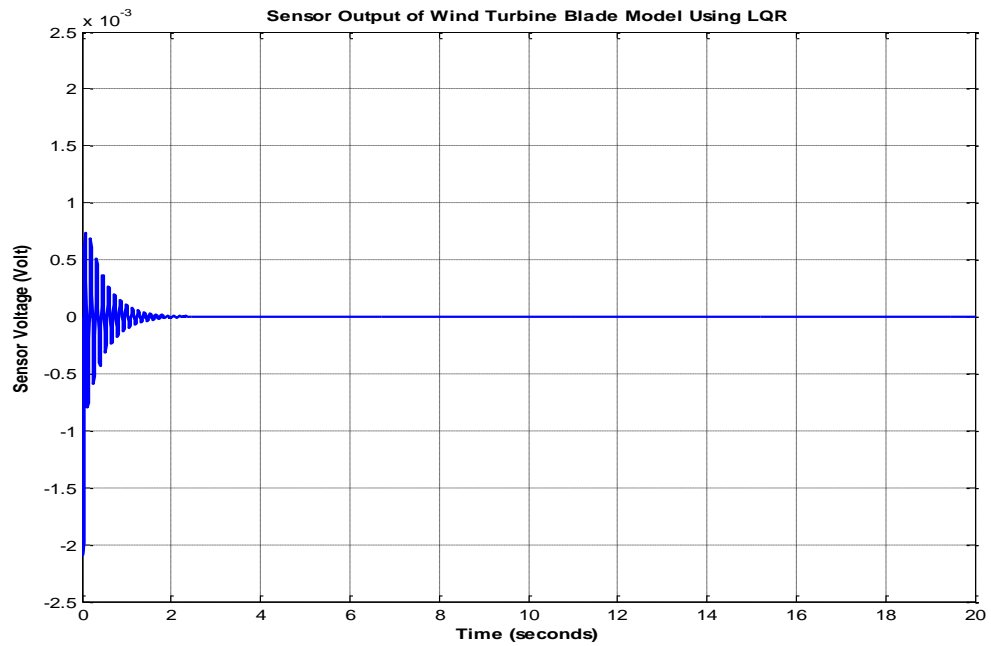
Figure 5-38: Response of wind turbine blade (Width=0.107m and thickness=0.001m)
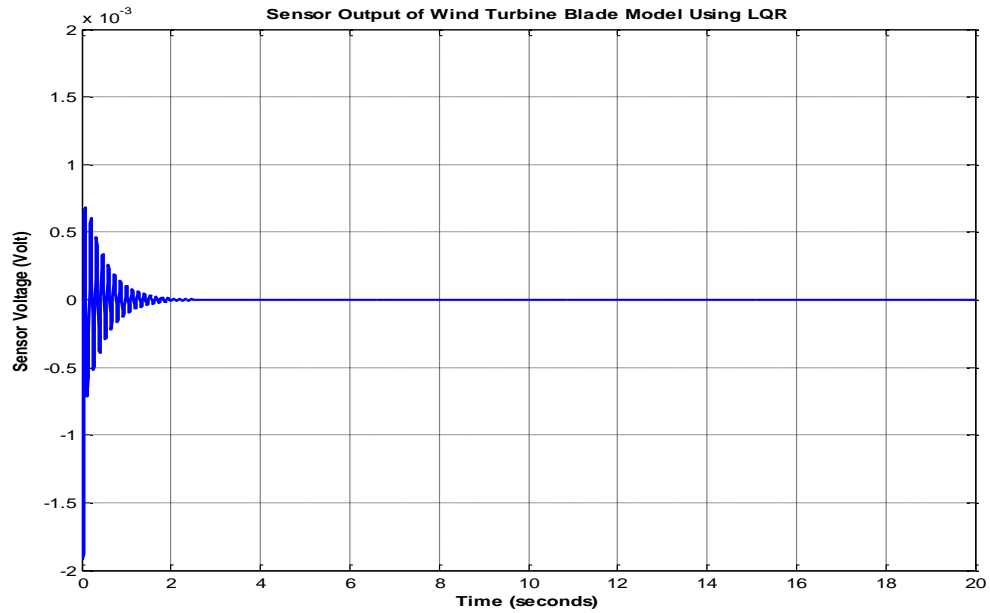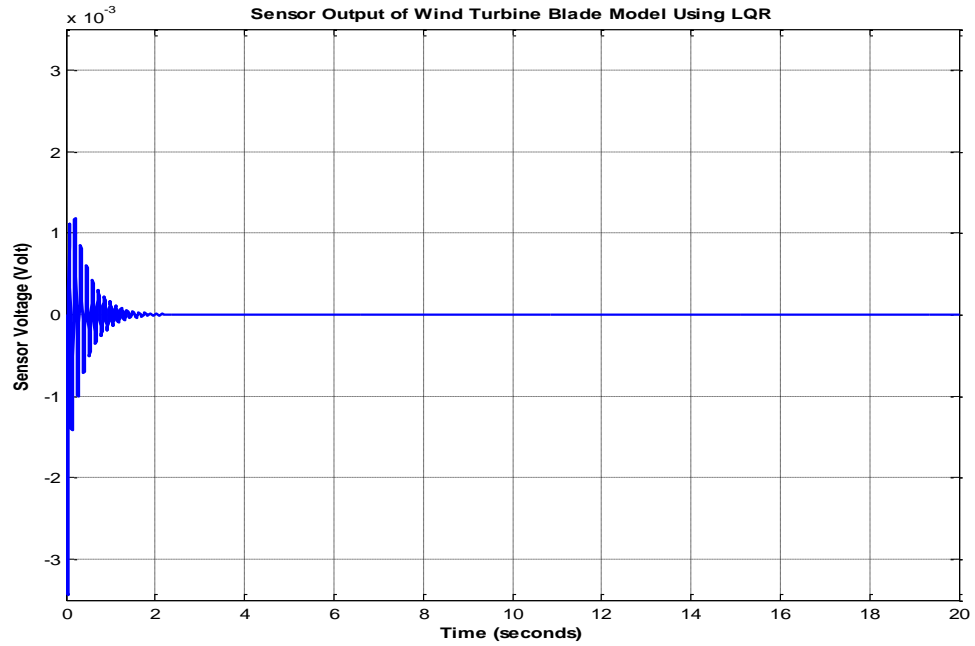
Figure 5-39: Response of wind turbine blade (Width=0.107m and thickness=0.01m)
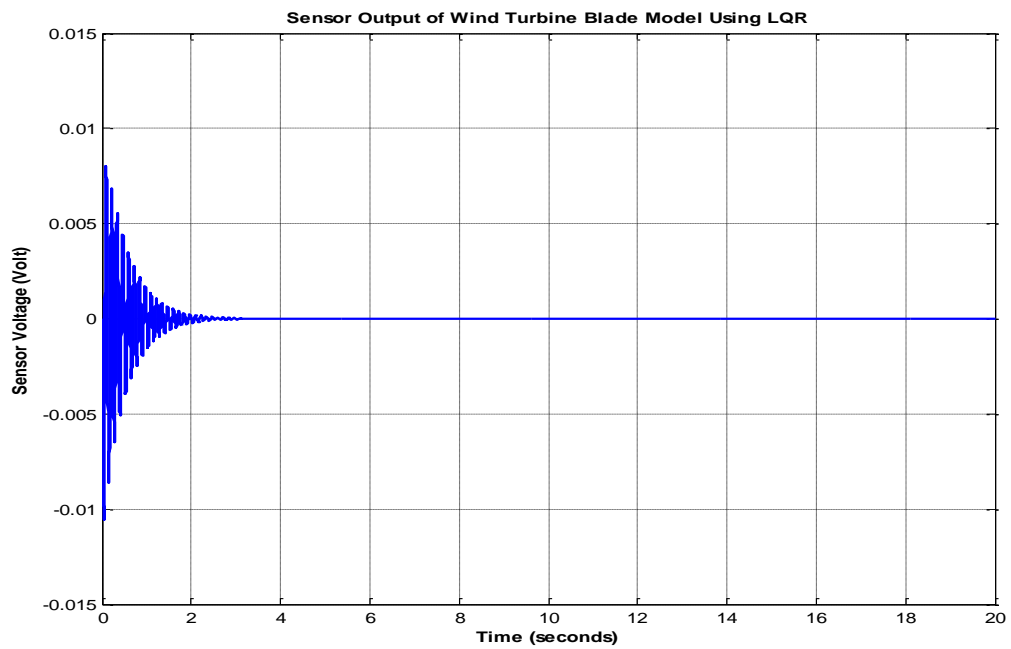
Figure 5-40: Response of wind turbine blade (Width=0.107m and thickness=0.12m)

Table 5-4: The effect of different values of width with adding LQR controller

	Case 1 (Width=0.1 and thickness=0.0005)	Case 2 (Width=0. 15 and thickness=0.0005)	Case 3 (Width=0.2 and thickness=0.0005)	Case 4 (Width=0.25 and thickness=0.0005)
Max disp (m)	0.0017	0.0016	0.0015	0.0014
Peak amp (V)	0.0019	0.0026	0.0032	0.0037
Act force (V)	87.34	64.96	49.87	39.306
Settling time (s)	0.673	0.737	0.8605	0.983

Table 5-5: The effect of different values of thickness with adding LQR controller

	Case 5 (Width=0.107 and thickness=0.0001)	Case 6 (Width=0.107 and thickness=0.001)	Case 7 (Width=0.107 and thickness=0.01)	Case 8 (Width=0.107 and thickness=0.12)
Max disp (m)	0.0017	0.0017	0.0016	7.5636×10^{-4}
Peak amp (V)	0.0019	0.0021	0.0034	0.0105
Act force (V)	85.505	83.44	63.269	13.83
Settling time (s)	0.672	0.675	0.865	2.101

From the simulation results, the dimensions of piezoelectric patches are considered very important parameters. The results showed that when the width is increased, the maximum displacement and the actuation force decrease whereas the peak amplitude and the settling time increase [50]. From the results, the best width is between 0.1 and 0.2 m.

Also, in case of different values of thickness, the results revealed that when the thickness is increased, the maximum displacement and the actuation force decrease whereas the peak amplitude and the settling time increase [50]. From this investigation, the best thickness is between 0.1 and 1 mm.

5.4   Effect of Piezoelectric Material Properties

The material properties of piezoelectric patches are considered very important factors in vibration suppression and the performance of smart structures. The effects of different values of material properties of piezoelectric patches are investigated.

Three different values of material properties of piezoelectric patches are studied. The smart structure that is used in this investigation is the wind turbine blade model. The material properties are shown in Table 5-6.

Table 5-6: Three different values of material properties of piezoelectric patches

	Density (kg/m^3)	Young's Modulus (GPa)	d_{31} (m/V)	e_{31} (C/m^2)
BM500	7650	65	-175×10^{-12}	-11.9
PSI-5A4E	7800	52	-190×10^{-12}	-10.56
PSI-5H4E	7800	50	-320×10^{-12}	-20.37

The width and thickness of piezoelectric patches are 10.7 cm and 0.5 mm, respectively. The responses of smart wind turbine blade model are illustrated in Figure 5-41 to Figure 5-43. Summary of the three cases of different material properties of piezoelectric patches is shown in Table 5-7.
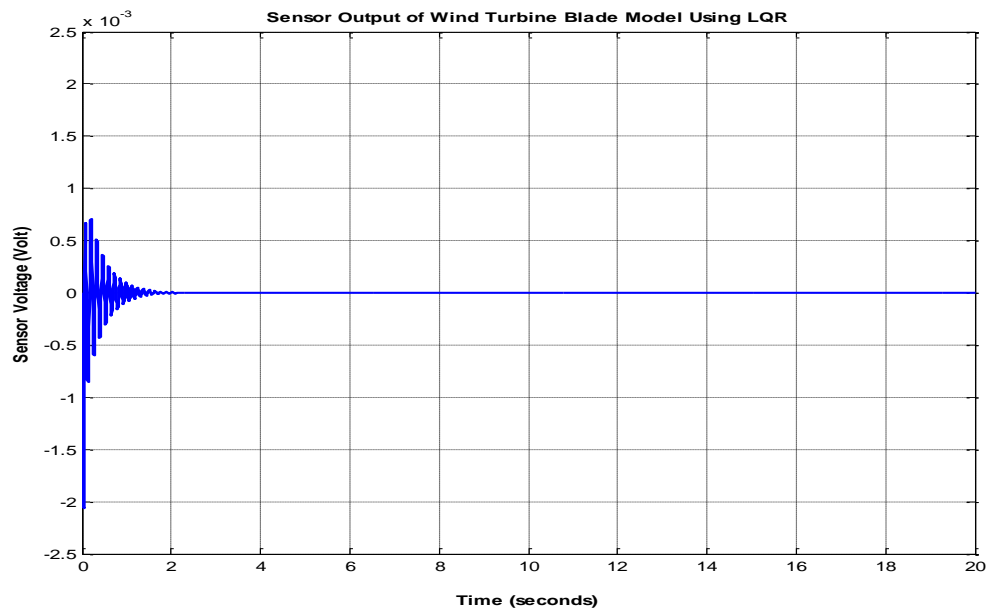
Figure 5-41: Response of wind turbine blade in case of BM500
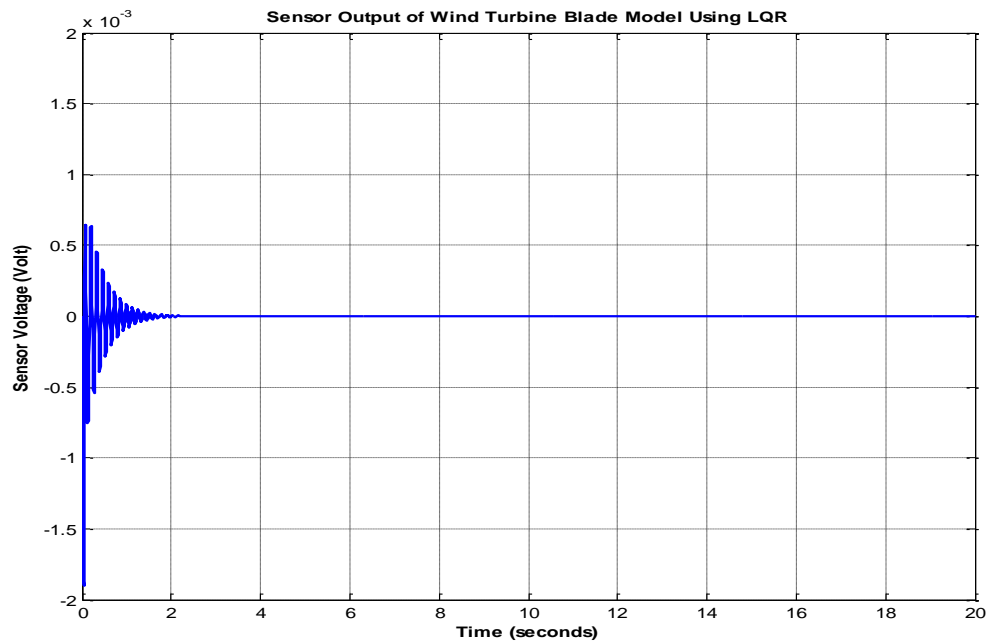
Figure 5-42: Response of wind turbine blade in case of PSI-5A4E
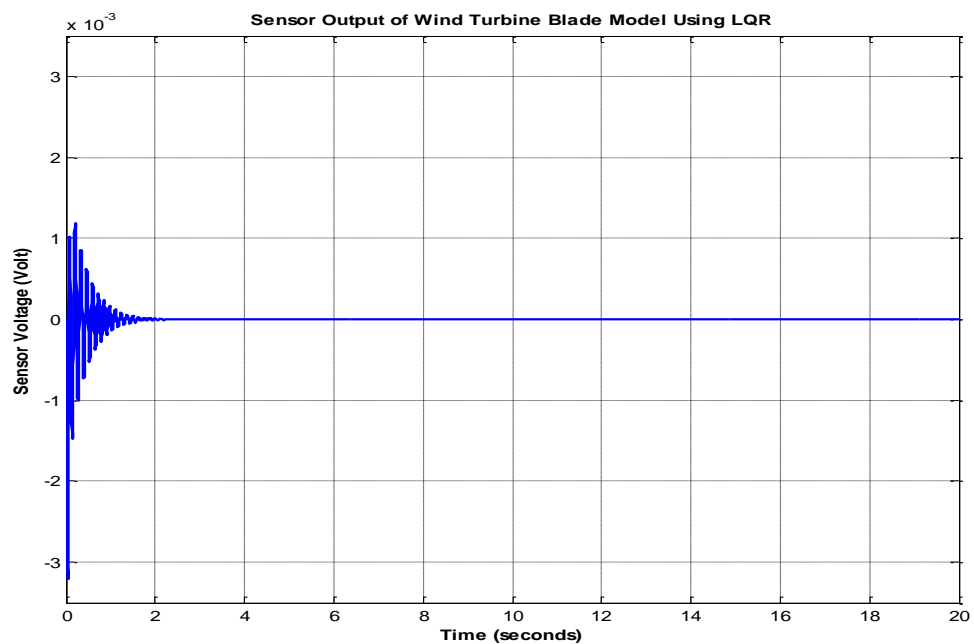
Figure 5-43: Response of wind turbine blade in case of PSI-5H4E

Table 5-7: The effect of different material properties of piezoelectric patches

	Case 1 BM500	Case 2 PSI-5A4E	Case 3 PSI-5H4E
Max displacement (m)	0.00159	0.0016	0.0014
Peak amp (V)	0.0021	0.0019	0.0032
Act force (V)	63.179	71.707	45.85
Settling time (S)	0.669	0.664	0.86

From the simulation results, the material properties of piezoelectric patches are considered very important parameters. The results showed that the actuation force, settling time, max displacement and peak voltage depend mainly on piezoelectric stress/charge constant (e_{31}). The results revealed that the maximum displacement and the actuation force increase when the values of piezoelectric stress/charge (e_{31}) increases (the magnitude value of e_{31} decreases) whereas the peak voltage (amplitude) and the settling time decrease with increasing (e_{31}) [50].

CHAPTER 6

CONCLUSIONS AND RECOMMENDATIONS

6.1   Conclusions

In this study, active vibration control of a horizontal axis wind turbine blade is conducted for reducing and monitoring the vibration response. Two systems are conduced to apply active vibration control on the wind turbine blade model, the first is a uniform cantilever beam and the other system is a non-uniform (tapered) cantilever beam. A single piezoelectric actuator and sensor are bonded on the upper and lower surface of smart systems, respectively. In the process of the design for active vibration control, the dynamic behavior and vibration analysis are required. The natural frequencies (eigenvalues) and mode shapes (eigenvectors) are obtained using the approximate analytical methods. The power of the approximate analytical methods is its ability to deal with many different cross sections with same method of solution. In the vibration control problems, vibration control is designed to control the first modes of smart structures because they contain the high vibrational level and low natural frequencies. An external aerodynamic force is applied to the smart structures. The shape of the distributed load is assumed to be cosine distribution. The entire structures are modeled in the state space form using the state space method, modal coordinates and piezoelectric theory. A controller strategy is considered one of the major elements for active vibration control technique. In this study, two types of controllers are designed to study the performance

of the piezoelectric active controller. The first is a Proportional-Derivative (PD) controller and the other controller is a Linear Quadratic Regulator (LQR). The simulated results showed that the Linear Quadratic Regulator (LQR) demonstrates better results for decreasing the settling time and actuation force whereas the Proportional-Derivative (PD) controller demonstrates better results for reducing the maximum displacement and peak voltage (amplitude). The effect of piezoelectric size is studied. The results showed that when the width is increased, the maximum displacement and the actuation force decrease whereas the peak amplitude and the settling time increase. On the other hand, when the thickness is increased, the maximum displacement and the actuation force decrease whereas the peak amplitude and the settling time increase. Also, the effects of piezoelectric materials are investigated. The results revealed that the maximum displacement and the actuation force increase when the values of piezoelectric stress/charge (e_{31}) increases (the magnitude value of e_{31} decreases) whereas the peak voltage (amplitude) and the settling time decrease when the values of piezoelectric stress/charge (e_{31}) increases. Active vibration control is considered one of the effective and efficient techniques for vibration suppression.

6.2   Recommendations and Future Work

This study can be extended for different types of structures, such as circular disks, shells and plates. For these shapes, the conclusions might be different from the cantilever beam. Also, different excitation forces can be applied on smart structures at different locations on the surface.

Furthermore, different types of controllers, such as fuzzy logic controller, Fast Output Sampling (FOS) and robust H_∞ can be designed to study their effectiveness, control input, performance, system response, robustness and efficiency.

Also, this work can be extended by using genetic algorithm, neural network and evolutionary computation for obtaining the optimal sizes and locations of piezoelectric actuators and sensors and for designing controllers, such as genetic algorithm based Linear Quadratic Regulator (LQR) to design the optimal control.

This study can be extended to develop some solutions for spillover phenomenon that increases due to the excitation of the residual modes by the controller.

REFERENCES

[1]   N. D. Zoric´, A. M. Simonovic´, Z. S. Mitrovic´, and S. N. Stupar, "Optimal vibration control of smart composite beams with optimal size and location of piezoelectric sensing and actuation," *J. Intell. Mater. Syst. Struct.*, vol. 24, no. 4, pp. 499–526, 2012.

[2]   N. D. Zoric´, A. M. Simonovic´, Z. S. Mitrovic´, and S. N. Stupar, "Active vibration control of smart composite beams using PSO-optimized self-tuning fuzzy logic controller," *J. Theor. Appl. Mech.*, vol. 51, no. 2, pp. 275–286, 2013.

[3]   M. Sathyajith, *Wind Energy: Fundamentals, Resource Analysis and Economics*. Springer, 2006.

[4]   E. Hau and H. Von Renouard, *Wind Turbines: Fundamentals, Technologies, Application, Economics*. Springer, 2013.

[5]   Awea.org, "AWEA - American Wind Energy Association." 2014.

[6]   C. W. De Silva, A. Borbely, J. F. Kreider, and L. R. Davis, *Vibration Damping , Control , and Design*. 2007.

[7]   piceramic.com, "Piezo Ceramic Technology, Piezo Actuators & Piezo Components from PI Ceramic," 2014.

[8]   A. Preumont, *Vibration Control of Active Structures: An Introduction*. Springer, 2011.

[9]   N. Jalili, *Piezoelectric-Based Vibration Control: From Macro to Micro/Nano Scale Systems*. Springer, 2009.

[10]   F. Casciati, G. Magonette, and F. Marazzi, *Technology of Semiactive Devices and Applications in Vibration Mitigation*. Wiley, 2006.

[11]   R. C. Ganesan, N. Engels, "Timoshenko beam finite elements using the assumed modes method," *J. Sound Vib.*, vol. 156, no. 1, pp. 109–123, 1992.

[12]   S. M. Han, H. Benaroya, and T. Wei, "Dynamics of Transversely Vibrating Beams Using Four Engineering Theories," *J. Sound Vib.*, vol. 225, no. 5, pp. 935–988, 1999.

[13] A. Bazoune and Y. A. Khulief, "A finite beam element for vibration analysis of rotating tapered timoshenko beams," *J. Sound Vib.*, vol. 156, no. 1, pp. 141–164, 1992.

[14] Y. A. Khulief, "Vibration frequencies of a rotating tapered beam with end mass," *J. Sound Vib.*, vol. 134, no. 1, pp. 87–97, 1989.

[15] Y. A. Khulief, "Vibration suppression in rotating beams using Active Modal Control," *J. Sound Vib.*, vol. 242, no. 4, pp. 681–699, 2001.

[16] Y. A. Khulief, "Active modal control of vibrations in elastic structures in the presence of material damping," *Comput. Methods Appl. Mech. Eng.*, vol. 190, pp. 6947–6961, 2001.

[17] N. Wereley, G. Wang, and A. Chaudhuri, "Demonstration of uniform cantilevered beam bending vibration using a pair of piezoelectric actuators," *J. Intell. Mater. Syst. Struct.*, vol. 0, pp. 1–10, 2010.

[18] K. Achawakorn and T. Jearsiripongkul, "Vibration Analysis of Exponential Cross-Section Beam Using Galerkin's Method," *Int. J. Appl. Sci. Technol.*, vol. 2, no. 6, pp. 7–13, 2012.

[19] Y. Zhen, R. Z. Zhao, and H. Liu, "Mode Analysis of Horizontal Axis Wind Turbine Blades," *TELKOMNIKA Indones. J. Electr. Eng.*, vol. 12, no. 2, pp. 1212–1216, 2014.

[20] E. F. Crawley and J. De Luis, "Use of piezoelectric actuators as elements of intelligent structures," *AIAA J.*, vol. 25, no. 10, pp. 1373–1385, 1987.

[21] G. Song, P. Qiao, and W. Binienda, "Active vibration damping of a composite beam using smart sensors and actuators," in *19th AIAA Applied Aerodynamics Conference*, 2001.

[22] S. Kapuria and M. Y. Yasin, "Active vibration suppression of multilayered plates integrated with piezoelectric fiber reinforced composites using an efficient finite element model," *J. Sound Vib.*, vol. 329, no. 16, pp. 3247–3265, 2010.

[23] A. Staino, B. Basu, and S. R. K. Nielsen, "Actuator control of edgewise vibrations in wind turbine blades," *J. Sound Vib.*, vol. 331, no. 6, pp. 1233–1256, 2012.

[24] J. Han, K. Rew, and I. Lee, "An experimental study of active vibration control of composite structures with a piezo-ceramic actuator and a piezo-film sensor," *Smart Mater. Struct.*, vol. 6, no. 5, pp. 549–558, 1997.

[25] T. C. Manjunath and B. Bandyopadhyay, "Vibration Control of a Smart Structure Using Periodic Output Feedback Technique," *Asian J. Control*, vol. 6, no. 1, pp. 74–87, 2004.

[26] T. C. Manjunath and B. Bandyopadhyay, "Fault tolerant control of flexible smart structures using robust decentralized periodic output feedback technique," *Smart Mater. Struct.*, vol. 14, no. 4, pp. 624–636, 2005.

[27] T. C. Manjunath and B. Bandyopadhyay, "Smart control of cantilever structures using output feedback," *Int. J. Simul. Syst. Sci. Tech*, vol. 7, no. 4–5, pp. 51–68, 2006.

[28] T. C. Manjunath and B. Bandyopadhyay, "Vibration control of Timoshenko smart structures using multirate output feedback based discrete sliding mode control for SISO systems," *J. Sound Vib.*, vol. 326, no. 1–2, pp. 50–74, 2009.

[29] G. Song and H. Gu, "Active Vibration Suppression of a Smart Flexible Beam Using a Sliding Mode Based Controller," *J. Vib. Control*, vol. 13, no. 8, pp. 1095–1107, 2007.

[30] J. Zhang, L. He, E. Wang, and R. Gao, "A LQR Controller Design for Active Vibration Control of Flexible Structures," in *Proceedings of the 2008 IEEE Pacific-Asia Workshop on Computational Intelligence and Industrial Application - Volume 01*, pp. 127–132, 2008.

[31] J. Zhang, L. He, E. Wang, and R. Gao, "Active Vibration Control of Flexible Structures Using Piezoelectric Materials," in *Proceedings of the 2009 International Conference on Advanced Computer Control*, pp. 540–545, 2009.

[32] N. U. Rahman and M. A. Alam, "Active vibration control of a piezoelectric beam using PID controller: Experimental study," *Lat. Am. J. Solids Struct.*, vol. 9, no. 6, pp. 657–673, 2012.

[33] W. Jarzyna, M. Augustyniak, M. Bocheński, and J. Warmiński, "PD and LQR controllers applied to vibration damping of an active composite beam," in *Przegląd Elektrotechniczny (Electrical Review)*, R. 88 NR 10b, pp. 128–131, 2012.

[34] T. Roy and D. Chakraborty, "Genetic algorithm based optimal control of smart composite shell structures under mechanical loading and thermal gradient," *Smart Mater. Struct.*, vol. 18, no. 11, 115006 (12pp), 2009.

[35] A. Z. Al-Garni, A. Jamal, A. M. Ahmad, A. M. Al-Garni, and M. Tozan, "Neural network-based failure rate prediction for De Havilland Dash-8 tires," *Eng. Appl. Artif. Intell.*, vol. 19, no. 6, pp. 681–691, 2006.

[36] A. Z. Al-Garni and A. Jamal, "Failure rate analysis of Boeing 737 brakes employing neural network," in *International Journal of Reliability, Quality and Safety Engineering*, pp. 1–25, 2007.

[37] A. Z. Al-Garni and A. Jamal, "Artificial neural network application of modeling failure rate for Boeing 737 tires," *Qual. Reliab. Eng. Int.*, vol. 27, no. 2, pp. 209–219, 2011.

[38] A. Kumar and D. Chhabra, "Design of Neural Network Controller for Active Vibration control of Cantilever plate with piezo-patch as sensor / actuator," *Int. J. Mod. Eng. Res.*, vol. 3, no. 4, pp. 2481–2488, 2013.

[39] I. Bruant, L. Gallimard, and S. Nikoukar, "Optimal piezoelectric actuator and sensor location for active vibration control, using genetic algorithm," *J. Sound Vib.*, vol. 329, no. 10, pp. 1615–1635, 2010.

[40] S. L. Schulz, H. M. Gomes, and A. M. Awruch, "Optimal discrete piezoelectric patch allocation on composite structures for vibration control based on GA and modal LQR," *Comput. Struct.*, vol. 128, pp. 101–115, 2013.

[41] Y. Qiao, J. Han, C. Zhang, J. Chen, and K. Yi, "Finite element analysis and vibration suppression control of smart wind turbine blade," *Appl. Compos. Mater.*, vol. 19, no. 3–4, pp. 747–754, 2012.

[42] S. Le, "Active vibration control of a flexible beam," 2009.

[43] J. F. Manwell, J. G. McGowan, and A. L. Rogers, *Wind Energy Explained: Theory, Design and Application*. Wiley, 2010.

[44] C. L. Ladson and L. R. Center, *Computer program to obtain ordinates for NACA airfoils*. National Aeronautics and Space Administration, Langley Research Center, 1996.

[45] K. J. Aström and R. M. Murray, *Feedback Systems: An Introduction for Scientists and Engineers*. Princeton University Press, 2010.

[46] Y. Li, J. Liu, and Y. Wang, "Design approach of weighting matrices for LQR based on multi-objective evolution algorithm," in *2008 International Conference on Information and Automation*, no. 2, pp. 1188–1192, 2008.

[47] G. Abreu, S. Conceicao, V. Lopes Jr., M. Brennan, and M. Alves, "System identification and active vibration control of a flexible structure," *J. Brazilian Soc. Mech. Sci. Eng.*, vol. 34, Special Issue, pp. 386–392, 2012.

[48] C. T. Chen, *Linear System Theory and Design*. Oxford University Press, 2009.

[49]   R. C. Nelson, *Flight stability and automatic control*. WCB/McGraw Hill, 1998.

[50]   W. G. Abdelrahman, A. Z. Al-Garni, and S. I. Abd El-Maksoud, "Active vibration suppression of a wind turbine blade using piezoelectric Materials," paper will be submitted for publication, 2014.

VITAE

Name   : SHERIF IBRAHIM ABD EL-MAKSOUD MOHAMED

Nationality   : Egyptian

Date of Birth   : 12/10/1989

Email   : eg.sherif89@gmail.com

Address   : Dhahran-Saudi Arabia

Academic Background   : Bachelor Degree in Aeronautical Engineering
                                From Institute of Aviation Engineering and Technology

                                Master Degree in Aerospace Engineering
                                From King Fahd University of Petroleum and Minerals

Research Interests

- Vibration Control

- Smart Materials

- Evolutionary computation and intelligent control

Research and Publications

- W. G. Abdelrahman, A. Z. Al-Garni, and S. I. Abd El-Maksoud, "Active vibration suppression of a wind turbine blade using piezoelectric Materials," paper will be submitted for publication, 2014.